A BROAD-SPECTRUM ANTI-BIOFILM PEPTIDE THAT TARGETS A CELLULAR STRESS RESPONSE

by

César de la Fuente-Núñez

Licenciado en Biotecnología (B.Sc. + M.Sc.), Universidad de León, 2009

A THESIS SUBMITTED IN PARTIAL FULFILLMENT OF

THE REQUIREMENTS FOR THE DEGREE OF

DOCTOR OF PHILOSOPHY

in

THE FACULTY OF GRADUATE AND POSTDOCTORAL STUDIES

(Microbiology and Immunology)

THE UNIVERSITY OF BRITISH COLUMBIA

(Vancouver)

October 2014

Abstract

Bacteria form multicellular communities known as biofilms that cause two thirds of all infections and demonstrate increased adaptive resistance to conventional antibiotics. Currently, there are no approved drugs that specifically target bacterial biofilms. In this work, I first identified peptide 1037, which inhibited biofilm formation in a broad-spectrum manner and proposed that this activity might be due to the effect of the peptide on biofilm-associated processes. However, these processes are not conserved in bacteria and therefore did not explain the broad-spectrum activity of the peptide. Additional screens identified 1018 as a potent anti-biofilm peptide that prevented biofilm formation and led to the eradication of mature biofilms in both Gram-negative and Gram-positive bacteria. Low levels of the peptide led to biofilm dispersal, while higher doses triggered biofilm cell death. To explain the broad-spectrum activity of the peptide, I hypothesized that it acted to inhibit a common stress response, and that the stringent response, mediating (p)ppGpp synthesis through the enzymes RelA and SpoT, was targeted. Consistent with this notion, increasing (p)ppGpp synthesis led to reduced susceptibility to the peptide. Furthermore, *relA* and *spoT* mutations blocking production of (p)ppGpp replicated the effects of the peptide, leading to reduced biofilm formation. Eliminating (p)ppGpp expression after 2 days of biofilm growth by removal of arabinose from a strain expressing *relA* behind an arabinose-inducible promoter, reciprocated the effect of peptide added at the same time, leading to loss of biofilm. NMR and chromatography studies showed that the peptide acted on cells to cause degradation of (p)ppGpp, and *in vitro* directly interacted with ppGpp. These results indicate that 1018 targets (p)ppGpp and marks it for degradation, thus providing an explanation for the broad-spectrum activity of the peptide. Further, the peptide was found to be synergistic with different classes of antibiotics to prevent and eradicate bacterial biofilms. Thus the peptide represents a novel strategy to potentiate antibiotic activity against biofilms. Further studies identified even more potent D-enantiomeric anti-biofilm peptides DJK-5 and DJK-6 that also prevented (p)ppGpp accumulation, were highly synergistic with conventional antibiotics and exhibited *in vivo* activity. Targeting biofilms represents a novel approach against drug-resistant bacterial infections.

Preface

A version of Chapter 1 has been published. **de la Fuente-Núñez C**, Reffuveille F, Fernández L, Hancock REW. Bacterial biofilm development as a multicellular adaptation: antibiotic resistance and new therapeutic strategies. Curr Opin Microbiol. 2013; 16:580-9.

A version of Chapter 2 has been published. **de la Fuente-Núñez C**, Korolik V, Bains M, Nguyen U, Breidenstein EB, Horsman S, Lewenza S, Burrows L, Hancock REW. Inhibition of bacterial biofilm formation and swarming motility by a small synthetic cationic peptide. Antimicrob Agents Chemother. 2012; 56:2696-704. C.D.L.F.-N. and R.E.W.H. conceived the project; C.D.L.F.-N. designed, performed and analyzed studies; V.K. helped with the initial peptide screen; S.H. and S.L. provided access to the flow cell apparatus and helped with the flow cell studies and further analyses of the results; L.B. and U.N. performed experiments using *Listeria monocytogenes*. C.D.L.F.-N. and R.E.W.H. wrote the paper; R.E.W.H. designed the research and supervised all studies.

A version of part of Chapter 3 and all of Chapter 4 has been published. **de la Fuente-Núñez C**, Reffuveille F, Haney EF, Straus SK, Hancock REW. Broad-spectrum anti-biofilm peptide that targets a cellular stress response. PLoS Pathog. 2014; 10: e1004152. C.D.L.F.-N. and R.E.W.H. conceived the project; C.D.L.F.-N. and F.R. designed, performed and analyzed studies; C.D.L.F.-N. wrote the paper; E.F.H. and S.K.S. performed and analyzed NMR studies; R.E.W.H. designed the research, supervised all studies and edited the paper.

A version of part of Chapter 3 has been accepted for publication. Reffuveille F, **de la Fuente-Núñez C**, Mansour S, Hancock, REW. A broad-spectrum anti-biofilm peptide enhances antibiotic action against bacterial biofilms. Antimicrob. Agents Chemother. 2014; 58:5363-71. C.D.L.F.-N. and R.E.W.H. conceived the project; F.R. and C.D.L.F.-N. designed, performed and analyzed studies; F.R., C.D.L.F.-N. and R.E.W.H. wrote the paper; R.E.W.H. designed research and supervised all studies.

A version of Chapter 5 has been submitted for publication. **de la Fuente-Núñez C**, Reffuveille F, Mansour SC, Reckseidler-Zenteno SL, Brackman G, Coenye T, Hancock REW. D-enantiomeric peptides that eradicate bacterial biofilms and protect *C. elegans* and *Galleria mellonella* from a lethal *Pseudomonas aeruginosa* infection. C.D.L.F.-N. and R.E.W.H. conceived the project; C.D.L.F.-N. and F.R. designed, performed and analyzed studies; S.L.R-Z was responsible for the BioFlux peptide screen; G.B. and T.C. performed and analyzed all *in vivo*

studies; C.D.L.F.-N. wrote the paper; R.E.W.H. designed research, supervised all studies and edited the paper.

Table of Contents

List of Tables

List of Figures

List of Abbreviations

Abbreviation	Meaning
AMP	Antimicrobial peptide
ANOVA	Analysis of variance
ATP	Adenosine triphosphate
BM2	Basal medium 2
CAA	Casamino acid medium
CDC	Center for Disease Control
Cf.	Compare
CF	Cystic fibrosis
CFU	Colony forming units
CIP	Ciprofloxacin
CTZ	Ceftazidime
c-di-GMP	bis-(3'-5')-cyclic dimeric guanosine monophosphate
DNA	Deoxyribonucleic acid
GTP	Guanosine triphosphate
HSL	Homoserine lactone
IMI	Imipenem
LB	Lysogeny broth
LPS	Lipopolysaccharide
MBIC	Minimal biofilm inhibitory concentration
MIC	Minimal inhibitory concentration
mM	Millimolar
MRSA	Methicillin-resistant *Staphylococcus aureus*
OD	Optical density
PI	Propidium iodide
PBS	Phosphate-buffered saline
PCR	Polymerase chain reaction
ppGpp	Guanosine tetraphosphate
pppGpp	Guanosine pentaphosphate
RNA	Ribonucleic acid

rRNA	Ribosomal ribonucleic acid
RT-PCR	Real-time polymerase chain reaction
SCVs	Small colony variants
SEM	Scanning electron microscopy
TOB	Tobramycin
tRNA	Transfer ribonucleic acid
WT	Wild-type
α	alpha
β	beta
Δ	delta; signifies here genetic deletion of a gene
μ	micro

Acknowledgements

Foremost, I would like to thank my PhD supervisor and mentor Dr. Bob Hancock for giving me the unique opportunity to work in his laboratory, for providing me freedom to think and explore ideas, for teaching me how to clearly explain complicated concepts, and overall for opening my eyes to the fascinating world of science.

I will always be grateful to Fundación "la Caixa" and Fundación Canadá for believing in me and for funding my ideas.

I have been very fortunate to have been surrounded by talented scientists during my PhD years. First, I would like to thank Dr. Fany Reffuveille for her friendship, invaluable experimental help and for the many hours spent talking about science.

Also, I would like to acknowledge members of the Hancock lab that have been supportive and have provided advice and knowledge over the years: Dr. Lucía Fernández, Dr. Elena Breidenstein, Dr. Jeff Xia, Sarah Mansour, Manjeet Bains, Reza Falsafi and Dr. Octavio Luiz Franco.

I would like to also thank my committee members Dr. Erin Gaynor, Dr. Rachel Fernandez and Dr. David Speert for being tremendously supporting and encouraging, and for their advice.

Unity makes strength. This definitely applies to my excellent collaborators Dr. Shawn Lewenza, Dr. Lori Burrows, Dr. John Smit, Jan Mertens, Dr. Tom Coenye and Dr. Shauna Reckseidler-Zenteno, whose expertise was key in different projects throughout my PhD.

I must not forget to also look back and remember the institutions that educated me over the years; I.E.S. Eusebio da Guarda in my hometown A Coruña and Universidad de León.

Nothing I have achieved or done would have been possible without my parents María Amparo Núñez Díaz and Raúl de la Fuente Fernández. They gave me life and then dedicated their own lives to educate me, love me and always encouraged me to try my best at whatever I decided to do. They also introduced me to the excitement of the unknown. Similarly, my brother Manoel de la Fuente Núñez and my sisters Milena de la Fuente Núñez and Vânia de la Fuente Núñez have been my comrades through life, have taught me invaluable lessons and have shaped who I am today. Lastly, special thanks to my partner and best friend Lily Canan Reynolds for her unconditional love, for her contagious passion for life, for her support and for always believing in me.

To my parents

Chapter 1: Introduction

1.1 Bacterial biofilm development

Biofilms are structured aggregations of microorganisms associated with surfaces that have been widely studied over the past few decades in part because they cause 65% or more of all infections, being particularly prevalent in device-related infections, infections on body surfaces (skin and soft tissue, lung, bladder, endocarditis, etc.) and chronic infections (Costerton et al., 1999; Hall-Stoodley et al., 2004; O'Toole et al., 2000). They are particularly problematic due to their resistance to host defence mechanisms and to conventional antimicrobial therapy, which substantially hinders their treatment in the clinic (Costerton et al., 1999; Hall-Stoodley et al., 2004; Kolter, 2010; O'Toole et al., 2000). From a broader perspective, biofilms are ancient phenotypic adaptations to the environment and are ubiquitous in nature (Hall-Stoodley L et al., 2004).

1.1.1 Biofilm development: an adaptive response to hostile environments

Bacteria have evolved the ability to form multicellular, surface-adherent communities called biofilms that allow survival in hostile environments. In clinical settings, bacteria are exposed to various sources of stress, including antibiotics, nutrient limitation, anaerobiosis, heat shock, etc., which in turn trigger adaptive responses in bacterial cells. The combination of these and other defense mechanisms results in the formation of highly (adaptively) resistant multicellular structures that are recalcitrant to host immune clearance mechanisms and very difficult to eradicate with the currently-available antimicrobial agents, which are generally developed for the eradication of free-swimming (planktonic) bacteria. However, novel strategies that specifically target the biofilm mode of growth have been recently described, thus providing the basis for future anti-biofilm therapy.

Biofilms appear early in the fossil record (~3.25 billion years ago), and are common in a broad range of organisms, including not only bacteria but also archaea and eukaryotic microbes such as fungi (Hall-Stoodley et al., 2004). The emergence of these primitive biofilms appears to have coincided with the first evidence of an evolutionary transition from unicellular to multicellular organization, which was provided by fossils of prokaryotic filamentous and mat-forming cyanobacteria-like organisms (Hall-Stoodley et al., 2004). This suggests that bacteria that transitioned into a biofilm lifestyle might have been the first multicellular life

forms. The deep evolutionary roots of this adaptation suggest that it must have been advantageous for survival in the harsh environment of early Earth. Indeed, a growing number of studies indicate that biofilm formation is closely linked to stress responses. With this in mind, we may speculate that around 3.25 billion years ago, a combination of stress signals triggered the activation of certain molecular pathways in bacteria. This eventually resulted in the emergence of the advantageous biofilm phenotype that increased the chances of survival under those particular conditions (Figure 1.1).

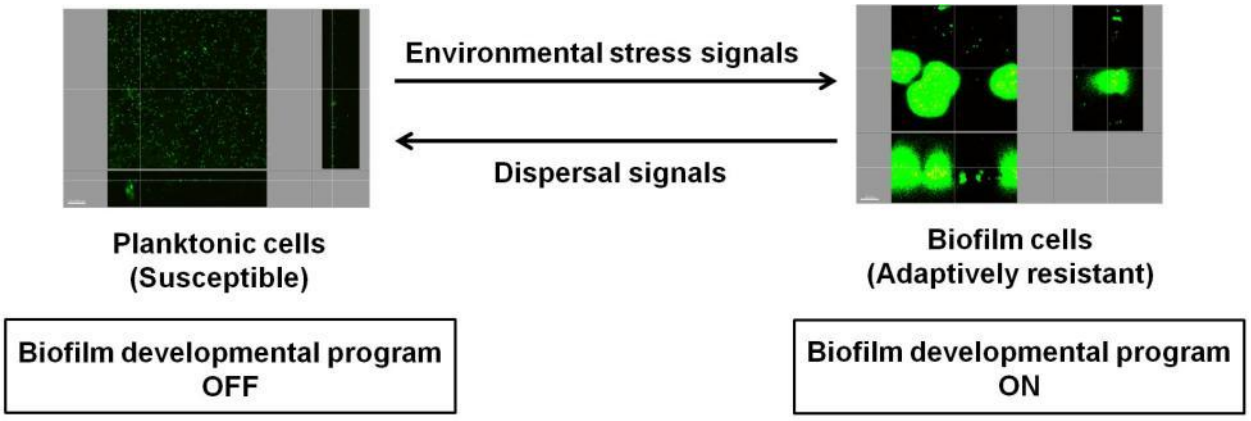

Figure 1.1. Bacterial biofilm development: from susceptible to resistant bacteria. Biofilm development initiates when flagella-propelled planktonic cells receive a stress signal from the environment. This stress signal, possibly combined with surface adherence, initiates the biofilm developmental program leading to increased (adaptive) resistance, enabling cell survival. Images shown correspond to *P. aeruginosa* biofilms grown in flow cell chambers, stained with SYTO-9 (green; live cells) and propidium iodide (red; dead cells) and visualized using confocal microscopy from above square panel and from two sides (bottom and right panels), demonstrating biofilm colonies as mounds arising from the surface. Reprinted from Curr. Opin. Microbiol., 16, de la Fuente-Núñez C, Reffuveille F, Fernández L, Hancock REW, Bacterial biofilm development as a multicellular adaptation: antibiotic resistance and new therapeutic strategies, 580-9, Copyright (2013), with permission from Elsevier.

Thus, while bacteria have traditionally been considered free-living, unicellular organisms, we now know that they predominantly exist as adherent multicellular biofilms in diverse environmental niches including the majority of clinically-relevant infections (Costerton et al., 1999; Hall-Stoodley et al., 2004; O'Toole et al., 2000). The transition from the planktonic state to biofilm growth occurs as a consequence of environmental changes that trigger the dysregulation of multiple regulatory networks (Costerton et al., 1999; Hall-Stoodley et al., 2004; O'Toole et al., 2000). Upon sensing a stress signal, free-living (planktonic) cells initiate attachment to a surface, which leads to the formation of a biofilm that has a greater

ability to withstand environmental challenges. Biofilm formation is therefore an environmentally driven developmental process that increases resistance to exogenous stresses, enabling bacterial survival under unfavorable conditions. Once the mature biofilm has developed, some cells within the population start to dissociate (disperse) from the sessile structure (O'Toole et al., 2000). This stage is termed dispersal and it is essential to complete the biofilm cycle by enabling the cells to spread and colonize new surfaces.

To avoid the death of the entire population, the response to stress has to be faster than the adverse action of the stress signal. Therefore, the development of biofilms in response to stress signals must be an extremely rapid and efficient process. Even before a structured biofilm is evident, a 'biofilm program' is activated, as evidenced by the differential expression of a substantial number of genes (Beloin and Ghigo, 2005; Whiteley et al., 2001). Initially this activation might be a response to cell association with a surface, which can occur through adhesion organelles including pili, flagella and external microbial layers, or due to immobilization of the bacteria (Costerton et al., 1999; O'Toole et al., 1998; O'Toole et al., 2000). As bacteria start to grow they attach more firmly and the increased numbers of co-localized microbes can trigger so-called quorum-sensing circuits that involve endogenous secreted signal molecules which, when accumulated to high enough local (threshold) concentrations, are taken up and trigger profound regulatory changes (O'Toole et al., 2000). One such signal molecule is the quorum-sensing signal 3-oxo-C12- homoserine lactone of *Pseudomonas aeruginosa*, which is required for the efficient differentiation of planktonic into biofilm cells (Davies et al., 1998). Mature biofilms eventually form and build prominent microcolonies that protrude from the surface, are held together by molecules termed collectively the extracellular matrix, including specific polysaccharides, proteins, and extracellular DNA (eDNA) (Whitchurch et al., 2002), and contain water-filled channels enabling enhanced access of nutrients into the biofilm (Costerton et al., 1999; Hall-Stoodley et al., 2004; Flemming and Wingender, 2010). The biofilm program includes the production of these matrix components, which may be protective, as well as the production of extracellular enzymes, the induction of mechanisms for excreting toxic compounds (e.g. efflux pumps), and changes in metabolism, especially a metabolic decline in bacteria living in the deepest layers of the biofilm structure (Costerton et al., 1999; Hall-Stoodley et al., 2004; Flemming and Wingender, 2010; O'Toole et al., 2000). This suggests that bacteria possess a biofilm genetic

program that is triggered by stressful conditions and propagated by association with surfaces and quorum sensing, impacting on both biofilm development and the characteristics of the resultant biofilm (Figure 1.1). Consequently, this program represents an advantageous adaptation that involves regulatory circuits that cause temporary rather than permanent genetic alterations. From this one can infer that biofilm formation is a deeply-wired genetic developmental process triggered by stress signals, which has been selected through evolution to enable bacterial survival in harsh conditions.

1.2 Biofilm formation in nature and in the clinic

Biofilms are formed in diverse environmental niches, including hydrothermal hot springs and deep-sea vents, freshwater rivers, rocks, etc. (Costerton et al., 1999; Hall-Stoodley et al., 2004). Additionally, these multicellular structures have been observed in various industrial and clinical settings (Breidenstein et al., 2011; Costerton et al., 1999; Hall-Stoodley et al., 2004; Høiby et al., 2010; Høiby et al., 2011). These observations suggest that stress signals in a great variety of natural and human ecosystems are able to drive bacteria to exist predominantly within the protective milieu of a biofilm structure. Cells within biofilms have been shown to be resistant to many different environmental insults, including a range of chemically diverse biocides and antibiotics used in industrial and clinical settings, as well as UV damage, metal toxicity, anaerobic conditions, acid exposure, salinity, pH gradients, desiccation, bacteriophages, amoebae, etc. (Costerton et al., 1999; Hall-Stoodley et al., 2004; Römling and Basalobre, 2012). Importantly, biofilms play a fundamental role in infectious diseases as they can form on any body surface and persist after treatment with diverse antimicrobial agents (Costerton et al., 1999). Biofilm cells can also withstand host immune responses (both innate and adaptive), being particularly resistant to phagocytosis, and are between 10- and 1000-fold more resistant to treatment with most conventional antibiotics than their planktonic counterparts (Costerton et al., 1999; Römling and Basalobre, 2012). Indeed, antibiotic development pipelines rarely test the susceptibility of recalcitrant biofilm cells or utilize animal models of biofilm-related infections.

It is estimated that the majority of all medical infections are caused by bacterial biofilms that colonize either non-biological or biological surfaces (Costerton et al., 1999; Høiby et al., 2011; Römling and Basalobre, 2012) (Table 1.1). Abiotic surfaces such as medical devices are commonly infected by biofilms. Examples include intravenous, endotracheal,

Hickman and dialysis catheters, prosthetic heart valves, orthopedic devices, tissue fillers, cardiac pacemakers and cerebrospinal fluid shunts (Costerton et al., 1999; Hall-Stoodley et al., 2004; Høiby et al., 2011; Römling et al., 2012). In fact, 60–70% of all nosocomial infections are due to the presence of biofilms on implants (Percival et al., 2012). The microorganisms most frequently associated with medical devices are the staphylococci (particularly *Staphylococcus epidermidis* and *S. aureus*), followed by the bacterium *P. aeruginosa* and a plethora of other environmental bacteria that opportunistically infect hosts compromised by invasive medical intervention, chemotherapy or a pre-existing disease state (Costerton et al., 1999; Hall-Stoodley et al., 2004; Høiby et al., 2011; Römling et al., 2012). In addition, biofilms can associate with living biological surfaces, including those provided by the human body (Table 1.1).

Table 1.1. Examples of different bacterial species involved in infections associated with biofilm development in immunocompromised patients and medical devices. Reprinted from Curr. Opin. Microbiol., 16, de la Fuente-Núñez C, Reffuveille F, Fernández L, Hancock REW, Bacterial biofilm development as a multicellular adaptation: antibiotic resistance and new therapeutic strategies, 580-9, Copyright (2013), with permission from Elsevier.

Bacterial species	**Surface on which biofilms form**	**Disease/infections associated with biofilms**
Aerobic/anaerobic bacteria	Surface/deep skin	Chronic wound
Burkholderia cepacia	Lungs	Cystic fibrosis
Enterococcus faecalis	Heart valves Central venous catheters Urinary catheters	Endocarditis
Escherichia coli	Urinary tract Middle ear Prostheses	Urinary tract infections Otitis media
Haemophilius influenzae	Middle ear	Otitis media
Klebsiella pneumoniae	Central venous catheters	
Mycobacterium tuberculosis	Lungs	Tuberculosis
Pseudomonas aeruginosa	Lungs Middle ear Contact lenses Central venous catheters Prostheses	Cystic fibrosis Otitis media Nosocomial infections
Staphylococcus aureus	Middle ear Bones Sutures Central venous catheters Prosthetic heart valves Prostheses	Otitis media Musculoskeletal infections Nosocomial infections

Bacterial species	**Surface on which biofilms form**	**Disease/infections associated with biofilms**
Staphylococcus epidermidis	Surface/deep skin Heart valves Central venous catheters Prostheses	Chronic wound Endocarditis
Streptococcus sp	Tooth surface	Dental caries

Indeed, biofilms play a significant role in human infections as diverse as dental caries, periodontitis, otitis media, chronic wounds, musculoskeletal infections, necrotizing fasciitis, biliary tract infection, osteomyelitis, bacterial prostatitis, native valve endocarditis, intra-amniotic infections, meloidosis, a wide range of nosocomial infections and cystic fibrosis (CF) pneumonia (Bryers, 2008; Costerton et al., 1999; Hall-Stoodley et al., 2004; Høiby et al., 2010; Høiby et al., 2011; Percival et al., 2012; Römling and Basalobre, 2012) (Table 1.1).

Bacterial colonization of the CF lung provides a good example of a biofilm-related infection. These lung infections are typically characterized by inflammation and tissue damage, as well as antibiotic and phagocytosis resistance (Breidenstein et al., 2011; Høiby et al., 2010). In particular, the lower respiratory tract of adolescents and early adult CF patients becomes colonized and chronically infected, predominantly by the bacterium *P. aeruginosa*, a model organism for the study of biofilms due to its tendency to develop well-structured biofilms (Høiby et al., 2010). These infections lead to lung tissue damage as a result of the combined action of bacteria and increased inflammation, frequently resulting in the death of the patient (the median life expectancy of CF patients is about 30–48 years) (Breidenstein et al., 2011; Høiby et al., 2010; Høiby et al., 2011). It has been demonstrated that *Pseudomonas* can form biofilms in the lungs of CF patients, which clearly contributes to the difficulty of eradicating these infections. In this specific case, *P. aeruginosa* presumably develops biofilms in response to stress signals present in the CF lung environment, such as microaerobiosis or antibiotic pressure. Once the biofilm has fully developed, subsequent strategies of host defense (immune cells especially phagocytes, reactive oxygen species, etc.) and/or antimicrobial therapy are often ineffective and fail to completely clear the organism. As mentioned in the previous section, this ability to resist under conditions of extreme stress is inherent to the nature of biofilms. Consequently, considerable efforts have been made to attain a greater understanding of the mechanisms that explain biofilm endurance. This information is critical for the development of novel therapeutic strategies.

1.3 Mechanisms of antibiotic resistance in biofilms

While many explanations have been advanced to explain the high antibiotic resistance displayed by bacterial biofilms, it constitutes a clear example of adaptive resistance, a phenomenon that is increasingly attracting the attention of clinical microbiologists (Fernández et al., 2011). The adaptive nature of biofilm resistance is evidenced by the fact that cells taken from a biofilm and brought back to the planktonic state generally recover their original susceptibility to antibiotics (Nickel et al., 1985). It is worth noting, however, that growth in a biofilm can favor the occurrence of processes that lead to the acquisition of inheritable resistance, such as horizontal gene transfer (Cook et al., 2011; Savage et al., 2013) or adaptive mutations (Driffield et al., 2008). The proposed underlying mechanisms of adaptive resistance in the biofilm state are numerous and diverse (Figure 1.2). Some of these mechanisms are rather general and relate to the drastically altered transcriptional program of biofilms or the inherent properties of biofilms, including their structure or composition, and as such they can be found in a wide range of species and affect the action of several antibiotic classes. In contrast, other mechanisms are very species-specific and/or antibiotic-specific. Here, I provide an overview of the different known factors contributing to biofilm resistance, most of which have been identified relatively recently (Figure 1.2).

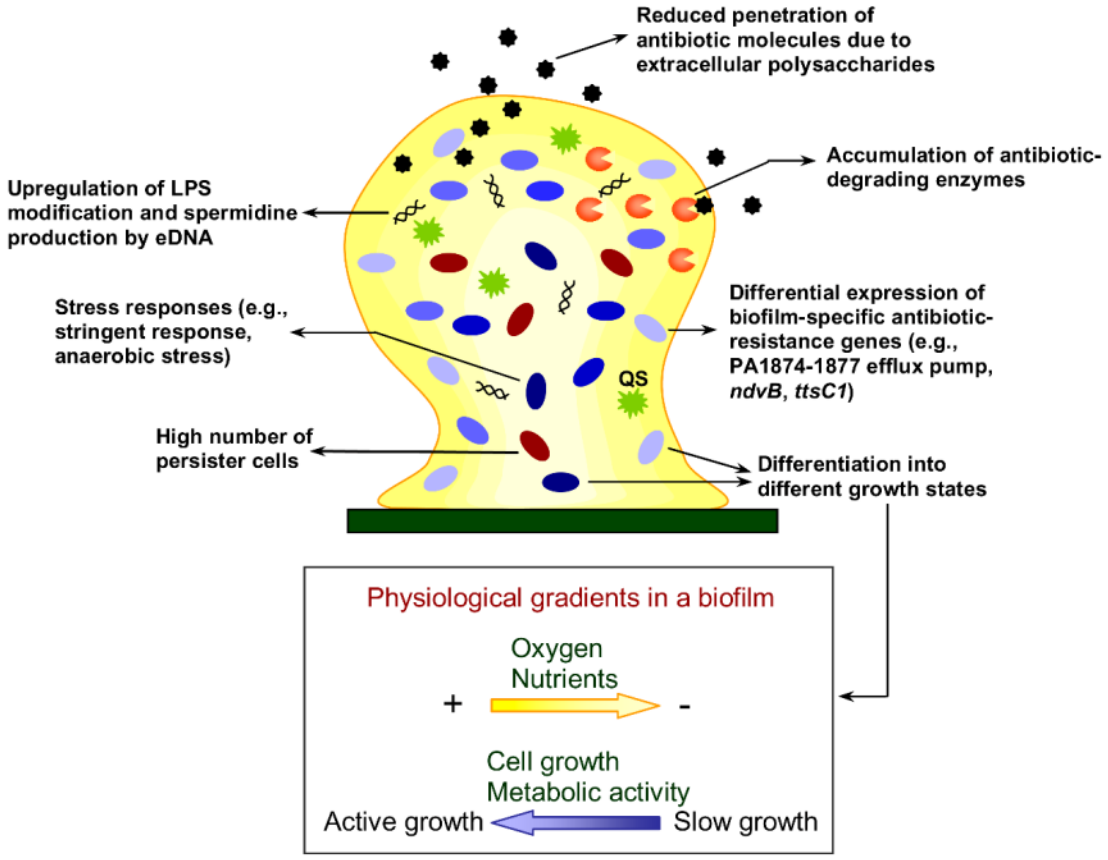

Figure 1.2. Schematic representation of a *P. aeruginosa* biofilm indicating various examples of adaptive resistance mechanisms exhibited during this multicellular growth state. The box below shows the gradients of oxygen and nutrients formed within the biofilm structure and how they relate to cell differentiation into different growth states. Abbreviations: QS, quorum-sensing signal; eDNA, extracellular DNA. Reprinted from Curr. Opin. Microbiol., 16, de la Fuente-Núñez C, Reffuveille F, Fernández L, Hancock REW, Bacterial biofilm development as a multicellular adaptation: antibiotic resistance and new therapeutic strategies, 580-9, Copyright (2013), with permission from Elsevier.

1.3.1. Stress responses

As discussed above, biofilm formation is closely linked to the adaptations triggered by exposure to environmental stresses, with adherence and quorum sensing also playing a role. Stress responses (as well as adherence and quorum sensing) cause hundreds of genes to change expression. Some of these changes are induced to better enable the bacterium to resist harmful conditions, including antibiotics and other chemicals. It is increasingly appreciated that the resistomes for many bacteria, representing the total number of genes that when altered in expression lead to decreased susceptibility to a given antibiotic, can be quite extensive; for example, the tobramycin and ciprofloxacin resistomes of *Pseudomonas* involve more than 100

separate gene products (Fernández et al., 2011). Certain stress responses, such as those exhibited under starvation conditions, are known to confer increased antibiotic tolerance. It was originally thought that the slower growth rate of biofilms per se conferred a greater ability to survive an antimicrobial insult. However, recent evidence shows that the antibiotic tolerance associated with nutrient limitation is a tightly controlled response involving complex regulatory pathways. Indeed, Nguyen et al. (Nguyen et al., 2011) have demonstrated that the activation of the stringent response was essential for increased antibiotic tolerance during starvation in *P. aeruginosa*. Similarly, in *E. coli* biofilms, the stringent response was found to participate in fluoroquinolone tolerance, although the possession of a fully functional DNA-stress SOS response is more important (Bernier et al., 2013). In the case of *Pseudomonas*, the SOS response has been shown to be important for fluoroquinolone resistance in planktonic cells (Breidenstein et al., 2012); as a result, it would be interesting to determine whether it also plays a role in biofilm formation. Another stress response that has been related to antibiotic resistance in *Pseudomonas* is the heat shock response, which impacts on susceptibility to aminoglycosides through the intracellular protease AsrA (Kindrachuck et al., 2011). Again, this link has only been demonstrated for planktonic cells, but it would be interesting to study its participation in the biofilm state. In other pathogens, such as *E. coli* and *Listeria monocytogenes*, genes encoding heat shock proteins are induced in biofilm cells; moreover, mutations affecting these genes exert a negative effect on biofilm formation (Kuczyńska-Wiśnik et al., 2010; van der Veen and Abee, 2010). Also worth noting are the adaptations related to growth under anaerobic conditions, as they too have been associated with antibiotic tolerance (Borriello et al., 2004), and anaerobiosis evidently impacts on biofilm formation. It has been demonstrated that low-oxygen conditions lead to the upregulation of certain efflux pumps in *P. aeruginosa* (Schaible et al., 2012). It would appear logical that such mechanisms might play a role in the resistance exhibited by cells from the oxygen-deprived deeper biofilm layers. Antibiotics themselves propagate adaptive resistance as it is well established that sub-inhibitory antibiotics lead to increased resistance (Fernández et al., 2011). In many cases, this has been shown to relate to altered regulation/expression of several resistance genes. Thus, any resistance that might occur due to other stress conditions, such as those encountered by cells in biofilms, would be amplified by antibiotic-mediated stress. For instance, exposure of *P. aeruginosa* biofilms to azithromycin induces the expression of the MexCD-OprJ efflux pump,

although no such response is observed when planktonic cells are grown in the presence of this macrolide (Gillis et al., 2005).

1.3.2. Heterogeneous population

Biofilm communities are very complex and typically consist of a heterogeneous population of cells in different growth states. This cell differentiation is proposed to be a consequence of the decreasing oxygen and nutrient gradients that exist between the surface and the deeper layers of the biofilm (Figure 1.2). Consequently, more metabolically-active cells at the surface and slow-growing cells in nutrient-deprived and oxygen-deprived layers exhibit markedly distinct responses when exposed to different antimicrobials. For instance, fluoroquinolones and tetracycline were only effective in killing the metabolically active cells in the upper layers of a *P. aeruginosa* biofilm (Pamp et al., 2008). In contrast, the lipopeptide colistin proved useful for the eradication of the slow-growing cells from deeper layers, but not the actively growing cells, which acquired adaptive resistance by upregulation of the LPS-modification (*arn*) operon (Pamp et al., 2008). Another phenomenon that contributes significantly to antibiotic resistance in biofilms is persistence, a property of the so-called persister cells, which are more numerous in biofilms than in planktonic populations (Lewis, 2008; Qu et al., 2010). Persister cells, which can withstand the presence of otherwise-inhibitory concentrations of antibiotics, have an increased capacity to overcome stressful conditions, including antibiotic challenges, likely due to altered transcriptional programming (Lewis, 2008). Indeed, possessing a large persister subpopulation has been described as the most significant resistance mechanism in *S. epidermidis* biofilms (Qu et al., 2010).

1.3.3. Extracellular matrix

Typically, the cells in a biofilm are embedded in a matrix of polysaccharides, extracellular DNA (eDNA) and proteins (Flemming and Wingender, 2010). In addition to providing structural stability, this matrix has been reported to protect the cells from different agents, including antibiotics. Originally, it was thought that this protection was due to a filtration effect such that the antibiotics failed to effectively penetrate the matrix (Kumon et al., 1994; Singh et al., 2010). However, it is now known that the extracellular matrix has large water-filled spaces and channels, which likely contradicts the filtration theory. Alternatively, the matrix could facilitate the accumulation of antibiotic-degrading enzymes such as β-lactamases (Anderl et al., 2000). Increasing evidence indicates that the extracellular matrix

might contribute by inducing additional adaptive resistance mechanisms. A clear example of this is the effect of eDNA exposure on *P. aeruginosa* cells. Thus, chelation of divalent cations by subinhibitory levels of the negatively charged eDNA mimics growth in a Mg^{2+}- limiting environment and triggers the activation of the PhoPQ and PmrAB two-component systems. This, in turn, leads to aminoarabinosylation of the lipid A and makes the cells adaptively resistant to cationic peptides and aminoglycosides (Mulcahy et al., 2008). Exposure to eDNA also results in the accumulation of spermidine on the cell surface, which exerts a protective effect against polymyxins and oxidative stress (Johnson et al., 2012).

1.3.4. Specific mechanisms

Conserved regulatory mechanisms underlying biofilm adaptive resistance are likely to exist in multiple species, but the effector mechanisms of resistance may vary considerably among species. The identification of genetic determinants of species-specific or antibiotic-specific biofilm resistance has been facilitated by screening strategies targeted at finding mutants that form supersusceptible biofilms. In this arena it is worth highlighting the participation of efflux pumps that are known to influence the rate at which antibiotics accumulate in cells and are synergistic with other mechanisms, such as low outer membrane permeability and β-lactamase mediated degradation. For instance, a novel pump from *P. aeruginosa* strongly influences resistance to aminoglycosides and fluoroquinolones in biofilms but not in the planktonic state (Zhang and Mah, 2008). Another efflux pump, YhcQ, partly explains the increased resistance of *E. coli* biofilms (Lynch et al., 2007). Expression of this gene was regulated by the helicase-like protein RapA that also controlled the expression of another gene, *yeeZ*, necessary for biofilm-specific resistance. The *yeeZ* gene product is thought to participate in polysaccharide production, thereby contributing by reducing antibiotic penetration into the biofilm, although as mentioned above this interpretation may not be correct. Nevertheless, a biofilm-specific upregulation of efflux pumps was observed in these cases. This is interesting in the context of recent data suggesting the participation of certain efflux pumps in the process of biofilm formation (Baugh et al., 2012; Matsumura et al., 2011). Another specific mechanism is the production of periplasmic glucans in *P. aeruginosa* biofilm cells, which requires the activity of the *ndvB* gene product. These glucans have been proposed to act by binding antibiotics before they reach their intracellular targets (Mah et al., 2003), although it was recently shown that they also increase the expression of ethanol oxidation

genes, which confer a protective effect against tobramycin (Beaudoin et al., 2012). Additionally, accumulation of these periplasmic glucans may have an impact on the Donnan potential, which refers to the distribution of ionic species between two ionic solutions separated by a membrane, thereby affecting the uptake of the antibiotics across the cell envelope. In other studies, a type VI secretion gene, *tssC1*, was found to be involved in biofilm antibiotic resistance, but not in biofilm formation, in *P. aeruginosa* (Zhang et al., 2011).

The above mechanisms highlight the diversity of the factors that participate in the decreased susceptibility of biofilm cells and there are many similar studies. Over the last few years, significant progress has been made towards understanding the nature of many of these mechanisms, despite the difficulties associated with the study of adaptive resistance due to its transient and often multi-genic nature. Nonetheless, considerably more work is required before we can fully decipher the molecular pathways that control this phenomenon and understand how it relates to biofilm formation and development.

1.4 New concepts in biofilm prevention and eradication

The traditional focus on discovering compounds that target the planktonic mode of growth, both *in vitro* and *in vivo*, and the insufficient level of understanding of the biofilm phenotype have resulted in a lack of available drugs that specifically target bacterial biofilms. In the clinic, biofilm infections are usually treated with combinations of antibiotics (Breidenstein et al., 2011; Høiby et al., 2010; Høiby et al., 2011; Römling and Basalobre, 2012). In the case of device-related biofilm infections, the device often has to be removed and replaced, a procedure that requires surgery, with all the costs, risks and complications involved (Høiby et al., 2011). These therapeutic approaches are clearly very aggressive but represent the only truly effective solutions currently available to clinicians. Fortunately, recent efforts have provided novel strategies to both prevent and eradicate bacterial biofilms (Figure 1.3). Cells within mature biofilms naturally produce compounds that induce their dispersal from the biofilm structure, to enable the colonization of new substrates; the resultant dispersed planktonic cells are then susceptible to conventional antibiotics. For example, Kolodkin-Gal et al. (Kolodkin-Gal et al., 2010) found that D-amino acids were produced by cells dispersing from *Bacillus subtilis* biofilms. Exogenous addition of low levels of these D-amino acids were then found to disrupt mature *B. subtilis* biofilms, and to additionally inhibit biofilm formation by the Gram-positive bacterium *S. aureus* and the Gram-negative pathogen *P. aeruginosa*

(Hochbaum et al., 2011). Mechanistically, in *B. subtilis* D-amino acids were found to trigger the release of amyloid fibers (encoded by the *yqxM-sipW-tasA* operon), which form part of the matrix linking cells within the biofilm. A subsequent study concluded that D-amino acids indirectly inhibit biofilm formation of *B. subtilis* by interfering with protein synthesis (Leiman et al., 2013). The same research group identified a second self-produced biofilm-dispersing molecule, the polyamine norspermidine (Kolodkin-Gal et al., 2012). This molecule led to the disassembly of *B. subtilis* biofilms by targeting the exopolysaccharide present in the biofilm matrix. Norspermidine also prevented biofilm development by *S. aureus* and *E. coli*. Interestingly, combinations of D-amino acids and norspermidine were more effective at preventing biofilm development and disrupting mature biofilms than either of the compounds alone (Kolodkin-Gal et al., 2012). However, recently published results are in conflict with these findings (Hobley et al., 2014). The signaling molecule nitric oxide (NO) has also been shown to disperse biofilms. For instance, treatment of *P. aeruginosa* biofilms with non-toxic levels of exogenously added NO stimulates c-di-GMP-degrading phosphodiesterases, which induce a switch to planktonic growth (Barraud et al., 2009). Polysaccharides produced by bacteria are structural components of the biofilm extracellular matrix. Indeed, it is well known that these polysaccharides are responsible for mediating cell-to-cell and cell-to-surface interactions, which are key in the overall architecture of biofilms. Interestingly, recent studies have identified polysaccharides released exclusively by mature biofilms. These polysaccharides, when added exogenously, limited biofilm formation by Gram-positive bacteria, and represent an interesting strategy for the prevention of biofilm development (Rendueles et al., 2011). Other strategies have been recently explored to target bacterial biofilms, although many of them are anticipated to be relatively species-specific in their action on biofilms. For instance, altering the biofilm developmental process might also be achieved by interfering with the signaling pathways involved. For example, targeting the quorum-sensing circuitry is a potentially attractive anti-biofilm approach that is being pursued (Balaban et al., 2007; Chung et al., 2011; Rasmussen et al., 2005). In addition, interfering with the second messenger signaling pathway (c-di-GMP, cAMP) has proven to be effective at inhibiting *Pseudomonas* biofilms (Boyd et al., 2012; Hengge, 2009; Pesavento and Hengge, 2009; Römling et al., 2013). Enzymes that interact with essential biofilm components are also of interest as anti-biofilm therapeutics. Some examples include DNAse I, an enzyme that

degrades eDNA, an essential structural component in developing biofilms (Whitchurch et al., 2002). Moreover, a glycoside hydrolase produced by *Actinobacillus* biofilms was capable of breaking down the β 1–6-N- acetylglucosamine polymers present in the peptidoglycan layer of bacterial cells. This enzymatic reaction led to the inhibition of biofilm formation without affecting growth and also dispersed preformed *Actinobacillus* biofilms (Kaplan et al., 2004; Ramasubbu et al., 2005). Surface appendages necessary for cell adhesion to other cells and surfaces and subsequently biofilm development have also been exploited as anti-biofilm targets, leading to the development of compounds that inhibited *E. coli* biofilm formation by blocking biogenesis and/or assembly of pili and curli (Cegelski et al., 2009). Other innovative strategies for the treatment of bacterial biofilms include the use of bacteriophages engineered to express a biofilm-degrading enzyme (Lu and Collins, 2007), iron chelators (iron being essential for biofilm formation) (Banin et al., 2006), and nanoparticles (Beyth et al., 2010; Lellouche et al., 2009). All the examples provided above show how the growing insight into the molecular mechanisms that participate in biofilm formation and dispersal has been essential for the development of new therapeutic strategies that specifically target these structures.

1.4.1 Host defence peptides as antimicrobial agents and biofilm inhibitors

Cationic host defense peptides have been considered as potential anti-infective agents primarily due to their antimicrobial or immunomodulatory properties (Easton et al., 2009; Hancock and Sahl, 2006; Scott et al., 2007). These peptides are typically 12 to 50 amino acids in length, and are amphiphilic, having 2 to 9 basic residues (R or K) and ~50% hydrophobic residues (Brogden, 2005; Hancock and Sahl, 2006). Their mechanism of action has been proposed to involve multiple targets, making them less prone to selecting for resistance compared to conventional antibiotics (Hancock and Sahl, 2006). Thus, cationic antimicrobial peptides target the bacterial cell with modest affinity through multiple coincident microbicidal mechanisms (Hancock and Sahl, 2006). Bacterial biofilms have been found to be particularly resistant to cationic antibiotics possibly due to the presence, in the biofilm matrix, of negatively charged polymers that bind and deactivate these antibiotics (Flemming and Wingender, 2010; Hancock and Sahl, 2006; Mulcahy et al., 2008). However, recently it was demonstrated that the natural human cathelicidin peptide LL-37 and the bovine peptide indolicidin were able to block *Pseudomonas aeruginosa* biofilm growth and cause dissolution of bacteria in mature

biofilms at concentrations below the MIC for planktonic bacteria (Overhage et al., 2008). These findings opened the door for the design and further optimization of synthetic variants based on these naturally-occurring host defence peptides, as performed in this thesis.

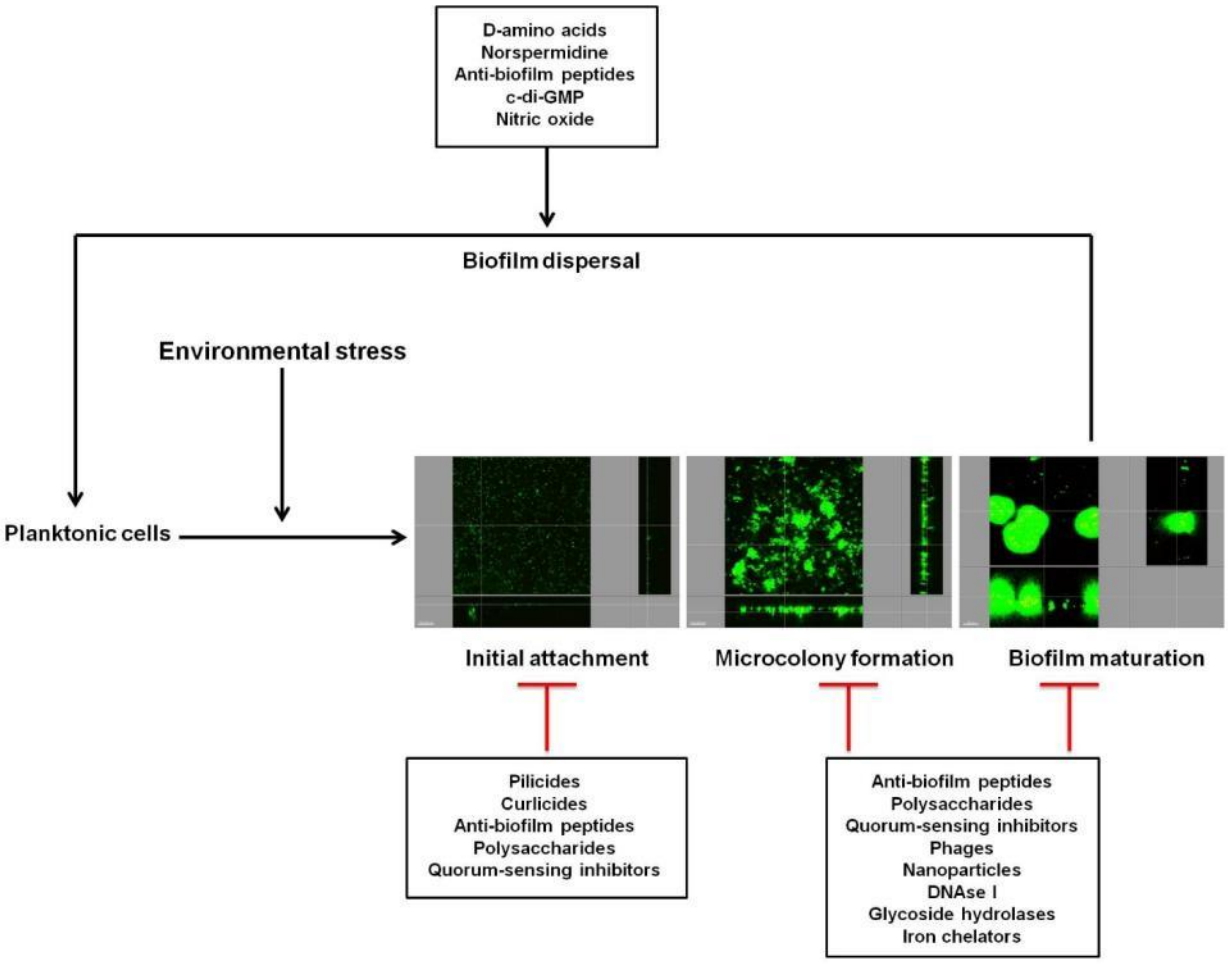

Figure 1.3. Examples of novel anti-biofilm therapeutics known to affect different stages of the biofilm developmental process. The black arrow in the upper box indicates molecules that work through induction of dispersal while the red lines represent inhibitory actions of the different molecules. The photographs represent confocal microscopy images of *P. aeruginosa* cells stained with SYTO-9. Reprinted from Curr. Opin. Microbiol., 16, de la Fuente-Núñez C, Reffuveille F, Fernández L, Hancock REW, Bacterial biofilm development as a multicellular adaptation: antibiotic resistance and new therapeutic strategies, 580-9, Copyright (2013), with permission from Elsevier.

1.5 (p)ppGpp signaling in bacteria: the environment as the trigger

During environmental stress, bacteria undergo the stringent response, which leads to the rapid production of the poly-phosphorylated nucleotides guanosine 5´-diphosphate 3´-diphosphate (ppGpp) and guanosine 5´-triphosphate 3´-diphosphate (pppGpp), collectively

known as (p)ppGpp. Accumulated ppGpp acts directly on RNA polymerase to alter the rate of transcription (Magnusson et al., 2005), thus resulting in reprogramming of bacterial metabolism by modulating the expression of around 500 genes (in the case of *E. coli*) to ensure survival (Maisonneuve et al., 2014). These nucleotides were first identified 45 years ago on autoradiograms containing extracts of amino acid-starved *Escherichia coli* (Cashel and Gallant, 1969) and are produced by the enzymes RelA and SpoT in most Gram-negative bacteria and by Rsh (Rel/Spo homolog) enzymes in Gram-positive bacteria (Potrykus and Cashel, 2008). The synthesis of these nucleotides has been most studied in *E. coli*, in which RelA is activated during amino acid starvation, whereas SpoT synthesizes (p)ppGpp during starvation for sources of carbon, nitrogen, phosphorus, iron or lipids as well as when stressed by heat or oxidation. SpoT is also responsible for degradation of ppGpp and pppGpp to GDP and GTP, respectively (Potrykus and Cashel, 2008). Furthermore, enzymes that hydrolize pppGpp to ppGpp (Keasling et al., 1993) and degrade ppGpp (Ooga et al., 2009) have been identified. Importantly, (p)ppGpp is produced by virtually all bacterial species and serves as a regulatory checkpoint that ensures bacterial survival by modulating the expression of numerous genes. In addition, (p)ppGpp has been suggested to play a role in biofilm formation in some bacterial species, as (p)ppGpp mutants were unable to produce structured biofilms (Aberg et al., 2006; Balzer and McLean, 2002; Chávez de Paz et al., 2012; Dahl et al., 2003; He et al., 2012; Klinkenberg et al., 2010; Lemos et al., 2004; Nguyen et al., 2011; Sugisaki et al., 2013; Taylor et al., 2002; Vogt et al., 2011). As mentioned earlier, (p)ppGpp can be induced by a plethora of environmental stress signals, thus resulting in increased (adaptive) resistance. For example, starvation for different nutrients has been widely studied, particularly in the case of amino acids, and is known to promote (p)ppGpp accumulation within bacterial cells (Potrykus and Cashel, 2008).

1.5.1 Stochastically-induced (p)ppGpp

Apart from being environmentally-induced, the second messenger signaling nucleotide (p)ppGpp has been recently identified as an important regulatory molecule that controls bacterial persistence in a stochastic manner (Maisonneuve et al., 2013). Persister cells are isogenic bacterial populations that, in response to high levels of antibiotics (or other stressors), produce cells that transiently become multidrug tolerant (Keren et al., 2004; Lewis et al., 2010). These persister cells differ from antibiotic-resistant bacteria in that their persistence

state is reversible, as upon removal of the antibiotic, the cells become susceptible (Maisonneuve et al., 2014). The second messenger (p)ppGpp has been shown to play a role in persistence, since increased levels of these nucleotides lead to the activation of toxin-antitoxin loci through a regulatory pathway that depends on inorganic polyphosphate and the Lon protease, and that amplifies (p)ppGpp synthesis through the inhibition of the enzyme glutamyl-tRNA synthetase by the toxin HipA (Germain et al., 2013; Kaspy et al., 2013; Maisonneuve et al., 2013) (Figure 1.4). HipA only inactivates $tRNA^{glu}$-bound glutamyl-tRNA synthetase by phosphorylating the conserved Ser^{239} near the active center of the enzyme, which consequently inhibits aminoacylation. The increased levels of uncharged $tRNA^{glu}$ in the cells activate RelA and subsequently trigger (p)ppGpp synthesis. Using a translational fusion that reported on the intracellular levels of (p)ppGpp in single *E. coli* cells, Maisonneuve and colleagues demonstrated that (p)ppGpp levels varied stochastically in exponentially growing cells, thus allowing bacteria to switch to the persistent state (Maisonneuve et al., 2013). Interestingly, RelA has been shown to be positively stimulated by its own product, (p)ppGpp (Shyp et al., 2012), suggesting that the synthesis of (p)ppGpp could be amplified through this positive feedback loop, leading to the generation of more persister cells.

1.5.2 The (p)ppGpp^0 phenotype

Conversely, it is well recognized that cells unable to produce (p)ppGpp [also known as (p)ppGpp^0 strains] are quite susceptible to antibiotics and other adverse environmental cues, and are deficient in biofim formation is some bacterial species (Aberg et al., 2006; Balzer and McLean, 2002; Chávez de Paz et al., 2012; Dahl et al., 2003; He et al., 2012; Klinkenberg et al., 2010; Lemos et al., 2004; Nguyen et al., 2011; Sugisaki et al., 2013; Taylor et al., 2002; Vogt et al., 2011). Furthermore, ppGpp has been shown to be necessary for the survival of bacterial pathogens in the course of infections (Dalebroux et al., 2010). In addition, as described above, (p)ppGpp production is involved in the formation of persister cells. Indeed, when the *relA* and *spoT* genes of *E. coli* are deleted, persister cell formation is almost eliminated (Korch et al., 2003; Maisonneuve et al., 2013).

1.5.3 (p)ppGpp as a regulator of bacterial drug resistance

Bacteria are capable of withstanding harmful environmental conditions in order to ensure their survival. This ability to adapt to adverse niches is a key underlying factor in the increasing development of bacterial resistance to currently available antibiotic therapies and

as described above (p)ppGpp controls adaptive resistance to some extent. There is convincing evidence that pathogenic bacterial strains isolated from persistent, difficult-to-treat infections, constitutively produce (p)ppGpp (Gao et al., 2010; Mwangi et al., 2013). Conversely, cells unable to produce (p)ppGpp are extremely susceptible to antibiotics and other adverse environmental cues both *in vitro* and *in vivo* (Dalebroux et al., 2010). Based on previously collected evidence, I propose (Figure 1.4) that (p)ppGpp is a central regulator of a variety of drug resistance-related processes and this highlights the need for developing therapeutic strategies that target (p)ppGpp in order to combat antibiotic resistance in bacteria.

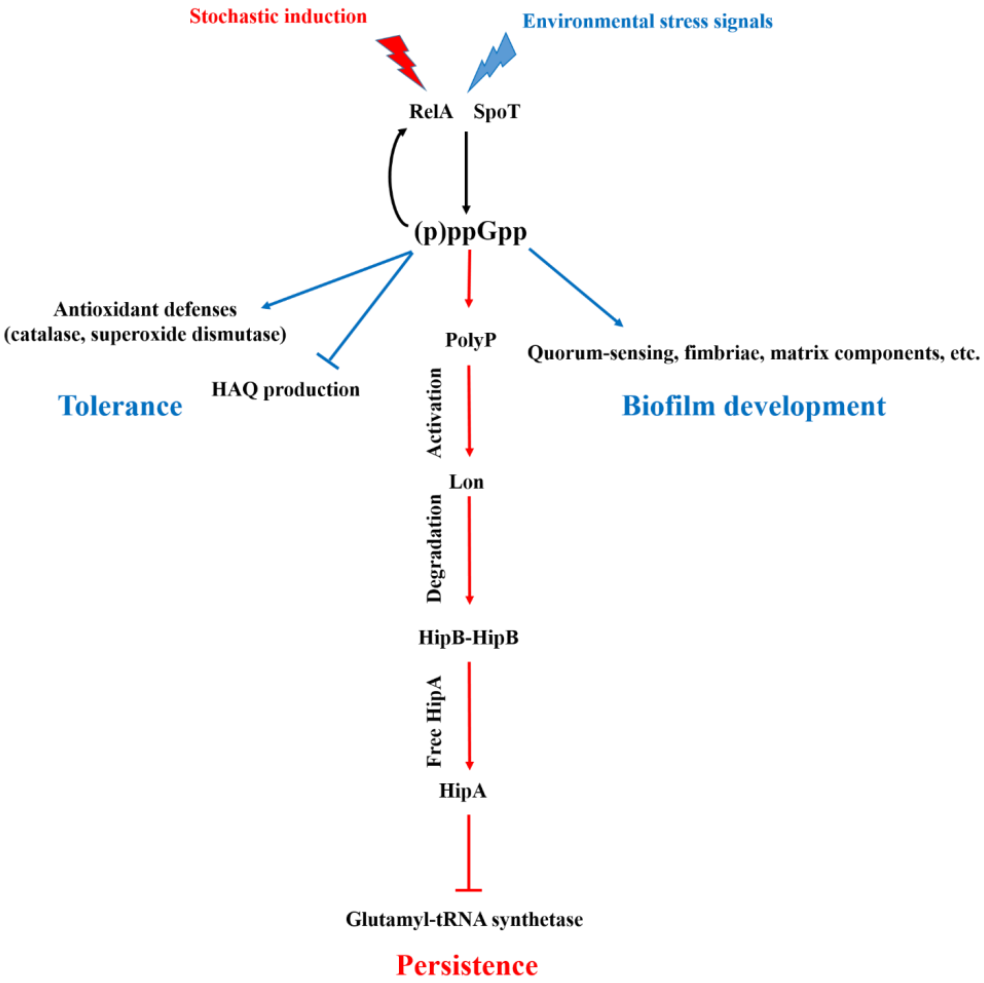

Figure 1.4. Working Hypothesis: (p)ppGpp as a regulator of bacterial drug resistance. Upon environmental stress, bacteria undergo the stringent response, which leads to the rapid production of ppGpp and pppGpp. Recently, the stringent response was shown to be essential for increased antibiotic tolerance during starvation in *P. aeruginosa*, thus linking tolerance to (p)ppGpp levels (Nguyen et al., 2011). Moreover, (p)ppGpp has been identified as an important regulatory molecule that controls persistence in *E. coli* in a stochastic manner

(Maisonneuve et al., 2013), leading to activation of toxin-antitoxin loci through a regulatory pathway that depends on inorganic polyphosphate and the Lon protease and that amplifies (p)ppGpp synthesis through the inhibition of the enzyme glutamyl-tRNA synthetase by the eukaryote-like serine-threonine kinase toxin HipA (Germain et al., 2013; Kaspy et al., 2013; Maisonneuve et al., 2013). Increased levels of uncharged tRNAglu in the cells activate RelA and subsequently trigger (p)ppGpp synthesis (Germain et al., 2013; Kaspy et al., 2013). In addition, (p)ppGpp has been suggested to play a role in biofilm formation in multiple bacterial species (Aberg et al., 2006; Balzer and McLean, 2002; Chávez de Paz et al., 2012; He et al., 2012; Lemos et al., 2004; Sugisaki et al., 2013; Taylor et al., 2002). The role of (p)ppGpp in different aspects of bacterial drug resistance (i.e., tolerance, persistence, biofilms) is summarized in the figure.

1.6 Aim of the thesis

The main objective of this thesis was to identify synthetic cationic peptides (conceptually derived from host defense peptides) that exhibited broad-spectrum anti-biofilm activity, synergized with conventional antibiotics and were active *in vivo*. Finally, a major goal was to elucidate the mechanism of action that explained the broad-spectrum anti-biofilm activity of one of our lead peptides.

The identification of broad-spectrum anti-biofilm peptides was achieved by screening peptide libraries against both Gram-negative and Gram-positive bacteria (Chapters 2, 3 and 5).

To evaluate synergistic interactions between peptides and conventional antibiotics to treat biofilms, checkerboard and follow-up flow cell studies were performed (Chapters 3 and 5).

The *in vivo* anti-biofilm activity of peptides was assessed in collaboration using two different invertebrate biofilm infection models (Chapter 5).

The mechanism of action of peptide 1018 was shown to involve targeting of the stringent response mediator molecule (p)ppGpp, as revealed by using a combination of techniques (Chapter 4).

Chapter 2: Broad-spectrum inhibition of bacterial biofilm formation by a small synthetic cationic peptide

2.1 Overview

Biofilms cause up to 80% of infections and are difficult to treat due to their substantial multi-drug resistance compared to their planktonic counterparts. Based on the observation that human peptide LL-37 is able to block biofilm formation at concentrations below its minimal inhibitory concentration, we screened for small peptides with anti-biofilm activity and identified a novel synthetic cationic peptide, peptide 1037, of only 9 amino acids in length. Peptide 1037 had very weak antimicrobial activity but at $1/30^{th}$ the MIC the peptide was able to prevent biofilm formation effectively (>50% reduction in cell biomass) by the Gram-negative pathogens *Pseudomonas aeruginosa* and *Burkholderia cenocepacia* and Gram positive *Listeria monocytogenes*. In assays using a flow cell system and a widefield fluorescent microscope, 1037 was shown to significantly reduce biofilm formation and led to cell death in biofilms. Using microarray and follow-up studies it was shown that in *P. aeruginosa*, 1037 directly inhibited biofilms by reducing swimming and swarming motilities, stimulating twitching motility, and suppressing the expression of a variety of genes involved in biofilm formation (e.g. PA2204). Comparison of microarray data from cells treated with peptides LL-37 and 1037 enabled the identification of 11 common *P. aeruginosa* genes that have a role in biofilm formation and were initially proposed to represent functional targets of these peptides.

2.2 Introduction

Bacteria growing on surfaces often form biofilms, which represent a complex bacterial lifestyle adaptation that provides protection from environmental stresses (Fux et al., 2005; López et al., 2010). Indeed, it has been estimated that cells in biofilms are up to 1000-fold more resistant to most antimicrobial agents than planktonic cells (Davies, 2003). An estimated 65-80% of all bacterial infections are biofilm-related (Davies, 2003; Fux et al., 2005). In addition to increased recalcitrance, biofilms are able to evade the host defense system thus hindering treatment (Davies, 2003; Fux et al., 2005). This explains why bacteria growing in biofilms cause a variety of infections, including chronic lung, wound and ear infections (Fux et al., 2005). Biofilms are also very adept at colonizing medical devices (e.g., catheters, implants, etc.), resulting in increased hospital stays and adding more than one billion dollars

per year to hospitalization costs in the U.S.A. alone (Fux et al., 2005). Despite the importance of biofilms, limited studies have focused on the identification of compounds able to specifically target and inhibit this mode of bacterial growth (Amer et al., 2010; Johansson et al., 2008; Junker and Clardy, 2007; Kolodkin-Gal et al., 2010; Lu and Collins, 2007; Riera et al., 2010; Valle et al., 2006). Instead, research has traditionally been focused on the development of anti-infective agents capable of killing a wide range of multidrug-resistant, disease-causing planktonic bacteria.

Recently, cationic host defense peptides have been considered as potential anti-infective agents primarily due to their antimicrobial or immunomodulatory properties (Brogden, 2005; Cherkasov et al., 2009; Easton et al., 2009; Hancock and Sahl, 2006; Hilpert et al., 2005). Natural cationic peptides are 12 to 50 amino acids in length, and are amphiphilic, having 2 to 9 basic residues (R or K) and ~50% hydrophobic residues (Brogden, 2005; Hancock and Sahl, 2006). Their mechanism of action has been proposed to involve multiple targets, making them less prone to selecting for resistance compared to conventional antibiotics (Brogden, 2005; Hancock and Sahl, 2006). Thus, cationic antimicrobial peptides target the bacterial cell with low affinity through several coincident microbicidal mechanisms (Brogden, 2005; Hancock and Sahl, 2006). Bacterial biofilms have been found to be particularly resistant to cationic antibiotics possibly due to the presence in the biofilm matrix of negatively charged polymers that bind and deactivate these antibiotics (Hoffman et al., 2005; Loutet and Valvano, 2011; Otto, 2006). However, recently we made the breakthrough observation that the natural human cathelicidin peptide LL-37 is able to block *Pseudomonas aeruginosa* biofilm growth and accelerate disintegration of pre-formed biofilms (Overhage et al., 2008).

Therefore our cationic peptide libraries were screened for peptides with effective anti-biofilm activity. Here, a small (9 amino acid) cationic peptide, peptide 1037, with very weak antimicrobial activity (MIC 304 μg/mL) is shown to work against biofilms formed by diverse bacterial species. Comparative analysis of transcriptomic data allowed the identification of novel dysregulated genes that are involved in biofilm formation and were initially thought to reflect the target for this peptide in inhibiting biofilm formation.

2.3 Methods and Materials

2.3.1 Bacterial strains

Pseudomonas aeruginosa wild-type strains PA14 and PA01, *Burkholderia*

cenocepacia 4813 and the food-borne pathogen *Listeria monocytogenes* 568 were used. All mutants utilized were obtained from the *P. aeruginosa* PAO1 library (Jacobs et al., 2003).

2.3.2 Peptide Synthesis

All peptides used in this study, including peptide 1037 (KRFRIRVRV-NH_2), were synthesized by GenScript (Piscataway, NJ, USA) using solid phase Fmoc chemistry and purified to a purity of >95% using reverse phase HPLC. Peptide mass was confirmed by mass spectrometry.

2.3.3 Minimal Inhibitory Concentration (MIC)

The broth microdilution method with minor modifications for cationic peptides (Wiegand et al., 2008) was used for measuring the MIC in BM2 glucose medium [62 mM potassium phosphate buffer (pH 7), 7 mM $(NH_4)_2SO_4$, 2 mM $MgSO_4$, 10 µM $FeSO_4$, 0.4% (wt/vol) glucose]. Peptides were dissolved in water and stored in glass vials and MIC assays were performed in sterile 96-well polypropylene microtitre plates (Cat. No. 3790, COSTAR). Peptides were added to the plate at the desired concentrations and the bacteria were inoculated to a final concentration of 5 x 10^5 CFU/mL per well. The plates were incubated at 37°C for 24 and 48 hours. The MIC was defined as the lowest concentration of peptide at which no growth was observed.

2.3.4 Growth curves

All strains used in this study were grown overnight in BM2 swarming medium (62 mM potassium phosphate buffer, [pH 7], 2 mM $MgSO_4$, 10 µM $FeSO_4$, 0.4% [wt/vol] glucose, 0.1% or 0.5% [wt/vol] Casamino Acids). If necessary, cultures were diluted to obtain equal optical densities. Five-µl portions of these cultures were added to 195 µl of fresh swarming medium in 96-well microtitre plates. The growth of these cultures at 37°C under shaking conditions was monitored with a TECAN Spectrofluor Plus by determining the absorbance at 620 nm every 20 min for 24 h. Two independent experiments were performed.

2.3.5 Biofilm assays

Biofilm formation was initially analyzed using a static abiotic solid surface assay as described elsewhere (Overhage et al., 2008). Dilutions (1/100) of overnight cultures were incubated in BM2 biofilm-adjusted medium [62 mM potassium phosphate buffer (pH 7), 7 mM $(NH_4)_2SO_4$, 2 mM $MgSO_4$, 10 µM $FeSO_4$, 0.4% (wt/vol) glucose, 0.5% (wt/vol) Casamino

Acids] in polypropylene microtitre plates (Falcon, United States) in the presence of peptide 1037 for 22 h at 37°C. Planktonic cells were removed, biofilm cells adhering to the side of the tubes were stained with crystal violet, and absorbance at 595 nm (600 nm for *L. monocytogenes*) was measured using a microtitre plate reader (Bio-Tek Instruments Inc., United States). *Listeria* biofilms were grown in Trypic soy broth (TSB) medium under shaking conditions (200 rpm) with medium replacement every 24 h for a total of 72 h. Peptide 1037 was added at time zero (prior to adding the diluted, overnight cultures) in varying concentrations, and the decrease in biofilm formation was recorded at 22 h for *Pseudomonas* and *Burkholderia* and at 72 h for *Listeria*.

2.3.6 Biofilm cultivation in flow chambers and microscopy

Biofilms were cultivated for 72 h in the presence of 20 μg/mL of peptide 1037 at 37°C in flow chambers with channel dimensions of 1 x 4 x 40 mm, with minor modifications to a previously described protocol (Yang et al., 2009). Silicone tubing (VWR, .062 ID x .125 OD x .032 wall) was autoclaved and the system was assembled and sterilized by pumping a 0.5% hypochlorite solution through the system at 6 rpm for 1 hour using a Watson Marlow 205S peristaltic pump. The system was then rinsed at 6 rpm with sterile water and medium for 30 min each. Flow chambers were inoculated by injecting 400 μl of mid-log culture diluted to an OD_{600} of 0.02 with a syringe. After inoculation, chambers were left without flow for 2 h after which medium was pumped though the system at a constant rate of 0.75 rpm (3.6 ml/h). Microscopy was done with a Leica DMI 4000 B widefield fluorescence microscope equipped with filter sets for monitoring of green (Ex 490/20, Em 525/36) and red (Ex 555/25, Em 605/52) fluorescence, using the Quorum Angstrom Optigrid (MetaMorph) acquisition software. Images were obtained with a 63 × 1.4 objective. Deconvolution was done with Huygens Essential (Scientific Volume Imaging B.V.) and 3D reconstructions were generated using the Imaris software package (Bitplane AG).

2.3.7 Swarming assays

Swarming experiments were performed on BM2 swarming agar plates (62 mM potassium phosphate buffer [pH 7], 2 mM $MgSO_4$, 10 μM $FeSO_4$, 0.4% [wt/vol] glucose, 0.1% [wt/vol] Casamino Acids (0.5% Casamino Acids for PA01), 0.5% [wt/vol] Difco agar), supplemented with different concentrations of peptide 1037 or controls. One μl aliquots of

mid-log-phase (i.e., OD_{600} of 0.4-0.6) cultures grown in BM2 glucose minimal medium were inoculated in 6-well plates. Each experiment was carried out three times with at least three replicates for each bacterial strain. All resulting dendritic colonies were analyzed by measuring the surface coverage on agar plates after 15 h of incubation at 37°C using Image J software. In the case of PAO1, due to its rounded swarming colony appearance, the swarming area was evaluated by measuring the diameter of the swarming colony.

2.3.8 Swimming and twitching motility assays

For swimming assays, LB medium plates with 0.3% (wt/vol) agar were used. One-µl aliquots of mid-log-phase cultures grown in LB broth were inoculated onto 6-well plates containing 10 ml LB (0.3% agar) and supplemented with increasing concentrations of peptide 1037. The diameters of the swimming zones were measured after incubation for 15 h at 37°C. Twitching was assessed as described previously (Overhage et al., 2008). Briefly 6-well plates containing 10 ml of LB medium supplemented with 1% (wt/vol) agar and increasing concentrations of peptide 1037, were inoculated by a toothpick stabbed through the agar to the agar:plastic interface, with one-µl of mid-log-phase cultures grown in LB broth. Twitching motility was determined by measuring the diameters of the twitching zones after 24 h of incubation. For both swimming and twitching assays, at least three independent experiments were performed.

2.3.9 DNA microarray experiment

P. aeruginosa PAO1 was grown on glass plates in the presence (20 µg/mL) or absence of peptide 1037. After 24 hours of incubation at 37 °C and shaking conditions, planktonic cells were washed off and biofilm cells were scraped from the glass surface. Once the cells were harvested, RNA isolation, cDNA synthesis, hybridization to microarray slides (The Institute for Genomic Research [TIGR], Pathogenic Functional Genomics Resource Center), and the analysis of DNA microarray slides using ArrayPipe version 1.7 were performed as previously described (Overhage et al., 2008). Only genes that exhibited a change, compared to the results for the untreated control, of two-fold or more with a P value of ≤0.05 were considered in this study. The microarray data were deposited in MIAME Express under accession number E-MTAB-962.

2.4 Results

2.4.1 Synthetic peptide screen

P. aeruginosa is one of the three leading causes of infections in hospitalized patients and is responsible for around 180,000 infections per year in North America (Hancock and Speert, 2000). This opportunistic human pathogen is also the most prevalent pathogen in patients with cystic fibrosis (CF), the most common eventually fatal recessive genetic disease in the Caucasian population (Breidenstein et al., 2011; Moureau-Marquis et al., 2008; Singh et al., 2000), and in this context commonly forms biofilms. The demonstrated ability of cationic peptide LL-37 to inhibit *P. aeruginosa* biofilms (Overhage et al., 2008) encouraged the design of new, improved anti-biofilm peptides. One of the main objectives was to minimize the size of the peptides, while conserving their anti-biofilm activity. We reasoned that smaller peptides would be less expensive to produce and that a reduction in the number of amino acids would allow for a more comprehensive understanding of the optimal amino acid sequence responsible for anti-biofilm activity. Therefore, we randomly selected around 50 peptides from previous libraries based loosely on the weakly active bovine peptide Bac2A, with the same size and similar overall amino acid compositions. Peptide Bac2A was developed to investigate antimicrobial activity against planktonic bacteria (Cherkasov et al., 2009), selecting both active and inactive peptides in this study. More than 50 derivatives were tested in 96-well plate biofilm assays, and 14 were found to have anti-biofilm activity with some peptides being able to inhibit biofilm formation by 45-65%. One of the best of these was HH15 (Table 2.1), a peptide with modest antimicrobial activity (Table 2.1).

Around 15 other peptides were then designed and synthesized with sequence or thematic similarity to HH15. Several had anti-biofilm activity including two, 1037 and 1029, which were only 9 amino acids in length. A 7-amino acid consensus sequence was apparent in the 5 best anti-biofilm peptides (Table 2.1) although we did not rigorously explore this consensus sequence. Peptide 1026 with an F3W change in the third residue to another aromatic amino acid retained good anti-biofilm activity, but peptide HH10 with an R8A change completely lost anti-biofilm activity as did HH2, HH7 and HH8 with this same change (in addition to an F3L change). Collectively these data are consistent with the possibility that the Arg residue in position 6 of the consensus is important for the anti-biofilm activity of these peptides.

Peptide 1037 that lacked only the last 3 amino acids of HH15 had a very high MIC (304 μg/mL) (Table 2.2), but paradoxically demonstrated the most potent decrease in biofilm mass (78% decrease) at lower concentrations (1/2 MIC) (Table 2.1). Substitution of Arg at position 2 with Gln in peptide 1029 led to a substantial improvement in MIC but a decrease in anti-biofilm activity, indicating that biofilm and antimicrobial activities were independent as confirmed by a number of peptides, including HH10, with good antimicrobial activity but no or minimal anti-biofilm activity (Table 2.1). Due to its small size and apparent selective potency towards biofilms, peptide 1037 was selected for further studies.

Table 2.1. Screening of peptide library. Example peptides.

Peptide	Amino acid sequence	MIC μg/mL	Biofilm Inhibition at ½ MIC (%)
LL-37	LLGDFFRKSKEKIGKEFKRIVQRIKDFLRNLVPRTES	31	57
Bac2a	RLARIVVIRVAR	50	0
HH15	KR**FRIRVRV**IRK	12	45
1026	VQW**RIRVRV**IKK	5	54
1029	KQ**FRIRVRV**	10	40
1036	VQ**FRIRVR**IVIRK	10	43
1037	KR**FRIRVRV**	304	**78**
Consensus	**FRIRVRV**		
HH2	VQL**RIRV**A**V**IRA	50	0
1002	VQRWLIVWRIRK	5	0
1003	IVWKIKRWWVGR	20	15
1004	RFWKVRVKYIRF	5	15
1008	RIKWIVRFR	20	0
HH7	VRL**RIRV**A**V**RRA	12	0
1010	IRW**RIRV**W**V**RRI	0	0
1011	RRWVVWRIVQRR	20	20
1012	IFW**R**RI**V**I**V**KKF	20	0
1013	VRL**RIRV**A	10	24
1016	LRIRWIFKR	20	30
HH8	VRL**RIRV**A**V**IRK	8	0
1020	VRL**RIR**WW**V**LRK	3	22
HH10	KR**FRIRV**A**V**RRA	0.8	0
1035	KRWRWIVRNIRR	40	15
1031	WRW**R**V**RV**W**R**	2.5	22

Table 2.2. Peptide 1037 MIC determination. Antimicrob. Agents Chemother, 56, 2012, 2696-704, doi: 10.1128/AAC.00064-12.

Bacterial strains	**MIC (µg/mL)**
PAO1	304 µg/mL
PA14	304 µg/mL
B. cenocepacia 4813	>608 µg/mL
L. monocytogenes LM568	25 µg/mL

2.4.2 Sub-inhibitory concentrations of 1037 inhibited bacterial biofilm formation in a broad-spectrum manner

Anti-biofilm activity was confirmed using static abiotic solid-surface assays (SSA) in which *P. aeruginosa* growing as biofilms was treated with increasing concentrations of peptide 1037 (Figure 2.1). As little as 10 µg/ml of peptide inhibited biofilm formation by ~50%. To determine whether the inhibitory effect on biofilm development was related to general growth inhibition or to a change in the bacterial growth rate, growth was measured in BM2 glucose biofilm-adjusted medium treated with increasing concentrations of peptide 1037 under shaking conditions at 37°C. These experiments underlined the specific inhibitory effect of peptide 1037 on biofilms, since sub-MIC levels of the peptide did not affect the planktonic growth of *P. aeruginosa* (data not shown).

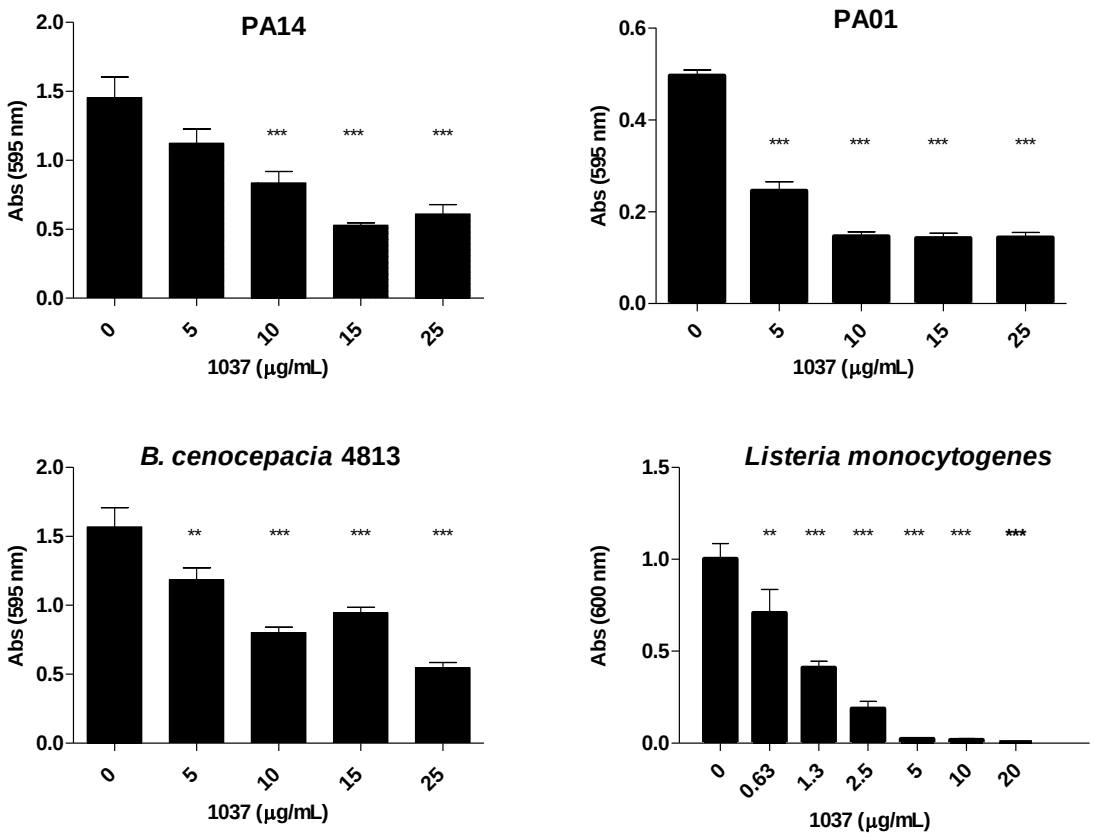

Figure 2.1. Dose dependent anti-biofilm effect of peptide 1037 on Gram-negative and Gram positive bacteria. Different bacterial strains were grown under biofilm conditions in the presence of 1037. After growth at 37°C for 22 h, biofilm growth was assessed by crystal violet staining and quantified at 595 nm. All experiments were done at least 3 times and statistical significance was determined using one-way ANOVA to compare the means between the untreated and treated groups (where ns reflects $p>0.05$, * $p<0.05$, ** $p<0.01$, and *** $p<0.001$). Copyright © American Society for Microbiology, Antimicrob. Agents Chemother, 56, 2012, 2696-704, doi: 10.1128/AAC.00064-12.

To further evaluate and confirm the anti-biofilm properties of the peptide, a more sophisticated flow chamber biofilm model based on a flow cell system and microscopy was employed. When biofilm cells of either PAO1 or PA14 were treated with sub-lethal concentrations of the peptide (20 µg/mL; 1/15 MIC), biofilm formation was clearly repressed with a strong decrease in the height of biofilms (Figure 2.2). Strikingly, treated samples demonstrated a moderate increase in the number of dead biofilm cells indicating that levels of 1037 that were more than 15-fold below the planktonic MIC were able to lead to the death of biofilm cells (Figure 2.2).

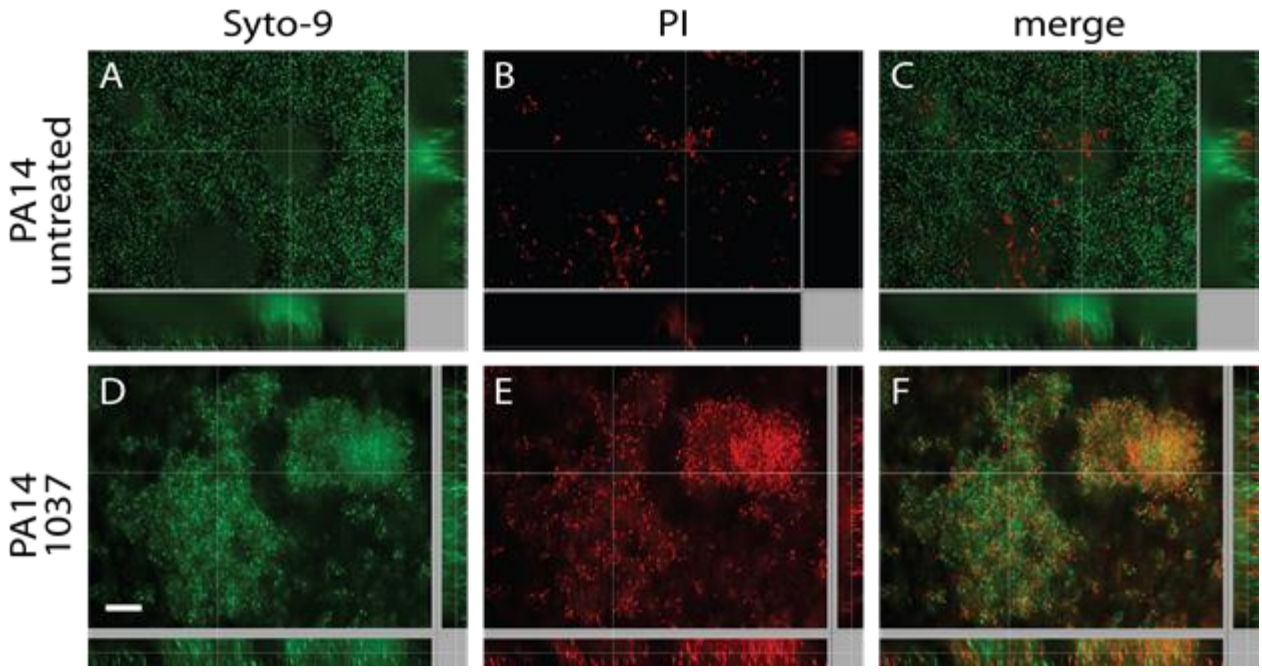

Figure 2.2. Flow cell analysis of *P. aeruginosa* PA14 biofilm formation in the absence and presence of 20 µg/mL of peptide 1037. *P. aeruginosa* biofilms were cultivated in minimal medium for 72 hours in the presence of 20 µg/mL of 1037 peptide at 37°C in flow chambers. Biofilms were stained and visualized using SYTO-9 to stain live biofilm cells green and propidium iodide, a normally cell impermeable stain, to stain dead cells red and examined by widefield fluorescent microscopy. The scale bar represents 15 µm in length and each panel shows xy, yz and xz dimensions. A-C. PA14 biofilm untreated. Images correspond to (A) PA14 biofilm stained with SYTO-9, (B) PA14 biofilm stained with propidium iodide, (C) merged image. D-F. PA14 biofilm treated with 20 µg/mL of peptide 1037. Images correspond to (D) PA14 biofilm stained with SYTO-9, (E) PA14 biofilm stained with propidium iodide and (F) merged image. Copyright © American Society for Microbiology, Antimicrob. Agents Chemother, 56, 2012, 2696-704, doi: 10.1128/AAC.00064-12.

To determine whether the anti-biofilm action of peptide 1037 was broad-spectrum, we evaluated its activity on static biofilm cultures of *B. cenocepacia*, and the Gram positive pathogen *L. monocytogenes*. *B. cenocepacia*, a prominent CF pathogen, can cause chronic infections (in a biofilm growth mode) as well as cepacia syndrome, a fatal pneumonia accompanied by septicemia (Loutet and Valvano, 2010). It was selected as it is notoriously resistant to the killing action of antimicrobial peptides (Moore and Hancock, 1986). *L. monocytogenes* is a ubiquitous, intracellular pathogen that causes foodborne disease and deadly listeriosis (Freitag et al., 2009), and whose biofilm mode of growth is thought to be involved in its persistence in the environment and foods. Treatment with peptide 1037 resulted in a substantial reduction in biofilm growth in both organisms (Figure 2.1). In particular,

Listeria biofilm formation was reduced by as little as 0.63 μg/ml, while 5 μg/ml caused complete inhibition of biofilm organisms even though 20 μg/ml caused no inhibition of planktonic cells (data not shown).

2.4.3 Transcriptome determination

To obtain insight into the molecular mechanism(s) by which peptide 1037 inhibits bacterial biofilms, we evaluated the effect of the peptide on gene expression of *P. aeruginosa* PAO1 biofilms. For this, we used microarray technology to analyze the global gene expression of biofilms grown in the presence and absence of peptide 1037. A total of 398 genes (selected genes are shown in Table 2.3) were shown to be significantly dysregulated ($P < 0.05$ by Student's *t* test) by at least 2-fold in the presence of peptide 1037. Of these, 138 were down-regulated and 260 were up-regulated. Genes were selected and further analyzed based on their involvement in biofilm-related processes that would likely impact on biofilm formation (Table 2.3).

Table 2.3. Selected *P. aeruginosa* genes dysregulated by peptide 1037 in biofilms.

Probe ID	Gene	Protein	Fold Change	P value
Flagella				
PA1077	*flgB*	flagellar basal-body rod protein FlgB	-3.84	5E-08
PA1078	*flgC*	flagellar basal-body rod protein FlgC	-2.19	0.0002
PA1079	*flgD*	flagellar basal-body rod modification protein	-2.52	0.0002
PA1081	*flgF*	flagellar basal-body rod protein FlgF	-2.27	0.01
Chemotaxis				
PA4953	*motB*	chemotaxis protein MotB	6.06	0.003
PA0176	*aer2*	aerotaxis transducer Aer2	3.64	0.03
PA1608	PA1608	probable chemotaxis transducer	8.05	0.0005
PA2788	PA2788	probable chemotaxis transducer	2.28	0.05
PA3704	*wspE*	probable chemotaxis sensor/effector fusion	4.85	0.008
Anaerobic growth				
PA0519	*nirS*	nitrite reductase precursor	-3.56	0.004
PA0523	*norC*	nitric-oxide reductase subunit C	-11.51	5E-08
PA3392	*nosZ*	nitrous-oxide reductase precursor	-4.71	0.01
Others				
PA4959	*fimX*	type IV pilus Assembly	5.49	0.004
PA3361	*lecB*	fucose-binding lectin PA-IIL	-4.79	0.007

Probe ID	Gene	Protein	Fold Change	P value
PA4479	*mreD*	rod shape-determining protein MreD	4.43	0.007
PA5053	*hslV*	heat shock protein HslV	11.84	4E-05
PA3478	*rhlB*	rhamnosyltransferase chain B	-3.45	0.005
PA4230	*pchB*	salicylate biosynthesis protein PchB	-2.64	0.03
PA4228	*pchD*	pyochelin biosynthesis protein PchD	-2.88	0.001
PA4226	*pchE*	dihydroaeruginoic acid synthetase	-2.70	0.03
PA1202	PA1202	probable hydrolase	-2.41	0.026
PA2145	PA2145	hypothetical protein	-3.28	0.047
PA2204	PA2204	probable binding protein of ABC transporter	-3.58	0.0023
PA2330	PA2330	hypothetical protein	-3.93	0.035
PA2781	PA2781	hypothetical protein	-2.17	0.038
PA3369	PA3369	hypothetical protein	-7.93	2.5E-08
PA4739	PA4739	hypothetical protein	-5.31	2E-07
PA0267	PA0267	hypothetical protein	3.57	0.033
PA3234	*actP*	probable sodium:solute symporter	2.73	0.0164
PA3903	*prfC*	peptide chain release factor 3	8.57	0.0003
PA4454	PA4454	hypothetical protein	4.77	0.009

2.4.4 Inhibition of swimming and swarming motility and stimulation of twitching motility

Flagella are known to be involved in swimming motility and play a role in biofilm formation and swarming motility (Breidenstein et al., 2011; Fux et al., 2005; Köhler et al., 2000; López et al., 2010). Interestingly, several genes related to flagella were down-regulated by two- to three-fold in the presence of peptide 1037 (Table 2.3). In contrast, chemotaxis genes were up-regulated by up to eight-fold (Table 2.3). Genes associated with denitrification (i.e., anaerobic respiration; Sauer et al., 2002; Yoon et al., 2002) were found to be down-regulated by up to 11-fold in the treated samples.

To further validate the microarray results, the effect of peptide 1037 on processes related to biofilm formation (i.e., swimming, swarming and twitching motilities) was determined. Peptide 1037 reduced flagella-dependent swimming motility in a broad-spectrum fashion, affecting this type of motility in PA14, PAO1 and *B. cenocepacia* 4813 (Figure 2.3). These results were particularly interesting since flagella play a role both in biofilm formation and swarming motility. Swarming motility, which like biofilm formation is a complex adaptation dependent on flagellin and quorum sensing (but otherwise quite distinct), was

significantly and nearly completely knocked-down ($p<0.001$ by one-way ANOVA) by the action of 1037 in both *P. aeruginosa* and *Burkholderia* (Figure 2.4).

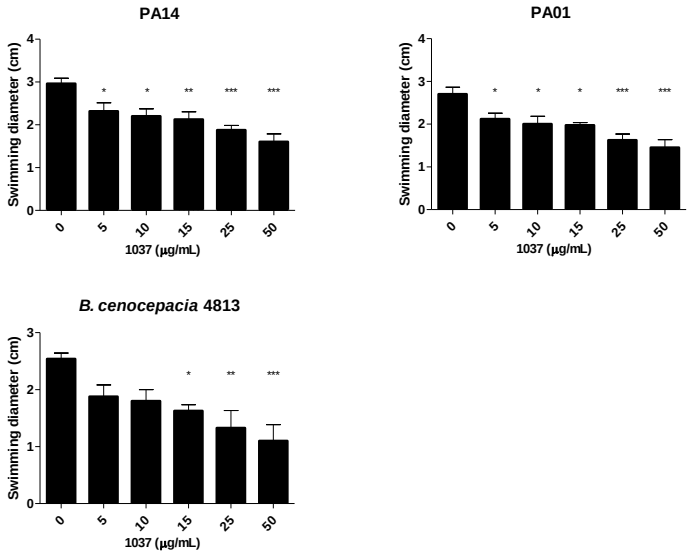

Figure 2.3. Swimming motility in the presence of peptide 1037. Swimming motility was evaluated on LB plates containing 0.3 % (w/v) agar and different concentrations of peptide 1037. The diameters (in cm) of the swim zones were measured after incubation for 20 h at 37°C. All experiments were done at least 3 times and statistical significance was determined using one-way ANOVA (where ns reflects $p>0.05$, * $p<0.05$, ** $p<0.01$, and *** $p<0.001$). Copyright © American Society for Microbiology, Antimicrob. Agents Chemother, 56, 2012, 2696-704, doi: 10.1128/AAC.00064-12.

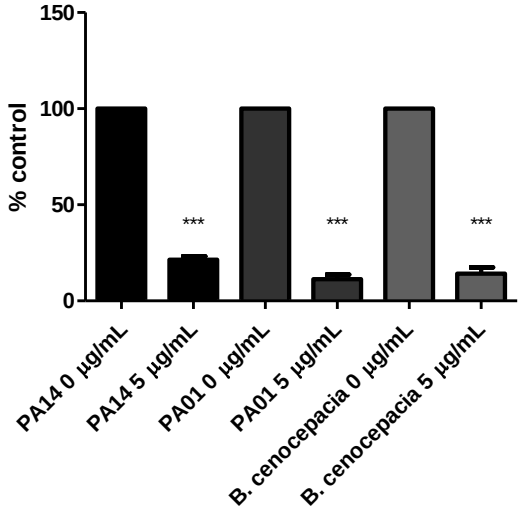

Figure 2.4. Bacterial swarming in the presence of peptide 1037. Swarming was examined on BM2-swarm plates containing 0.5 % (w/v) agar (Difco) after incubation for 20 h at 37°C. Swarming colonies were quantified as described in the Methods and materials section. All experiments were done at least 3 times and statistical significance was determined using one-

way ANOVA (where *** indicates P<0.001). Copyright © American Society for Microbiology, Antimicrob. Agents Chemother, 56, 2012, 2696-704, doi: 10.1128/AAC.00064-12.

Pilus-mediated twitching motility involves the movement of *Pseudomonas* on solid surfaces. Twitching motility has been shown to be involved in the disassembly of biofilm structures (Picioreanu et al., 2007; Singh et al., 2002). Array results demonstrated that a gene required for twitching motility (*fimX;* Kazmierczak et al., 2006) was up-regulated by more than 5-fold. Consistent with this result, sub-MIC concentrations of peptide 1037 significantly ($p<0.05$ by one-way ANOVA) enhanced twitching motility by about 45% (Figure 2.5).

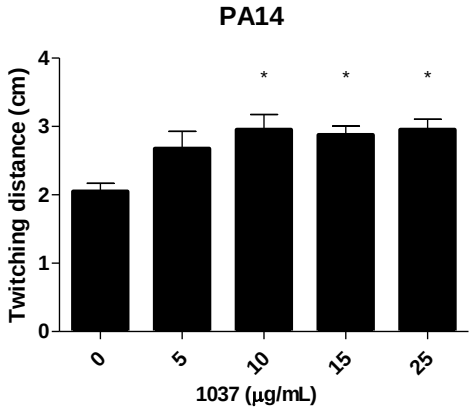

Figure 2.5. Twitching motility of *P. aeruginosa* PA14 in the presence of peptide 1037. *P. aeruginosa* cells were spot inoculated on LB plates with 1% (wt/vol) agar and increasing concentrations of peptide 1037. Twitching motility was determined by measuring the diameter of the twitching zones after 24 hours of incubation at 37ºC. Four independent experiments were performed and statistical significance was determined using one-way ANOVA (* indicates $p<0.05$). Copyright © American Society for Microbiology, Antimicrob. Agents Chemother, 56, 2012, 2696-704, doi: 10.1128/AAC.00064-12.

2.4.5 Screening of genes dysregulated by the action of cationic peptides LL-37 and 1037

Since peptide 1037, like LL-37, is a cationic amphipathic peptide with anti-biofilm activity, we wondered whether these peptides inhibited biofilms using similar mechanisms. We therefore compared microarrays evaluating the effects on *P. aeruginosa* biofilms of LL-37 (Overhage et al., 2008) and peptide 1037 (de la Fuente-Núñez et al., 2012). A common set of 14 genes, out of more than 400 dysregulated, was found to be dysregulated in biofilms treated with either peptide, including 10 down-regulated genes and 4 up-regulated genes (Figure 2.6). To assess the involvement of these genes in biofilm formation, transposon mutants in each gene were grown in static biofilm cultures. Among the down-regulated genes,

mutants in all but one (PA2781) exhibited varying deficiencies in biofilm formation by 13-83% (Figure 2.6A). Prominent biofilm deficiency phenotypes were found for mutants in the nitrogen metabolism gene PA0519 (*nirS*), the flagella gene *flgB* (PA1077) and, particularly in a gene predicted to be a probable ABC transporter binding protein (PA2204). Mutants corresponding to the up-regulated genes were also grown in static cultures to determine their biofilm phenotypes. Two mutants demonstrated significantly increased biomass (PA3234 and PA4454) when compared to the wild-type strain (Figure 2.6B).

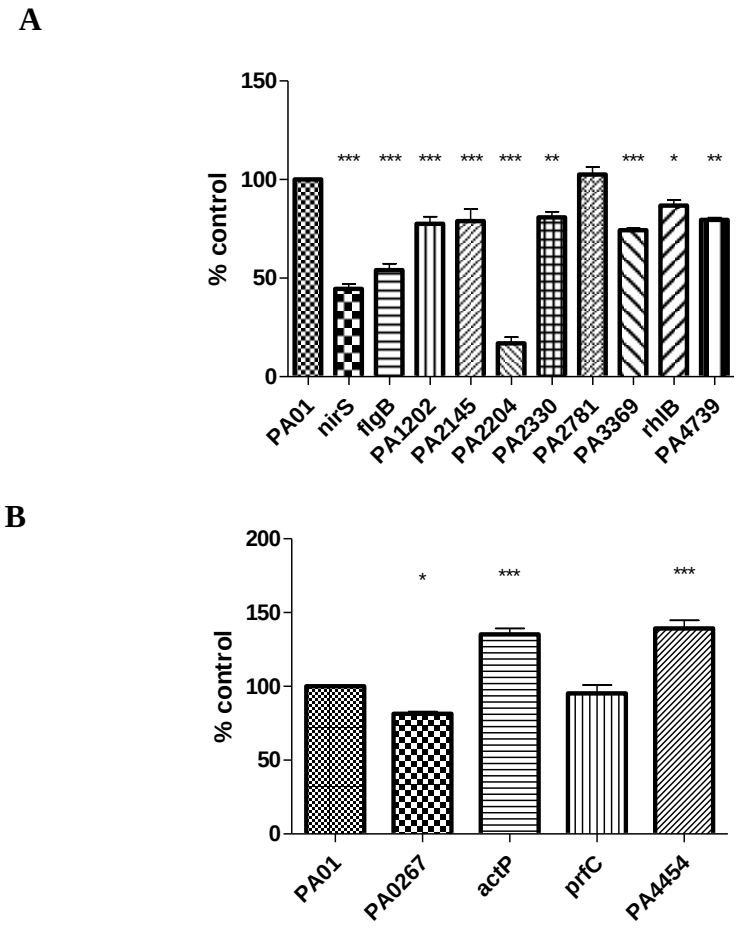

Figure 2.6. Mechanism of action of anti-biofilm activity: Comparison of the LL-37 and 1037 microarrays. Biofilm formation by mutants of genes (A) down-regulated by both LL-37 and 1037 and (B) up-regulated by both peptides. Transposon mutants corresponding to genes dysregulated in biofilm cells by the action of both LL-37 and 1037 were grown in polypropylene microtitre plates at 37°C for 22 h and residual biofilm formation assessed by crystal violet staining All experiments were done at least 3 times and statistical significance was determined using one-way ANOVA (where ns reflects $P>0.05$, * $P<0.05$, ** $P<0.01$, and

*** P<0.001). Copyright © American Society for Microbiology, Antimicrob. Agents Chemother, 56, 2012, 2696-704, doi: 10.1128/AAC.00064-12.

2.5 Discussion

The objective of the experiments presented in this Chapter was to identify a very short peptide with good anti-biofilm activity. Here we identified a novel 9 amino acid peptide, 1037, capable of knocking down bacterial biofilms. By comparing the primary structures of a series of peptides that exhibited reasonable anti-biofilm activity (Table 2.1), a consensus amphipathic sequence (FRIRVRV) was identified, with 3 cationic residues (i.e., R) and 4 hydrophobic amino acids, analogous to host defense peptides.

Interestingly, peptide 1037, one of the smallest peptides that we designed, was found to have the most potent anti-biofilm activity (Table 2.1). Indeed, levels of peptide 1037 more than 30-fold lower than the MIC for planktonic cells were able to significantly reduce biofilm formation in both Gram-negative (*P. aeruginosa*, *B. cenocepacia*) and Gram positive (*L. monocytogenes)* bacteria (Table 2.2; Figure 2.1).

Intriguingly peptide 1037, as well as altering the thickness and morphology of biofilms, led to a decreased number of biofilm cells of *P. aeruginosa* (Figure 2.2) even though, paradoxically, it failed to show significant direct antimicrobial activity against planktonic cells (Table 2.2). This indicates that the peptide is able to trigger uptake of a normally impermeable stain propidium iodide (usually interpreted as cell death), or released DNA to which it binds, by acting on a target that is either selectively expressed in biofilm cells, or is under-expressed and thus more susceptible to inhibition. Both Figure 2.6 and a previous report (Overhage et al, 2008) present a large number of candidate genes, but given the penchant of the antimicrobial peptides to demonstrate multiple targets, including cell membranes, cell wall biosynthesis, RNA, protein and DNA synthesis, cell division, autolytic enzymes, and inhibition of particular enzymes (Hancock and Sahl, 2006), it seemed likely that such a mechanism would be quite complex. The lack of large amounts of propidium iodide staining DNA outside the biofilm cells suggested that the peptide might not be inducing cell lysis, but rather might be compromising the cytoplasmic membrane, as indicated by the presence of propidium iodide inside a subset of the cells (Figure 2.2).

Cationic peptides are known to be able to freely translocate into cells (Hancock and Sahl, 2006; Powers et al., 2006), bind to DNA in a sequence-specific manner (He and

Furmanski, 1995) and alter directly gene expression (current study and Overhage et al, 2008). Microarray technology and *in vitro* assays demonstrate here that very low concentrations of 1037 affect the development of biofilms in a variety of ways. First, flagella-dependent swimming motility was reduced in a concentration-dependent manner (Figure 2.3). Inhibition of swimming motility might limit the number of bacterial cells reaching the surface, therefore decreasing biofilm formation (Breidenstein et al., 2011; Köhler et al., 2000; López et al., 2010). Second, peptide 1037 potently inhibited bacterial swarming (Figure 2.4), which is known (in a nutritionally conditional fashion) to impact on (Shrout et al., 2006), and share regulatory relationships with (Breidenstein et al., 2011), biofilm formation. As swarming cells are thought to be relevant to growth on mucosal surfaces and demonstrate increased resistance to antimicrobial agents and overproduction of virulence factors (Butler et al., 2010; Overhage et al., 2008), the anti-swarming effect of peptide 1037 might contribute to its potential therapeutic value. Importantly, the modest anti-swimming and potent anti-swarming properties of peptide 1037 were not observed with LL-37 (C. de la Fuente-Núñez, unpublished observations). Third, peptide 1037 was found to stimulate twitching motility (Figure 2.5), a type of surface motility that promotes the disassembly of biofilm structures (Picioreanu et al., 2007; Singh et al, 2000).

As expected, flagellar genes were down-regulated, as were genes (*nirS*, *norC* and *nosZ*) known to play a role in anaerobic biofilm developmental processes by encoding proteins involved in anaerobic respiration (Sauer et al., 2002; Yoon et al., 2002). Other down-regulated genes involved in biofilm formation included the quorum sensing-regulated gene *rhlB*, which is involved in rhamnolipid production (Overhage, Bains et al., 2008), and the fucose-binding lectin gene *lecB*, which is required for biofilm formation (Johansson et al., 2008).

Since LL-37 served as a general model for the design of peptides culminating in peptide 1037, we questioned whether these peptides inhibited biofilms in a similar manner. To answer this question, the impact of peptide 1037 on bacterial global gene expression was compared with results previously reported by our lab using LL-37 (Overhage et al., 2008). LL-37 causes up-regulation of 311 genes and down-regulation of 475 genes, while 1037 was found to induce the expression of 260 genes, repressing 138. However, only 10 genes were found to be commonly down-regulated by both peptides (Figure 2.6A). Transposon mutants corresponding to each gene were utilized to evaluate the potential impact of decreased expression of these 10 genes on biofilm formation. All but one of these mutants led to significant reductions in biofilm

formation (Figure 2.6A). Three mutants led to more substantial biofilm deficiencies: a *nirS* mutant, consistent with a role for anaerobic respiration in biofilm development (Sauer et al., 2002; Yoon et al., 2002), the *flgB* mutant in the flagella basal body, and a gene encoding the unknown ABC periplasmic transporter gene (PA2204).

On the other hand, 4 genes were up-regulated by both LL-37 and 1037 (Figure 2.6B). In this case, two mutants (PA3234 and PA4454) grew significantly more biofilm than the control consistent with a role for these proteins in suppression of biofilm formation. Indeed, a previous study showed that PA3234, a probable sodium:solute symporter, was repressed in biofilms (Whiteley et al., 2001). Moreover, expression of the ABC superfamily gene *yrbD* (PA4454) is known to increase gradually during biofilm formation (Ito et al., 2009). Interestingly, PA4454 was also found to be up-regulated in a biofilm-deficient *phoQ* mutant (Gooderham et al., 2009). Taken together, our results indicate that LL-37 and peptide 1037 induce the dysregulation of relatively few common genes, possibly implying that these dysregulated genes likely play an active role in biofilm development that is antagonized by their dysregulation by peptide 1037.

In conclusion, we have demonstrated a small peptide, peptide 1037 that improves on the previously described anti-biofilm activity of its predecessor (LL-37), and additionally is able to inhibit another complex adaptation, swarming motility. Despite its conceptual similarity to antimicrobial peptides, the biological properties of peptide 1037, confirmed by results for other peptides, clearly demonstrated that direct antimicrobial activity and anti-biofilm activity are separately determined. Peptide 1037 exhibited very weak activity against planktonic bacteria, and inhibited biofilm production even in *Burkholderia* that is completely resistant when growing planktonically, to all cationic peptides and polymyxin B. In the process of library screening we identified a consensus sequence (FRIRVRV) present in several peptides with anti-biofilm activity that will serve as a basis for iterative design of improved peptides. Small cationic peptides that simultaneously target biofilms and swarming while retaining either direct antimicrobial or immunomodulatory activities might provide the basis for a new generation of anti-infective agents. Alternatively, the combination of peptide 1037 plus a second agent with antimicrobial properties might also provide a good therapeutic strategy.

2.6 Summary

This chapter shows the ability of a very short peptide (9 amino acids) termed peptide 1037 to prevent biofilm formation in both Gram-negative and Gram-positive bacteria. In flow cell experiments, peptide 1037 substantially reduced biofilm formation and led to cell death of *P aeruginosa* biofilms. Furthermore, peptide 1037 affected biofilm-associated cellular processes in *P. aeruginosa* such as swimming, swarming and twitching motilities and suppressed the expression of genes involved in biofilm formation (e.g. PA2204). Comparison of microarray data from cells treated with peptides LL-37 and 1037 enabled the identification of 11 common *P. aeruginosa* genes that have a role in biofilm formation and are proposed to represent functional targets of these peptides.

Chapter 3: Peptide 1018 as a potent broad-spectrum anti-biofilm agent that enhanced antibiotic action against bacterial biofilms

3.1 Overview

Bacteria form multicellular communities known as biofilms that cause two thirds of all infections and demonstrate a 10- to 1000- fold increase in adaptive resistance to conventional antibiotics. Currently, there are no approved drugs that specifically target bacterial biofilms. In this chapter, peptide 1018 was identified and characterized as a potent broad-spectrum anti-biofilm agent. At concentrations that did not affect planktonic growth, peptide treatment completely prevented biofilm formation and led to the eradication of mature biofilms in representative strains of both Gram-negative and Gram-positive bacterial pathogens including *Pseudomonas aeruginosa*, *Escherichia coli*, *Acinetobacter baumannii*, *Klebsiella pneumoniae*, methicillin- resistant *Staphylococcus aureus*, *Salmonella* Typhimurium and *Burkholderia cenocepacia*. Low levels of the peptide led to biofilm dispersal, while higher doses triggered biofilm cell death. Further, peptide 1018 demonstrated synergistic interactions with various classes of antibiotics, to potently prevent and eradicate bacterial biofilms formed by multidrug-resistant "ESKAPE" pathogens. Combinations of peptide 1018 and antibiotics ceftazidime, ciprofloxacin, imipenem, or tobramycin were synergistic in 50% of assessments, and decreased, by 2- to 64-fold, the concentration of antibiotic required to treat biofilms formed by *Pseudomonas aeruginosa, Escherichia coli, Acinetobacter baumannii, Klebsiella pneumoniae, Salmonella enterica* and methicillin-resistant *Staphylococcus aureus*. Furthermore, in flow cell biofilm studies, combinations of low, sub-inhibitory levels of the peptide (0.8 μg/ml) and ciprofloxacin (40 ng/ml) decreased dispersal and triggered cell death in mature *P. aeruginosa* biofilms. In addition, short-term treatments with the peptide in combination with ciprofloxacin prevented biofilm formation and reduced pre-existing biofilms of *P. aeruginosa* PA14. Thus this peptide provides a new strategy for potentiating antibiotic activity against biofilms formed by multidrug-resistant pathogens.

3.2 Introduction

As described above, biofilms are structured multicellular communities of microorganisms associated with surfaces. They cause at least 65% of all human infections, and represent a major health problem worldwide due to their resistance to host defence mechanisms

and to conventional antimicrobials, which generally target free-swimming (planktonic) bacteria (Costerton et al., 1999; de la Fuente-Núñez et al., 2013). Thus, there is an urgent need to identify compounds that effectively clear biofilm-related infections alone or in combination with conventional antibiotics.

In Chapter 2, synthetic cationic peptides conceptually derived from natural host defence peptides such as the human cathelicidin LL-37 and the bovine peptide indolicidin (Overhage et al., 2008), were identified as biofilm inhibitory compounds. It was demonstrated that anti-biofilm peptides, although similar to cationic antimicrobial peptides (that are active against planktonic bacteria) in comprising both cationic and hydrophobic amino acids (de la Fuente-Núñez et al., 2012), have substantially different structure-activity relationships. Thus, in Chapter 2 I described peptides with good anti-biofilm but virtually no activity vs. planktonic bacteria (i.e., very high MIC values), and *vice versa*; similarly these peptides inhibited *B. cepacia* in the biofilm form despite the complete resistance of this species to cationic peptides (Moore and Hancock, 1986; Scott et al., 1999).

Here, synthetic peptide 1018, previously characterized as an immunomodulatory peptide (Achtman et al., 2012; Wieczorek et al., 2010) with weak direct antimicrobial activity was identified as a relatively potent broad-spectrum anti-biofilm peptide that prevented biofilm formation and eradicated existing biofilms formed by 4 of the so-called ESKAPE pathogens. Furthermore, the synergistic interactions, against biofilms, of anti-biofilm peptide 1018 in conjunction with different classes of antibiotics commonly used in the clinic were investigated.

3.3 Methods and materials

3.3.1 Bacterial Strains

Strains utilized included wild-type strains of *Pseudomonas aeruginosa* PAO1, strain H103, and PA14 and clinical isolates *E. coli* O157, *Salmonella enterica* serovar Typhimurium (clinical isolate 14028S), *Staphylococcus aureus* MRSA (clinical isolate #SAP0017), *Klebsiella pneumoniae* ATTC 13883 (a colistin-heteroresistant reference strain from American Type Culture Collection, Rockville, MD), *Acinetobacter baumannii* SENTRY C8 (a polymyxin B-resistant blood clinical isolate from the U.S.A. obtained through the SENTRY surveillance system) and *Burkholderia cenocepacia* genomovar IIIa (Vancouver Children's Hospital clinical isolate 4813).

3.3.2 Peptide synthesis

Peptide 1018 (VRLIVAVRIWRR-NH_2) used in this study was synthesized by CPC Scientific using solid-phase 9-fluorenylmethoxy carbonyl (Fmoc) chemistry and purified to a purity of ~95% using reverse-phase high-performance liquid chromatography (HPLC). Peptide mass was confirmed by mass spectrometry.

3.3.3 Growth conditions

The medium used was generally BM2 minimal medium (62 mM potassium phosphate buffer, pH 7.0, 7 mM [$(NH_4)_2SO_4$, 2 mM $MgSO_4$, 10 μM $FeSO_4$] containing 0.4% (wt/vol) glucose as a carbon source, except for *Staphylococcus aureus* HG001 wild-type for which BM2 glucose + 0.5% casamino acids (CAA) was used, and *Salmonella enterica* SL1344 that was grown in Luria Broth. *Escherichia coli* MG1655 was grown in BM2 + 0.1% CAA.

3.3.4 Minimal Inhibitory Concentration (MIC, $MBIC_{50}$, $MBIC_{100}$) assays

The broth microdilution method with minor modifications for cationic peptides (Wiegand et al., 2008) was used for measuring the MIC of peptide 1018. Minimal biofilm inhibitory concentrations leading to a 50% decrease in biofilm growth ($MBIC_{50}$) were obtained using 96-well plate assays and crystal violet staining of adherent biofilms as described in Chapter 2. The minimal peptide concentrations that completely inhibited biofilm formation ($MBIC_{100}$) were obtained using flow cells at different input concentrations of peptide.

3.3.5 Biofilm cultivation in flow cell chambers and microscopy

Biofilms were grown in flow chambers with channel dimensions of 1x4x40 mm, as previously described for 72 h at 37°C (Chapter 2) in the absence or presence of the desired concentration of peptide 1018. Flow cell chambers were inoculated by injecting 400 μl of an overnight culture diluted to an OD_{600} of 0.05. After inoculation, chambers were left without flow for 2 h to enable initial adherence, after which the medium (with or without sub-inhibitory concentrations of 1018) was pumped through the system at a constant rate of 2.4 ml/h. In all cases, after 3 days of growth the flow rate (90 rpm) was increased so as to limit the amount of planktonic and loosely-attached cells within the flow cell chamber. All media used (see above) in flow cell assays supported the planktonic growth of the bacterial species tested, as determined by growth curves. Except where otherwise specified, the concentrations of peptide 1018 used were 10 μg/ml for *Pseudomonas aeruginosa*, *Escherichia coli* 0157, *Acinetobacter*

baumannii SENTRY C8 and *Burkholderia cenocepacia* genomovar IIIa 4813, 20 µg/ml for *Salmonella enterica* sv. Typhimurium 14028S experiments, 2 µg/ml for *Klebsiella pneumoniae* ATTC13883, and 2.5 µg/ml for methicillin resistant *Staphylococcus aureus* MRSA #SAP0017. The different concentrations used corresponded to the measured $MBIC_{100}$ of the peptide against the different bacterial species as shown in Table 3.1. For inhibition studies, peptide was added to the flow-through medium immediately after the initial adherence phase, and maintained for 3 days. For treatment of existing biofilms, bacteria were allowed to develop into structured 2-day old biofilms prior to peptide treatment by addition into the flow cell flow-through medium for the following 24 h. Biofilm cells were stained using the LIVE/DEAD BacLight Bacterial Viability kit (Molecular Probes, Eugene, OR) or Syto-9 alone prior to microscopy experiments. A ratio of Syto-9 (green fluorescence, live cells) to propidium iodide (PI) (red fluorescence, dead cells) of 1:5 was used. Microscopy was done using a confocal laser scanning microscope (Olympus, Fluoview FV1000) and three-dimensional reconstructions were generated using the Imaris software package (Bitplane AG). Quantification of the overall biofilm biovolume (μm^3) and the percentage of live and dead cell volume was performed using Imaris software as previously described (Chávez de Paz et al., 2010; Sun et al., 2013). Experiments were performed at least in triplicate.

For inhibition of biofilm growth, the treatment was applied from the beginning of the experiment. For treatment of pre-formed biofilms, bacteria were allowed to develop structured 2-day-old biofilms prior to peptide and antibiotics treatment for the following 24 h. For "shot" experiments, injection of peptide and antibiotic diluted in medium was done directly in the flow cell chamber. The flow was stopped during application of the treatment (2 h for inhibition and 1 h for eradication).

3.3.6 Dispersal biofilm cell assay

Cell counts of live dispersed bacteria from flow cell biofilms were performed using strain *P. aeruginosa* PA14 grown in BM2 minimal glucose medium. *P. aeruginosa* PA14 biofilms were grown in the flow cell system for 2 days as described above and treated with either 0.8 µg/ml, 10 µg/ml of peptide 1018, 40 ng/ml of ciprofloxacin or the combination of 0.8 µg/ml of 1018 and 40 ng/ml of ciprofloxacin. To count the dispersed viable cells, 1.5 ml of the output flow was collected at the designated times (time 0 and after 3 and 23 h) and serially diluted 10-fold. One hundred-µl portions from these serial dilutions were then plated

onto LB agar plates. Plates were incubated at 37°C overnight, and colony counts were performed to obtain total CFU/ml at each time point. Experiment was repeated at least 3 times.

3.4 Results

3.4.1 Peptide 1018 as a potent broad-spectrum anti-biofilm agent

While screening for peptides with anti-biofilm activity, I identified the previously unknown ability of the immunomodulatory peptide IDR (innate defense regulator)-1018 (VRLIVAVRIWRR-NH_2; abbreviated here as peptide 1018) (Rivas-Santiago et al., 2013) to specifically target and kill biofilm cells (Figure 3.1), at much lower concentrations than previously described peptides (Chapter 2). At concentrations that had no effect on planktonic growth (Table 3.1), this peptide was able to potently prevent biofilm formation (Figure 3.1, middle panels) and eradicate, kill or alter preformed (2-day old) biofilms (Figure 3.1, right hand panels) formed by diverse species of Gram-negative bacteria and the Gram-positive bacterium *Staphylococcus aureus*.

Table 3.1. Peptide 1018 exhibited potent broad-spectrum direct anti-biofilm activity but weak antibacterial activity for planktonic cells. Comparison of planktonic cell MIC to $MBIC_{50}$ and $MBIC_{100}$, which are the minimal biofilm inhibitory concentrations leading to 50% and 100% decrease in biofilm growth, respectively. Reprinted from: de la Fuente-Núñez C, Reffuveille F, Haney EF, Strauss SK, Hancock REW. (2014). Broad-spectrum anti-biofilm peptide that targets a cellular stress response. PLoS Pathog. 10: e1004152.

	Activity (μg/ml)		
Bacterial strains	**MIC**	**$MBIC_{50}$**	**$MBIC_{100}$**
Pseudomonas aeruginosa PA01	64	5	10
Pseudomonas aeruginosa PA14	64	5	10
Burkholderia cenocepacia IIIa 4813	>256	2	10
Escherichia coli 0157	32	8	10
Acinetobacter baumannii SENTRY C8	128	2	10
Klebsiella pneumoniae ATTC13883	8	2	2
Salmonella enterica sv Typhimurium 14028S	64	3.2	10
S. aureus MRSA #SAP0017	64	2	2.5

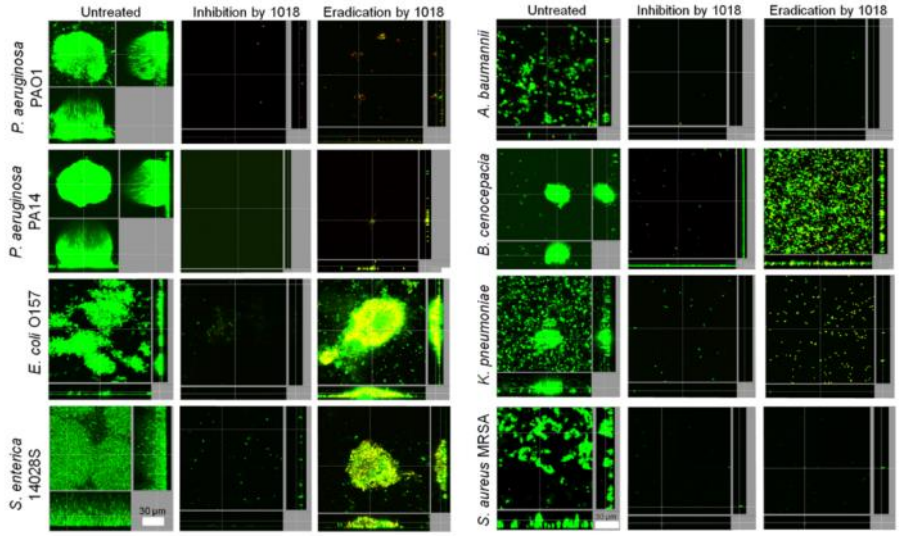

Figure 3.1. Peptide 1018 potently inhibited bacterial biofilms at concentrations that did not affect planktonic cell growth. Sub-inhibitory concentrations of peptide 1018 prevented biofilm development and eradicated or reduced existing biofilms of Gram-negative and Gram-positive bacteria. Concentrations of peptide 1018 used were 10 µg/ml for *Pseudomonas aeruginosa* (labelled as strains PA14 and PAO1) *Escherichia coli* 0157, *Acinetobacter baumannii* and *Burkholderia cenocepacia*, 20 µg/ml for *Salmonella enterica* serovar Typhimurium 14028S experiments, 2 µg/ml for *Klebsiella pneumoniae* experiments, and 2.5 µg/ml for methicillin resistant *Staphylococcus aureus* (MRSA) experiments. Inhibition of biofilm development was tested by immediately adding 1018 into the flow-through medium of the flow cell apparatus and then monitoring biofilm formation for 3 days. Eradication conditions involved waiting two days before addition of 1018 into the flow-through medium. After 3 days, bacteria were stained green with the all bacteria stain Syto-9 and red with the dead-bacteria stain propidium iodide (merge shows as yellow to red) prior to confocal imaging. Each panel shows reconstructions from the top in the large panel and sides in the right and bottom panels (xy, yz and xz dimensions). Reprinted from: de la Fuente-Núñez C, Reffuveille F, Haney EF, Strauss SK, Hancock REW. (2014). Broad-spectrum anti-biofilm peptide that targets a cellular stress response. PLoS Pathog. 10: e1004152.

I investigated the role of peptide 1018 in biofilm cell dispersion and killing of *P. aeruginosa* PA14 2-day old biofilms, in collaboration with Dr. Fany Reffuveille. At very low concentrations (0.8 µg/ml), the peptide increased live cell dispersion from existing biofilms by ~4-fold after 23 h of treatment (Figure 3.2), resulting in an average of 8.2 ± 6.6% residual biofilm biovolume compared to the untreated controls ($P<0.05$). Only 26 ± 7.4% of the cells that remained attached within the flow cell chambers were killed by treatment with 0.8 µg/ml of peptide 1018. Conversely, higher concentrations of peptide (10 µg/ml) did not trigger live biofilm cell dispersal (Figure 3.2), and most of the cells remaining bound to the surface were

dead, as judged by uptake of the normally impermeant stain propidium iodide (67 ± 7.7% red cells compared to 2.5 ± 1.0% in the untreated controls; P<0.05).

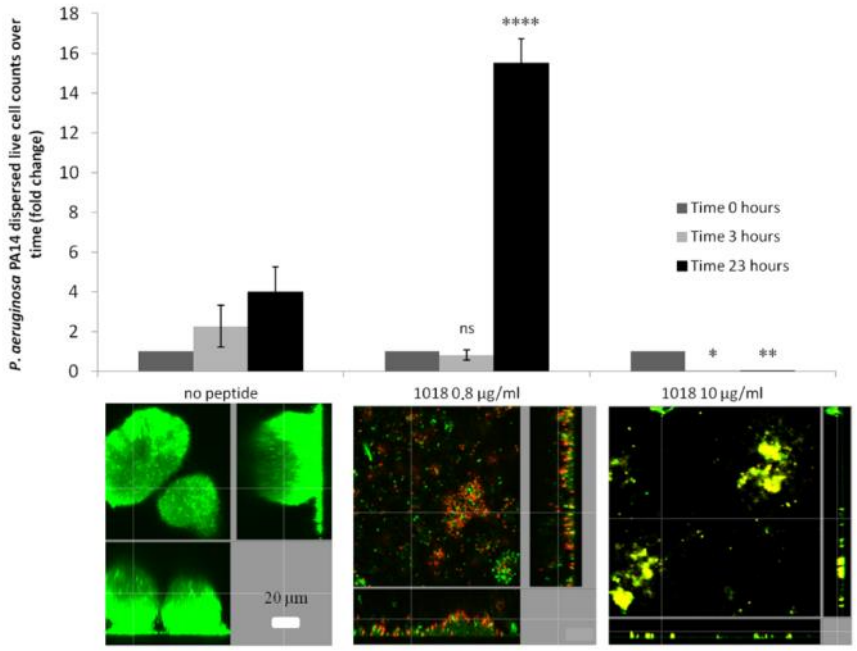

Figure 3.2. Low levels of peptide 1018 led to biofilm dispersion while higher levels triggered biofilm cell death. Dispersed cells from mature *P. aeruginosa* flow cell biofilms were collected and viable cell counts performed after 0, 3 and 23 h of treatment with different concentrations of the peptide (0.8 and 10 µg/ml). Representative confocal images of the remaining cells present in the flow cell chambers after peptide treatment are shown for each condition. Statistical significance comparing peptide-treated groups to untreated was determined using Student's *t* test (ns, P > 0.05; *, P < 0.05; **, P < 0.01; ****, P < 0.0001). Reprinted from: de la Fuente-Núñez C, Reffuveille F, Haney EF, Strauss SK, Hancock REW. (2014). Broad-spectrum anti-biofilm peptide that targets a cellular stress response. PLoS Pathog. 10: e1004152.

In experiments with pre-grown, 2-day old biofilms, only *E. coli* 0157, *S. enterica* 14028S and *B. cenocepacia* samples consistently had attached cells after peptide treatment (Figure 3.1, right hand panels). However, the remaining cell population was mostly dead in the case of *E. coli* 0157 as, on average, there was a significant increase in dead cell number in treated samples (54.4 ± 3.1%) compared to untreated samples (1.5 ± 0.9%; P<0.05). On the other hand, the peptide caused more substantial dispersal but lesser cell death in *S. enterica* 14028S and *B. cenocepacia* biofilms. *Salmonella* biofilms treated with 1018 had 29.2 ± 19.0%

dead cells as opposed to just 0.54 ± 0.69% in samples without peptide ($P<0.05$). *B. cenocepacia* biofilms exhibited no significant increase in cell death (7.9 ± 3.4% cf. 3.8 ± 2.4% in the untreated controls).

3.4.2 Synergy between anti-biofilm peptide 1018 and antibiotics to inhibit biofilm formation

Synergy between anti-biofilm peptide 1018 and conventional antibiotics ciprofloxacin, ceftazidime, imipenem or tobramycin was determined in collaboration with Dr. Fany Reffuveille using a checkerboard titration assay, as previously described (Hall et al., 1983), except that the effect of peptide diluted in one dimension and antibiotic in another on biofilms formed by bacterial adherence to the surface of microtitre wells was measured (de la Fuente-Núñez et al., 2012). The lowest peptide/antibiotic concentration combination that led to complete inhibition of biofilm growth (minimal biofilm inhibitory concentration; MBIC) was determined and the fractional inhibitory concentration (FIC) was calculated based on the MBIC of each compound alone and in combination (Hall et al., 1983), which represents the minimal concentration required to fully prevent biofilm formation. The FIC provides a measure of the degree of synergy between two antimicrobial agents against a particular microorganism. FIC values below 0.5 indicate synergy, those between 0.5 and 1 correspond to additive effects with numbers just above 0.5 indicating a 2-fold change in MBIC for one agent and a very large change in MBIC for the other, and those above 2 show antagonistic interactions (de la Fuente-Núñez et al., 2014; Hall et al., 1983).

Anti-biofilm peptide 1018 exhibited synergistic interactions with all of the antibiotics tested in this study against biofilms formed by at least one of the 6 tested bacterial species (Table 3.2) with 50% of all combinations giving synergy ($FIC\leq0.5$) and 16.7% giving close to synergy ($FIC<0.53$). Addition of the peptide in 20 of 24 cases reduced, by 4 to 64 fold, the levels of antibiotic needed to completely inhibit biofilm formation (Table 3.2).

Some variability was observed for different species and different antibiotics. Sub-MBIC levels of the peptide in combination with all antibiotics tested led to synergistic (FIC=0.14 - 0.5) inhibition of *P. aeruginosa* PA14 biofilm formation. Particularly significant was the case of ciprofloxacin (FIC=0.14) that showed a 16-fold decrease in the concentration of ciprofloxacin required to inhibit biofilm growth when used in combination with 1018 (Table 3.2). Synergy (FIC=0.16-0.25) was also observed between peptide 1018 and three of the

antibiotics tested against Gram-positive methicillin resistant *S. aureus* (MRSA) biofilms, while tobramycin showed near synergy with peptides due to a 64-fold reduction in the effective concentration of this antibiotic (Table 3.2). Combinations of the peptide with ceftazidime (FIC=0.37) and tobramycin (FIC=0.38) were synergistic against biofilms formed by *A. baumannii* SENTRY 8, while the other two antibiotics were 8-32 fold more effective in the presence of peptide.

Table 3.2. Anti-biofilm peptide 1018 showed synergy with conventional antibiotics in a broad-spectrum manner. Checkerboard titrations were performed to assess synergistic interactions between peptide 1018 and conventional antibiotics to prevent biofilm formation. Briefly, one compound (e.g. peptide) was diluted along the rows of a microtitre plate and the other compound (e.g. antibiotic) was diluted along the columns. In this method, one is looking for a reduction in the Minimal biofilm inhibitory concentration (MBIC) of each compound in the presence of the other. The result is expressed as the fractional inhibitory concentration (FIC) index as described in Methods and materials. In all cases, peptide 1018 when combined with antibiotics reduced the antibiotic MBIC when used alone, here depicted as fold decrease in antibiotic concentration at the FIC. CTZ: ceftazidime; CIP: ciprofloxacin; IMI: imipenem; TOB: tobramycin.

Strains	FIC				Fold Decrease in Antibiotic Concentration			
	CTZ	**CIP**	**IMI**	**TOB**	**CTZ**	**CIP**	**IMI**	**TOB**
P.aeruginosa PA14	**0.38**	**0.14**	**0.5**	**0.5**	16X	16X	4X	2X
E. coli 0157	1	0.69	0.75	**0.38**	4X	4X	4X	4X
A. baumannii	**0.37**	0.52	0.53	**0.38**	16X	32X	8X	4X
K. pneumoniae	0.75	0.63	0.53	**0.31**	4X	2X	32X	16X
S. enterica	**0.31**	1	1	0.75	4X	2X	2X	4X
S. aureus MRSA	**0.16**	**0.25**	**0.25**	0.52	32X	64X	4X	64X

Peptide 1018 was also synergistic with the aminoglycoside antibiotic tobramycin (FIC=0.38) in inhibiting biofilm formation by *E. coli* O157 (Table 3.2) although other combinations were only additive. Conversely with the related species *S. enterica* serovar Typhimurium synergy was only observed when combining 1018 with ceftazidime (FIC=0.31). For *K. pneumoniae* ATCC 13883, synergy was observed when using peptide 1018 in combination with tobramycin (FIC=0.31), while additive effects were observed for the other three antibiotics tested, with the MBIC for imipenem being notably reduced by 32 fold (Table 3.2). Thus synergy was highly dependent both on the particular species being tested and the

antibiotic used in combination.

3.4.3 Synergy of anti-biofilm peptide 1018 with conventional antibiotics assessed in flow cells

The best combination obtained in the checkerboard microtitre plate assay for each bacterial species (peptide/antibiotic combinations that led to the lowest FIC values) was used to confirm the synergistic interactions using the more sophisticated flow cell system. Biofilms were allowed to develop for 3 days in flow cell chambers with constant flow of BM2 glucose minimal medium across the developing biofilms. Peptide and/or the different antibiotics tested were added to the flow medium during the entire 3 days of the experiment, after which the resulting surface adherent cells/biofilm was stained for total cells (stained green with the fluorescent dye Syto-9) and dead cells (stained red with normally-impermeant propidium iodide) and visualized using confocal laser scanning microscopy as previously described (de la Fuente-Núñez et al., 2014).

Synergy was confirmed using this system since in all cases the combination of peptide plus antibiotic significantly increased the biofilm inhibitory activity of each compound when used alone (based on lack of live adherent biofilm colonies; Figure 3.3). For example, *P. aeruginosa* biofilm formation was inhibited by 0.8 μg/ml of peptide 1018 combined with 40 ng/ml ciprofloxacin leading to a significant reduction in biofilm thickness, while the few small microcolonies observed were mostly composed of dead cells (Figure 3.3). A few cells remained attached to the surface of flow cell chambers after combination treatment of *E. coli* 0157 (1.6 μg/ml tobramycin plus 8 μg/ml 1018), *K. pneumoniae* (0.1 μg/ml tobramycin plus 2 μg/ml 1018), *S. aureus* (8 μg/ml ceftazidime plus 8 μg/ml 1018) and *A. baumannii* (32 μg/ml ceftazidime plus 32 μg/ml 1018) (Figure 3.3). However, these cells appeared dead as determined by propidium iodide uptake (yellow-to-red color when merged with Syto-9). No attached *S. enterica* cells were observed after the application of the 2 μg/ml peptide and 62.5 ng/ml ceftazidime (Figure 3.3). These results confirmed the results obtained using the checkerboard assay and clearly showed that anti-biofilm peptide 1018 acted in synergy with conventional antibiotics, thus markedly reducing the concentration of antibiotic needed to prophylactically treat bacterial biofilm formation.

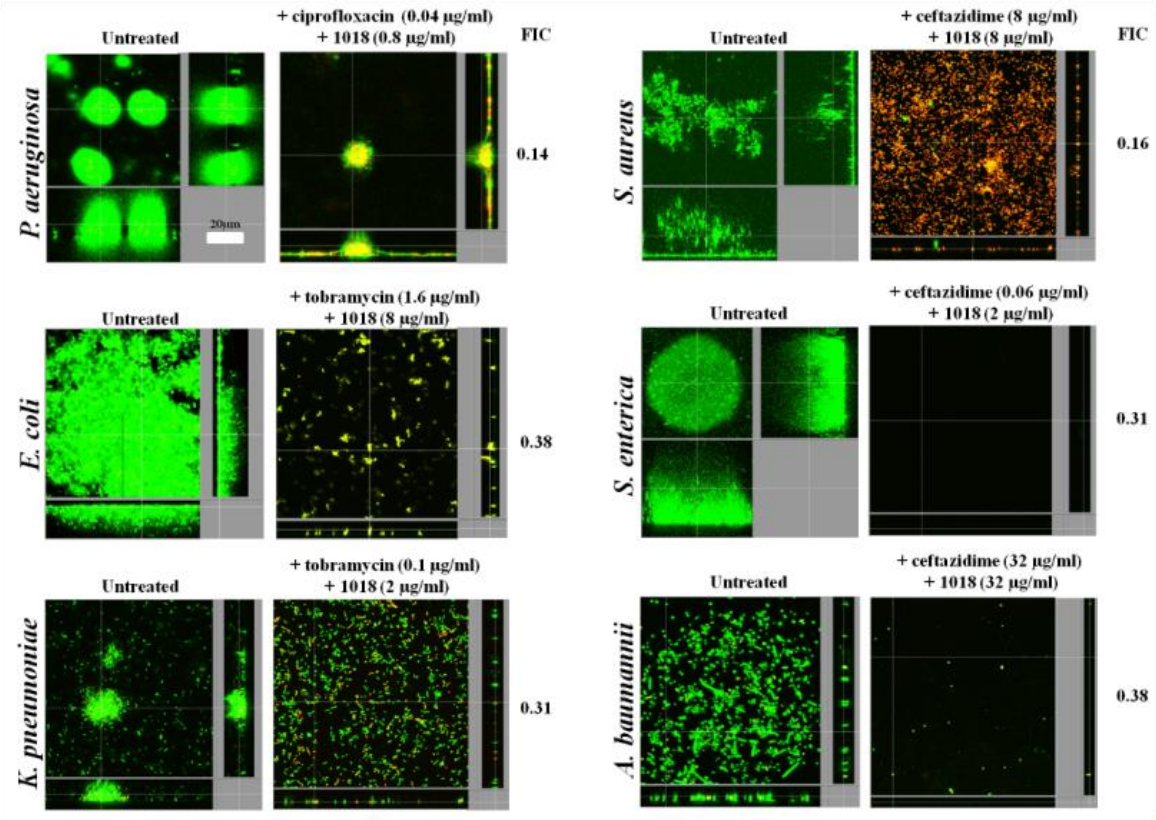

Figure 3.3. Anti-biofilm peptide 1018 synergized with conventional antibiotics to inhibit biofilm formation. Biofilms were grown in a flow cell system (Methods and materials). Treatment (antibiotic/peptide combination) was added to the flow through medium at the beginning of the experiment and maintained for the entire 3 days of the experiment. After 3 days, bacteria were stained green with the all bacteria stain Syto-9 and red with the dead-bacteria stain propidium iodide (merge shows as yellow to red) prior to confocal imaging. Each panel shows reconstructions from the top in the large panel and sides in the right and bottom panels (xy, yz and xz dimensions). FIC values provided were those calculated using checkerboard assays (Table 1) and are provided to the right of each image (synergy if FIC<0.5). Copyright © American Society for Microbiology, Reffuveille F, de la Fuente-Núñez C, Mansour S, Hancock REW. (2014). A broad-spectrum anti-biofilm peptide enhances antibiotic action against bacterial biofilms. Antimicrob. Agents Chemother. 58:5363-71.

3.4.4 Eradication of pre-formed biofilms by the combination of peptide 1018 with antibiotics

The same combinations of peptides and antibiotics used in the inhibition studies (and first determined in the checkerboard assays) were also used to treat pre-existing biofilms. Biofilms were grown for 2 days in flow cells, after which they had already formed biofilm colonies and were then treated for the last 24 h of the experiment. As a comparative control,

we first tested the susceptibility of *P. aeruginosa* PA14 biofilms to ciprofloxacin (Figure 3.4). Biofilm resistance to ciprofloxacin was observed as treatment with the antibiotic at its MIC, 10xMIC or 100xMIC did not eradicate 2-day old *P. aeruginosa* PA14 biofilms (Figure 3.4), and only triggered some cell death of inner biofilm clusters at 10xMIC and 100xMIC (Figure 3.4).

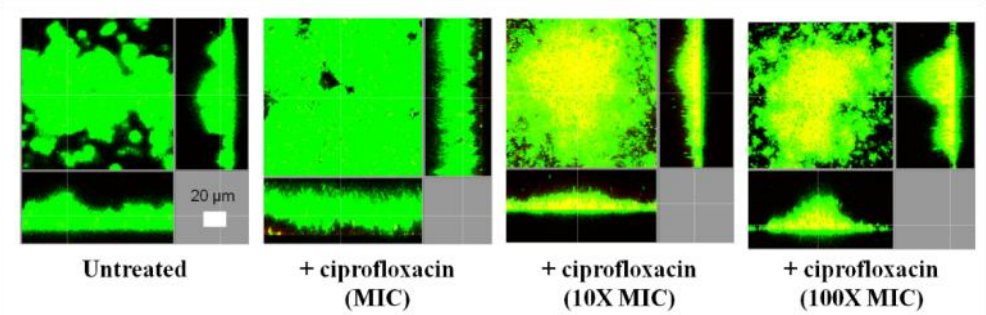

Figure 3.4. *Pseudomonas aeruginosa* PA14 pre-formed biofilms were highly resistant to ciprofloxacin. Biofilms were grown in flow cell system. Ciprofloxacin at its MIC (160 ng/ml), 10xMIC and 100xMIC concentrations were applied on a 2 days-old biofilm, for 24 hours. After 3 days, bacteria were stained green with the all bacteria stain Syto-9 and red with the dead-bacteria stain propidium iodide (merge shows as yellow to red) prior to confocal imaging. Each panel shows reconstructions from the top in the large panel and sides in the right and bottom panels (xy, yz and xz dimensions). Copyright © American Society for Microbiology, Reffuveille F, de la Fuente-Núñez C, Mansour S, Hancock REW. (2014). A broad-spectrum anti-biofilm peptide enhances antibiotic action against bacterial biofilms. Antimicrob. Agents Chemother. 58:5363-71.

Next, a combination of peptide and antibiotic or each compound individually was tested. In all cases, treatment with conventional antibiotics alone did not clear pre-formed biofilms and did not significantly induce biofilm cell death (Figure 3.5). Treatment with low levels of the anti-biofilm peptide 1018 alone led to decreased biofilm thickness, and disrupted the overall biofilm structure and triggered some cell death (Figure 3.5), as previously observed with peptide 1018 (de la Fuente-Núñez et al., 2014). These effects were significantly increased in the presence of low concentrations of antibiotics that by themselves did not affect pre-formed biofilms (Figure 3.5). For example, combined treatment with ceftazidime and peptide 1018 completely cleared mature biofilms formed by *A. baumannii* (Figure 3.5). The same combination of antimicrobials at lower concentrations disrupted *S. aureus* MRSA mature biofilms and led to cell death (Figure 3.5). Peptide 1018 in combination with tobramycin led to biofilm clearance in *K. pneumoniae* and killed biofilm cells in *E. coli* 0157 (Figure 3.5).

Similarly, *P. aeruginosa* PA14 mature biofilms treated with 1018 and ciprofloxacin led to very small microcolonies composed of dead cells (Figure 3.5). On the other hand, treatment with the peptide and ceftazidime did not clear mature biofilms formed by *S. enterica*; however, it did reduce biofilm thickness and led to substantial cell death (Figure 3.5). Therefore it can be concluded that, when used in combination with conventional antibiotics, peptide 1018 potently enhanced antibiotic action to both prevent biofilm formation and treat mature biofilms formed by multidrug-resistant pathogens.

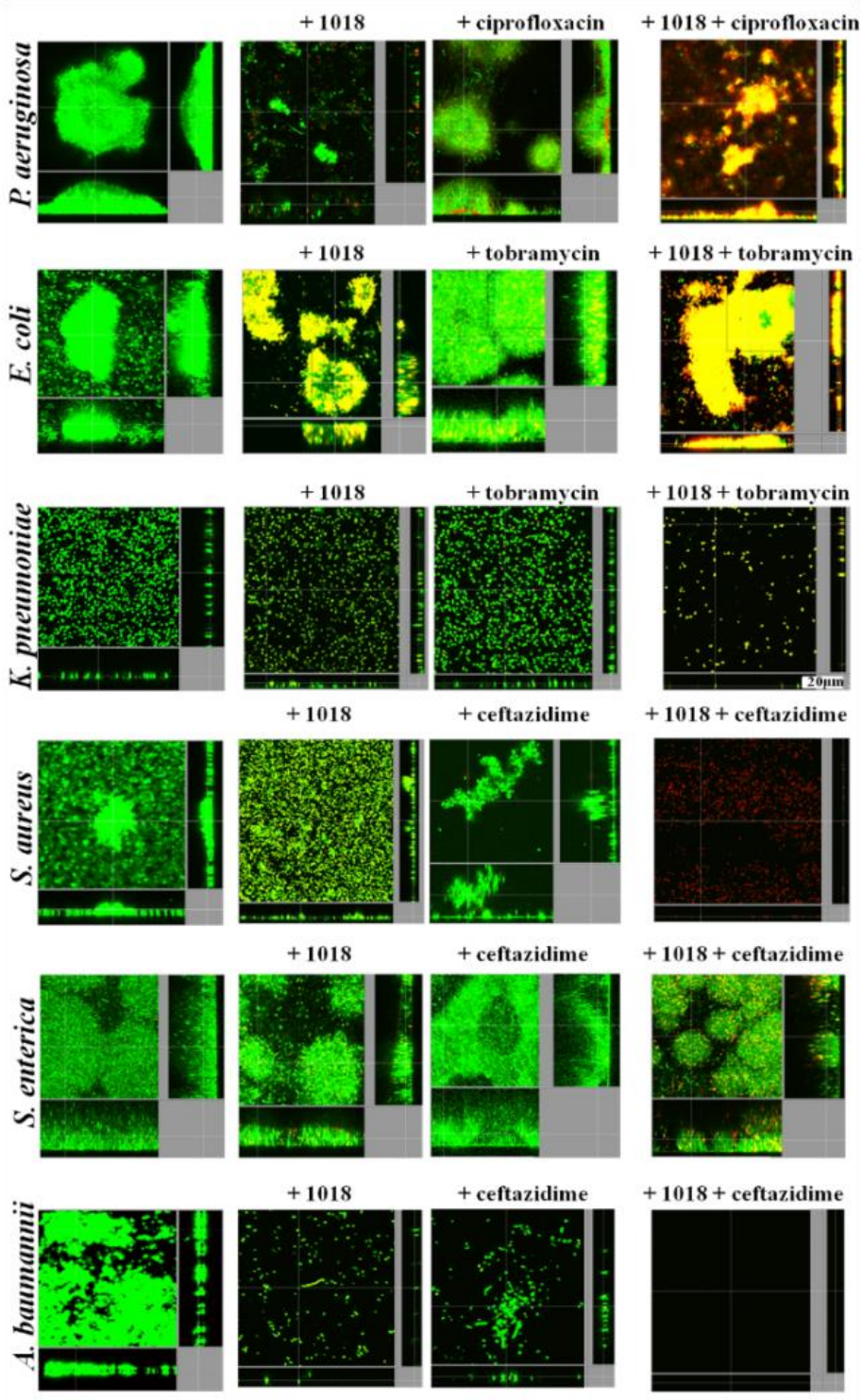

Figure 3.5. Synergy between anti-biofilm peptide 1018 with conventional antibiotics in eradicating pre-formed biofilms. Bacteria were grown as biofilms in a flow cell system. Treatments (antibiotic, peptide or combinations as specified in the figure 3.3) were added after 2 days of biofilm growth for a subsequent 24 hours. After 3 days, bacteria were stained green with the all bacteria stain Syto-9 and red with the dead-bacteria stain propidium iodide (merge

shows as yellow to red) prior to confocal imaging. Each panel shows reconstructions from the top in the large panel and sides in the right and bottom panels (xy, yz and xz dimensions). Copyright © American Society for Microbiology, Reffuveille F, de la Fuente-Núñez C, Mansour S, Hancock REW. (2014). A broad-spectrum anti-biofilm peptide enhances antibiotic action against bacterial biofilms. Antimicrob. Agents Chemother. 58:5363-71.

3.4.5 Combinations of peptide and ciprofloxacin significantly reduced dispersal of viable cells from *P. aeruginosa* mature biofilms

The lowest FIC obtained in checkerboard assays corresponded to the combined use of peptide 1018 with ciprofloxacin against *P. aeruginosa* PA14 (FIC= 0.14 at 40 ng/ml of ciprofloxacin and 0.8 μg/ml of peptide 1018; Table 3.2). To further assess the effect of this combined therapy on dispersal of cells and cell death in *P. aeruginosa* PA14 mature biofilms, cell dispersal assays were performed in collaboration with Dr. Fany Reffuveille measuring the numbers of cells collected from the flow-through medium. Briefly, biofilms were allowed to grow untreated for 2 days and subsequently treated with ciprofloxacin alone or in combination with peptide 1018 (Figure 3.6). Cells dispersed from the biofilms in the flow cell chambers were collected in tubes, and plated on LB agar for assessment of viable cell counts. Treatment with 40 ng/ml ciprofloxacin led to no increase in the number of live dispersed cells ($p>0.05$; Figure 3.6). Conversely, when the same concentration of ciprofloxacin was used together with 0.8 μg/ml of peptide 1018, the number of dispersed cells was significantly reduced after both 3 and 23 h (Figure 3.6). This can be contrasted with observations of the cells remaining attached to the flow cell that formed very small microcolonies composed largely (>61% cf. 2.5±2% in the control; $p<0.001$) of dead cells (Figure 3.5). In contrast biofilms treated only with ciprofloxacin remained virtually unaffected ($p>0.05$).

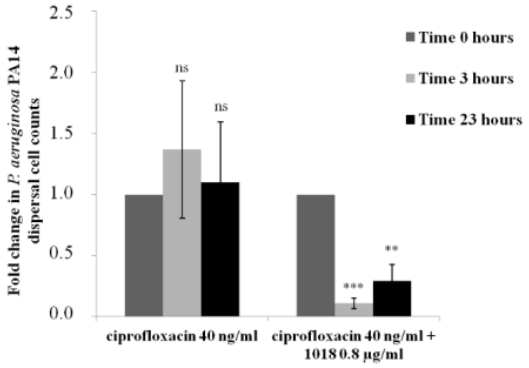

Figure 3.6. Low levels of peptide 1018 in combination with ciprofloxacin decreased dispersal of viable cells from *P. aeruginosa* PA14 biofilms. Dispersed cells from 2 days-old biofilm grown in the flow cell system were collected after 0, 3 and 23 h of treatment with 40

ng/ml of ciprofloxacin or 40 ng/ml of ciprofloxacin and 0.8 µg/ml of 1018 peptide and enumerated by plate counts. Student's *t* test was done to compare different time points to time 0 and determine the statistical significance (**, p< 0.01; ***, p< 0.001). Copyright © American Society for Microbiology, Reffuveille F, de la Fuente-Núñez C, Mansour S, Hancock REW. (2014). A broad-spectrum anti-biofilm peptide enhances antibiotic action against bacterial biofilms. Antimicrob. Agents Chemother. 58:5363-71.

Moreover, the ciprofloxacin, ceftazidime and tobramycin susceptibilities of dispersed cells from *P. aeruginosa* PA14 biofilms treated with 0.8 µg/ml of peptide 1018 were identical to those of dispersed cells from untreated biofilms (MICs of 0.16, 3.2 and 0.8 µg/ml for ciprofloxacin, ceftazidime and tobramycin respectively), indicating that live dispersed cells from samples treated with low levels of the peptide did not develop adaptive resistance to any of these antibiotics.

3.4.6 Short-term therapy using combinations to treat *P. aeruginosa* PA14 mature biofilms

To further evaluate the anti-biofilm potential of peptide 1018 in combination with ciprofloxacin, first short-term combined treatments using 10 µg/ml of peptide 1018 alone were performed on *P. aeruginosa* PA14 biofilms (Figure 3.7). Treatment with 1018 for 2 h at the beginning of biofilm growth prevented biofilm growth (Figure 3.7; upper right panel), however two 1-hour treatments on days 2 and 3 were required to eradicate established biofilms (Figure 3.7; lower right panel cf. lower left panel).

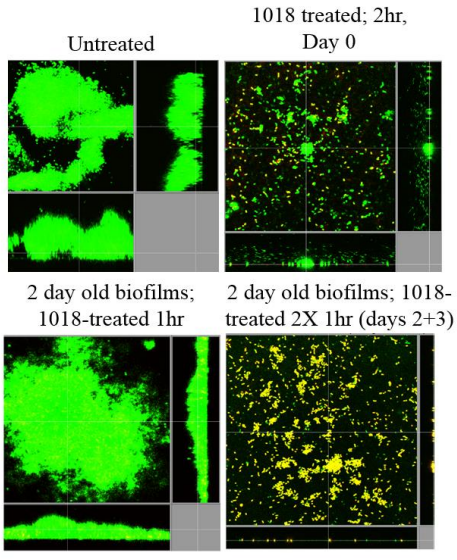

Figure 3.7. Short-term peptide 1018 treatments (10 µg/ml) led to biofilm inhibition and eradication. *P. aeruginosa* PA14 biofilms (untreated controls top left image) were treated for

2 hours from the beginning of biofilm growth on day 0 (top right image), for 1 hour at day 2 (bottom left image) or treated twice for 1 hour at days 2 and 3 (bottom right image). In all cases, after 3 days, attached cells within flow cells were stained using SYTO-9 and imaged with confocal microscopy.

Then, we performed short-term treatments on *P. aeruginosa* PA14 biofilms using the combination of 1018 (0.8 μg/ml) and ciprofloxacin (40 ng/ml). Treatment with both compounds for only 2 h at the beginning of biofilm growth (inhibition conditions) substantially inhibited biofilm formation leaving only a few aggregated cells post-treatment (Figure 3.8).

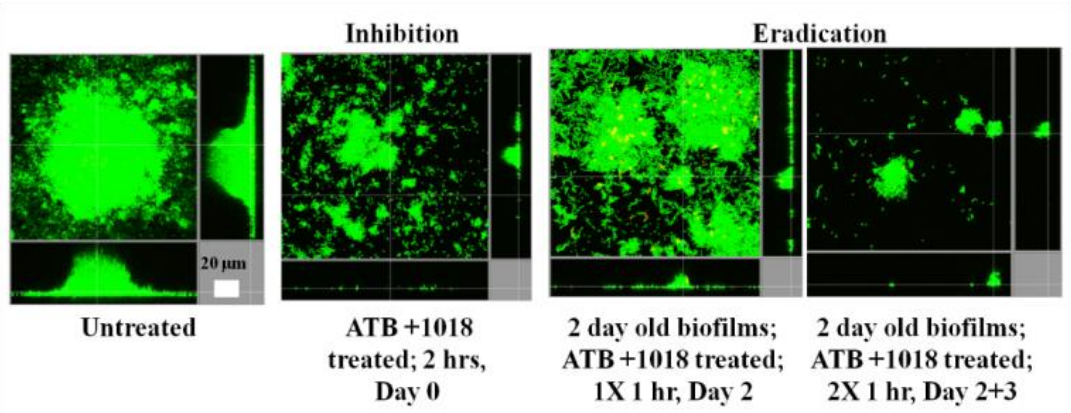

Figure 3.8. Short-term treatments with combinations of low concentrations of peptide 1018 and ciprofloxacin still inhibited biofilm formation. Peptide 1018 (0.8 μg/ml) and ciprofloxacin (40 ng/ml) were injected for 2 h at the beginning of *P. aeruginosa* PA14 biofilm formation, or with 2 day-old *P. aeruginosa* PA14 biofilms for 1 h on day 2, or for 1 h on day 2 plus 1 h on day 3. After 3 days, bacteria were stained green with the all bacteria stain Syto-9 and red with the dead-bacteria stain propidium iodide (merge shows as yellow to red) prior to confocal imaging. Each panel shows reconstructions from the top in the large panel and sides in the right and bottom panels (xy, yz and xz dimensions). Copyright © American Society for Microbiology, Reffuveille F, de la Fuente-Núñez C, Mansour S, Hancock REW. (2014). A broad-spectrum anti-biofilm peptide enhances antibiotic action against bacterial biofilms. Antimicrob. Agents Chemother. 58:5363-71.

Eradication conditions involved growing *P. aeruginosa* PA14 biofilms untreated for 2 days before treating them with peptide 1018 and ciprofloxacin. Two-day old biofilms treated once with peptide 1018+ciprofloxacin for 1 h demonstrated modest effects with decreased biofilm thickness and altered overall biofilm structure (Figure 3.8), while treating the biofilms twice on days 2 and 3 for 1 h each time virtually eradicated *Pseudomonas* biofilms (Figure 3.8).

3.5 Discussion

The increase in antibiotic resistance during biofilm infections is a substantial problem in public health, and solutions need to be provided. In this Chapter it was demonstrated that anti-biofilm peptide 1018 inhibited biofilm formation and eradicated pre-formed biofilms formed by Gram-negative and Gram-positive multidrug-resistant pathogens. In addition, 1018 was shown to disperse mature biofilms at low concentrations (0.8 µg/ml) and kill biofilm cells at higher concentrations (10 µg/ml).

To evaluate one possible clinical modality for this broad-spectrum anti-biofilm peptide, its synergy with conventional antibiotics was also tested. Using checkerboard assays and performing confirmatory studies using the flow cell methodology, it was demonstrated that peptide 1018, in combination with 4 conventional antibiotics used in the clinic, prevented biofilm formation and eradicated pre-formed biofilms formed by bacterial pathogens that are notorious for their high antibiotic resistance. Interactions between the peptide and antibiotics led to synergy in half of the tested combinations and substantial reductions (up to 64-fold) in the concentrations of antibiotic required to inhibit biofilm formation (Table 3.2). This might have significant potential in treating chronic infections that usually involve biofilms and are highly recalcitrant to treatment. Indeed to treat chronic infections, the antibiotic dose is often increased but can still fail to clear the infection, thus leading to high level antibiotic resistance (Høiby et al., 2011). The use of agents like peptide 1018 may provide a solution to this problem due to its ability to potentiate the anti-biofilm activity of conventional antibiotics that are otherwise largely only effective against planktonic bacteria.

Low concentrations of peptide 1018 (0.8 µg/ml) were able to increase biofilm dispersal after 23 h of treatment. Dispersal of cells from biofilms represents a potential danger in the clinical setting as this may lead to infection at other sites or even septic shock (Hall-Stoodley et al., 2004; Hall-Stoodley and Stoodley, 2005). Critically when the peptide was combined with ciprofloxacin at sub-MIC concentrations, the number of live dispersed cells dropped dramatically by ~20-fold compared to the normal level of cells dispersed from wild-type biofilms (Figure 3.6). This may be due to the increase in cell death in biofilms. These results indicate that combination treatment with peptide 1018 and antibiotic (ciprofloxacin) may be a good strategy to treat biofilm infections while avoiding potential future infections derived from cells dispersed from biofilms.

3.6 Summary

The steady rise in antibiotic resistance is one of the most significant threats to human medicine. This is further exacerbated by adaptive resistance that is dependent on the growth state of bacteria and is especially important for biofilms that cause two thirds of all infections. In this Chapter, I identified and characterized a small peptide 1018 that potently prevented biofilm formation and eradicated pre-existing biofilms formed by both Gram-negative and Gram-positive multi-drug resistant (MDR) bacterial pathogens. In addition, peptide 1018 demonstrated substantially enhanced effectiveness in combination with commonly used antibiotics in inhibiting biofilm formation and eradicate pre-existing biofilms formed by these strains. Indeed combinations were often synergistic and the presence of peptide substantially decreased the concentration of antibiotics needed to treat biofilms. Thus the inclusion of an anti-biofilm peptide like 1018 serves as a novel anti-resistance strategy, overcoming adaptive (biofilm-mediated) resistance.

Chapter 4: Role for the stringent response in peptide 1018 action and role of (p)ppGpp in biofilm development.

4.1. Overview

Since peptide 1018 exhibited broad-spectrum anti-biofilm activity, I hypothesized that the peptide acted to inhibit a common stress response in target species, and that the stringent response, mediating (p)ppGpp synthesis through the enzymes RelA and SpoT, was targeted. Consistent with this, increasing (p)ppGpp synthesis by addition of serine hydroxamate or over-expression of *relA* led to reduced susceptibility to the peptide. Furthermore, *relA* and *spoT* mutations blocking production of (p)ppGpp replicated the effects of the peptide, leading to a reduction of biofilm formation in the four tested target species. Also, eliminating (p)ppGpp expression after 2 days of biofilm growth by removal of arabinose from a strain expressing *relA* behind an arabinose-inducible promoter, reciprocated the effect of peptide added at the same time, leading to loss of biofilm. NMR and chromatography studies showed that the peptide acted on cells to cause degradation of (p)ppGpp within 30 minutes, and *in vitro* directly interacted with ppGpp. Thus it is proposed that peptide 1018 targets (p)ppGpp and marks it for degradation in cells. Targeting (p)ppGpp represents a new approach against biofilm-related drug resistance.

4.2. Introduction

The mechanisms suggested for the activity of peptide 1037 (Chapter 2) and LL-37 (Ovehage et la, 2008) are hard to rationalize with the very broad-spectrum activity of anti-biofilm peptides like 1018 since motility, adherence, quorum sensing, and the specific targets suggested based on the results from Figure 2.6, vary substantially between different species. The ability of peptide 1018 to inhibit biofilm formation in both Gram-negative and Gram-positive bacteria indicated that the peptide might act by interfering with a widespread cellular process in bacteria. Bacteria are known to respond to stressful environmental conditions (such as starvation) by activating a widespread cellular response called the stringent response (SR) (Potrykus and Cashel, 2008). As a consequence, the cell synthesizes two small signaling nucleotides, guanosine 5´-diphosphate 3´-diphosphate (ppGpp) and guanosine 5´-triphosphate 3´-diphosphate (pppGpp), collectively denoted (p)ppGpp (Potrykus and Cashel, 2008). They are synthesized from adenosine triphosphate (ATP) and either guanosine diphosphate (GDP)

to make ppGpp or guanosine triphosphate (GTP) to make pppGpp. These serve as a second messenger response that is induced by a variety of stress conditions, is highly conserved in both Gram-negative and Gram-positive species (Magnusson et al., 2005; Potrykus and Cashel, 2008), regulates the expression of a plethora of genes (Potrykus and Cashel, 2008), and is known to play a role in biofilm formation in certain species (Aberg et al., 2006; Balzer and McLean, 2002; Chávez de Paz et al., 2012; He et al., 2012; Lemos et al., 2004; Sugisaki et al., 2013; Taylor et al., 2002), although some variability has been observed (Balzer and McLean, 2002; Chávez de Paz et al., 2012; Lemos et al., 2004; Nguyen et al., 2011). Since (p)ppGpp production is conserved in bacteria in response to stress signals and plays an important role in biofilm formation, I hypothesized here that (p)ppGpp might be a target of peptide 1018.

4.3 Methods and materials

4.3.1 Bacterial Strains

P. aeruginosa PAO1 (p)ppGpp mutant Δ*relAspoT* [(Δ*relA* (Δ181-2019) Δ*spoT* (Δ200-1948)] and its complemented strain Δ*relAspoT*+SR were a kind gift from D. Nguyen (Nguyen et al., 2011). *S. aureus* parent strain HG001, its (p)ppGpp mutant HG001 rsh_{syn} (Δ942-950nt) and the strain complemented with full length *rsh* were kindly provided by T. Geiger (Geiger et al., 2010). *S. enterica* serovar Typhimurium parent strain SL1344 and its (p)ppGpp mutant SL1344 Δ*relAspoT* (Δ*relA*71::kan *rpsL* Δ*spoT*281::cat) were provided by K. Tedin (Tedin and Norel, 2001). *Escherichia coli* parent strain (MG1655), *E. coli* Δ*relAspoT* [Δ*relA*:: kan (Δ209-2302) Δ*spoT*:: cat (Δ700-2355)] deletion insertion mutant and *E. coli relA*+ (p)ppGpp positive control ptac::*relA* (pALS10) were also provided by D. Nguyen and obtained as previously described (Svitil et al., 1993; Xiao et al., 1991). For the expression of *relA* in the *P. aeruginosa* mutant strain PAO1Δ*relAspoT*, the pHERD20T plasmid carrying an arabinose-inducible promoter was used (Qiu et al., 2008). A 3.2 kb DNA fragment containing the *relA* gene was amplified with primers relAF (5'-GCTAGGATGCCTGCGTAATC-3') and relAR (5'-GAGATCGCCATCGAGGAATA-3') and cloned into a TOPO Zero-Blunt cloning vector (Invitrogen) and then into the pHERD20T vector. This construct was then electroporated into electrocompetent *P. aeruginosa* PAO1Δ*relAspoT* cells. Positives clones carrying the plasmid were selected on LB plus 500 µg/ml of carbenicillin, and *relA* overexpression upon induction was confirmed by RT-qPCR. In all experiments 0.01% arabinose was used to induce the

promoter.

4.3.2 Biofilm cultivation in flow cell chambers and microscopy

In experiments testing the effect of enhanced (p)ppGpp production of biofilm susceptibility to peptides, *E. coli* strain MG1655 expressing *relA* from a *lac* promoter on plasmid pALSl0 (Svitil et al., 1993) was grown in flow cells for 3 days in BM2 + 0.1% CAA containing 20 μg/ml of peptide 1018 and in the presence or absence of 100 μM isopropyl β-D-1-thiogalactopyranoside (IPTG). *P. aeruginosa* PAO1 and *S. aureus* HG001 strains were grown as described above but in the presence or absence of serine hydroxamate (SHX).

4.3.3 (p)ppGpp measurement by thin layer chromatography

Bacteria were grown overnight in modified MOPS minimal medium containing 0.4% glucose, 2 mM phosphate (KH_2PO_4), and 0.2% CAA. The cells were then diluted 1:20 in the same MOPS minimal medium except containing 0.4 mM phosphate (KH_2PO_4) and 500 μM SHX to induce (p)ppGpp synthesis, in the presence or absence of peptide 1018, colistin, tobramycin or polymyxin B and cells were labelled with 10 μCi/ml ^{32}P for 3 h. For experiments evaluating the ability of the peptide (or different antibiotics) to directly lead to degradation of (p)ppGpp, the cells were induced with SHX and allowed to synthesize (p)ppGpp (for 3 h) prior to peptide treatment. Samples were then extracted with frozen 13 M formic acid by three cycles of freeze-thaw. Aliquots (7.5 μl) of the supernatants were applied to 20×20 cm PEI cellulose TLC plates, resolved with 1.5 M KH_2PO_4 (pH 3.4) for 4 h. After chromatography, nucleotides were visualized by autoradiography and quantified with a MolecularImager FX PhosphorImager and Quantity One software (Bio-Rad). Unlabeled GTP was spotted on the plates as markers and visualized after chromatography by UV light-induced fluorescence.

4.3.4 Nucleotide co-precipitation

The ability of peptide 1018 to co-precipitate with nucleotides with varying phosphate content was examined as described previously by Hilpert et al. (Hilpert et al., 2010). Peptide 1018 was mixed separately with ppGpp, GTP, GDP, ATP, ADP or NaH_2PO_4 in 50 mM Tris buffer at pH 7.4. ppGpp was purchased from TriLink BioTechnologies and all other nucleotides were purchased from Sigma. Nucleotide concentrations ranging from 0.25 to 0.008 mM were mixed in a microtitre plate with 0.25 nmoles of peptide 1018 in a final volume of 100 μl per well. Samples were also prepared containing only peptide 1018 or the nucleotide of

interest at each concentration. The co-precipitation of peptide 1018 with a nucleotide resulted in an increase in turbidity, which was quantified by measuring the A_{620} using a Powerwave X 340 microplate reader (BioTek Instruments Inc., Winooski, VT, USA).

4.3.5 ^{31}P-NMR spectroscopy

^{31}P-NMR spectroscopy was used to evaluate the binding of peptide 1018 to ppGpp and GTP. Samples containing 0.5 mM GTP or ppGpp were prepared in buffer (10 mM Tris, 50 mM NaCl, pH 7.4) and 1 mM phosphate was added as an internal chemical shift reference as well as for quantification. Separate samples containing 0.5 mM of peptide 1018 mixed with each nucleotide were prepared in the same way. Additional samples of 0.5 mM ppGpp, GTP and ATP with 1 mM phosphate were also prepared in 6.5 M formic acid for comparison to the samples prepared from the *P. aeruginosa* PAO1 extracts (see below). All samples contained 10% D_2O. Each NMR sample was briefly centrifuged on a benchtop centrifuge (~30 s) to pellet any precipitate that formed and the supernatant liquid was used as the NMR sample. ^{31}P spectra were acquired at 25 ºC on a Bruker Avance 500 MHz spectrometer, operating at a ^{31}P frequency of 202.272 MHz. A single pulse experiment, with a 90 degree pulse of 20 µs was used, on a BB 500 probe. 4096 scans were acquired for the pure nucleotide samples while 12288 scans were accumulated for samples that contained peptide. Spectra were processed with an exponential window and line broadening of 50 Hz. To evaluate the differential binding of peptide 1018 to ppGpp or GTP, samples containing an equimolar mixture of ppGpp and GTP (both at 0.5 mM) were prepared in Tris buffer. Peptide 1018 was added to separate nucleotide mixtures to achieve final peptide concentrations of 0.25, 0.5, 0.75 and 1 mM. The samples were again centrifuged to pellet the precipitate and the resulting supernatant was used in the NMR experiments. The experiments were performed as above, but the spectra were processed with a shifted sine bell window only. The phosphorous peak signal intensity resulting from unique chemical shift peaks from either ppGpp or GTP was determined at every concentration of peptide 1018 tested.

To examine the effect of peptide 1018 on ppGpp levels *in vivo*, 3 X 20 ml cultures of PAO1 (in BM2 media with 0.5% casamino acids) were grown overnight at 37°C in the presence of SHX (500 µM) to induce the production of ppGpp. Following overnight incubation, peptide 1018 was added to a final concentration of 20 µg/ml and the sample was grown for an additional hour at 37°C. For comparison, a separate culture was prepared with

no peptide 1018 added. The PAO1 cells were harvested by centrifugation for 20 min at ~ 2000 × g in a Beckman Coulter Allegra 6 centrifuge. All three bacterial pellets were resuspended in a total of 400 µl H_2O. To prepare the NMR sample, 400 µl of the bacteria suspension was added to 500 µl of 13 M formic acid and 100 µl of D_2O. The sample was subjected to three rounds of freezing and thawing using liquid nitrogen and a room temperature water bath. The sample was centrifuged at 4°C and 14000 rpm in a microcentrifuge and 500 µl of the resulting supernatant was used as the NMR sample. Spectra were acquired as described for the pure nucleotide samples but with an accumulation of 24576 scans. All NMR experiments were performed by Dr. Evan Haney and Dr. Suzana Straus.

4.4. Results

4.4.1 Evidence for a role for the stringent response in peptide action

The basis for the broad-spectrum activity of peptide 1018 was investigated. Previous studies, based on transcriptomic and biochemical investigations, suggested that peptides LL-37 (Overhage et al., 2008) and 1037 (de la Fuente-Núñez et al., 2012) act against *Pseudomonas* by modestly inhibiting attachment and quorum sensing as well as promoting twitching motility. However, although we could show that peptide 1018 had similar modest effects on these processes, it was difficult to rationalize these mechanisms with the observed broad-spectrum activity, since these processes vary substantially within the above-described target species. Thus we considered that there might be a common mechanism and hypothesized that the peptide acted to inhibit a common stress response in target species, namely the stringent response, mediating (p)ppGpp synthesis through the enzymes RelA and SpoT.

Overproducing the potential target of a given drug is a well-established method for identifying drug targets. Here we overproduced (p)ppGpp by addition of serine hydroxamate (SHX; a structural analogue of L-serine that induces the stringent response by inhibiting charging of seryl-tRNA synthetase (Tosa and Pizer, 1971), and by IPTG induction of the cloned *relA* gene, and observed resistance against peptide 1018 (Figure 4.1A,B). First we performed checkerboard microtitre plate assays, using established methods (Yan et al., 2001), to analyze the interaction between SHX addition at time 0 and peptide 1018 treatment in more detail. Minor modifications were made to previously described methodology (Yan et al., 2001) to quantify adherent biofilm biomass (as opposed to planktonic bacterial growth) using the

crystal violet assay (de la Fuente-Núñez et al., 2012). The crystal violet-stained biofilm was resuspended using 70% ethanol and quantified using a spectrophotometer at 595 nm. Three independent experiments were performed and statistical significance was determined using Student's *t* test. At concentrations of SHX (10 µM) that did not affect *P. aeruginosa* PAO1 planktonic growth (which required 250 µM SHX to inhibit growth), we observed increased biofilm formation by nearly 2-fold (to 188 ± 0.3% cf. the SHX untreated control; $P<0.05$). In these cells the minimal biofilm inhibitory concentration (MBIC) went from 10 µg/ml (Table 3.1) to 80 µg/ml of 1018 (leading to a reduction to 8.9 ± 0.02% biofilm volume cf. the peptide untreated control; $P<0.05$; no difference was observed at 40 µg/ml of the peptide, which led to 93.2 ± 0.04% biofilm formation cf. the peptide untreated control). These results showed that peptide resistance was not due to slow growth. At 320 µM SHX, whereby biofilm production was increased nearly 4-fold (to 395 ± 0.4% cf. the SHX untreated control; $P<0.01$), 160 µg/ml 1018 was required to fully inhibit biofilm formation (reduced to 4.7 ± 0.002% cf. peptide untreated control; $P<0.01$). Thus the amount of peptide required to inhibit biofilms depended on the concentration of SHX, and therefore on the levels of (p)ppGpp, since increasing the levels of SHX resulted in peptide resistance unless a higher dose of peptide was used. While SHX by itself clearly resulted in an increase in biofilm development over the 18 to 24 h of the assay, the peptide was present in these studies even before biofilms began to develop.

These results were confirmed and extended using flow cell methods. Overproduction of (p)ppGpp by SHX treatment of *P. aeruginosa* and *S. aureus* wild-type strains led to peptide resistance (Figure 4.1A). The fold-change in biovolume of *P. aeruginosa* PAO1 biofilms treated with 20 µg/ml of peptide 1018 was 0.095 ± 0.03 ($P<0.05$) compared to untreated controls. However, adding SHX restored the ability to form biofilms in the presence of the peptide (2.6 ± 0.5 fold-increase compared to untreated samples; $P<0.05$). Similarly, the biovolume of peptide 1018-treated *S. aureus* HG001 biofilms was only 0.6% that of untreated samples, which was complemented when adding SHX (1.65 ± 0.6 fold-change compared to untreated samples; $P<0.05$). Similar results were obtained by genetic means whereby peptide resistance was increased by overproduction of (p)ppGpp in an *E. coli* strain overexpressing the cloned *relA* gene under the control of an IPTG-inducible promoter (Figure 4.1B).

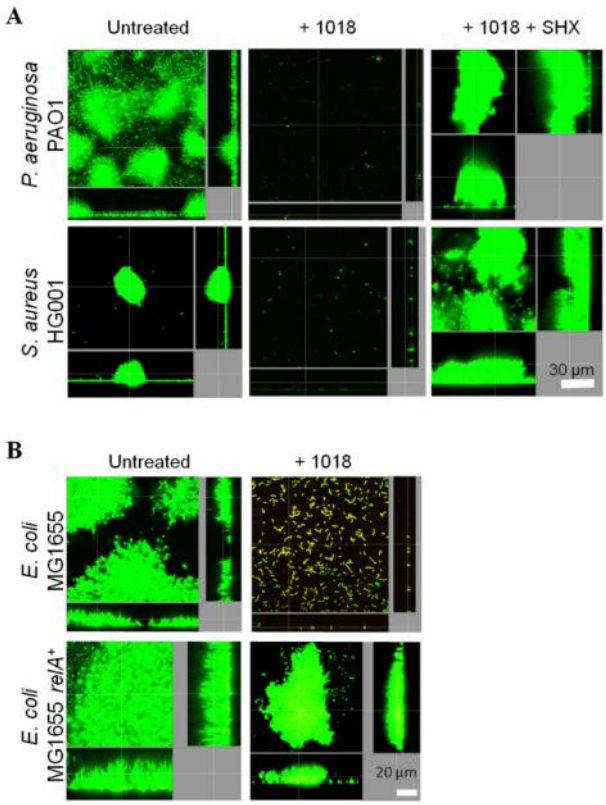

Figure 4.1. Enhanced (p)ppGpp production led to altered susceptibility of biofilms to peptides. (A) Addition of SHX, which leads to overproduction of (p)ppGpp, resulted in the resistance of biofilm development to 20 µg/ml of peptide 1018; **(B)** (p)ppGpp overproduction through *relA* overexpression led to anti-biofilm peptide resistance. **(A-B)** Inhibition of biofilm development was tested by immediately adding 20 µg/ml 1018 (± SHX or IPTG) into the flow-through medium of the flow cell apparatus and then monitoring biofilm formation for 3 days. After 3 days, bacteria were stained green with the all bacteria stain Syto-9 prior to confocal imaging. Each panel shows reconstructions from the top in the large panel and sides in the right and bottom panels (xy, yz and xz dimensions). Reprinted from: de la Fuente-Núñez C, Reffuveille F, Haney EF, Strauss SK, Hancock REW. (2014). Broad-spectrum anti-biofilm peptide that targets a cellular stress response. PLoS Pathog. 10: e1004152.

4.4.2 Role of (p)ppGpp in biofilm formation in various bacterial species

Previous studies have reported that mutants influencing (p)ppGpp production are biofilm-deficient, but not always completely defective, occasionally forming monolayers of attached cells or extremely-deficient biofilms (as opposed to well-structured biofilms) (Chávez de Paz et al., 2012; He et al., 2012; Lemos et al., 2004; Sugisaki et al., 2013; Taylor et al., 2002). To confirm that there was a correlation between the production of (p)ppGpp and biofilm production under the experimental conditions reported here, biofilm formation of (p)ppGpp-deficient mutants was compared to their respective wild-type strains in the Gram-negative

Pseudomonas aeruginosa and Gram-positive bacterium *Staphylococcus aureus* (Figure 4.2). Cells unable to synthesize (p)ppGpp showed a substantial decrease in their ability to adhere tightly to the plastic surface of flow cell chambers and were unable to develop structured biofilms, although they formed residual aggregates (Figure 4.2). Genetic complementation of the genes responsible for (p)ppGpp synthesis in *P. aeruginosa relA spoT* and *S. aureus rsh* mutants restored the full ability to form biofilms (Figure 4.2). In the un-complemented mutants (Figure 4.2), residual (p)ppGpp-deficient mutant cells appeared to be in the planktonic state as opposed to adhering to the surface, and often were dead or division-inhibited (demonstrating filaments). These poorly-attached cells could be cleared by increasing the flow rate. This might explain in part the variability in the defect in biofilm formation in mutants defective in (p)ppGpp production (i.e. due to flow rate, or other factors such as the age of the biofilms, temperature and media utilized here, which differed compared to previous reports; Balzer and McLean, 2002; Chávez de Paz et al., 2012; Lemos et al., 2004; Nguyen et al., 2011).

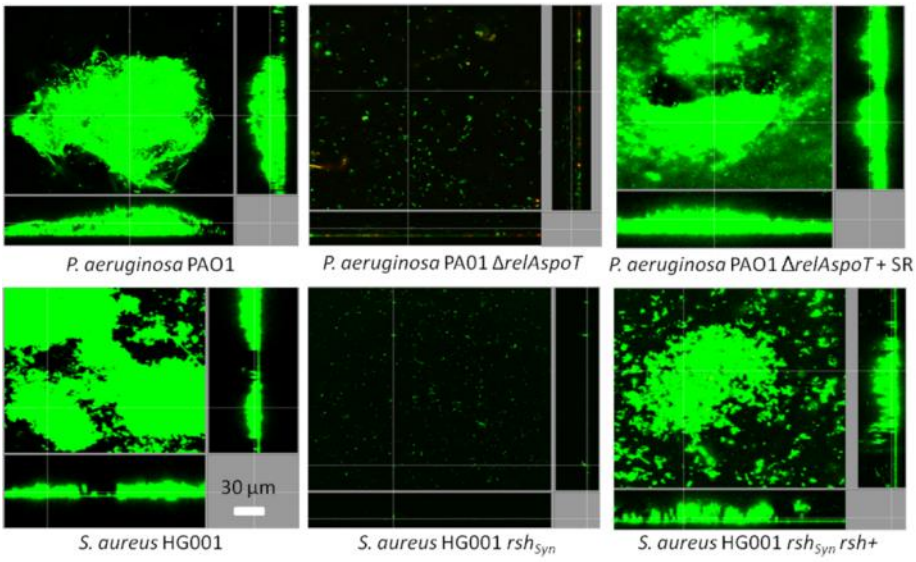

Figure 4.2. Genetic complementation of (p)ppGpp synthetase enzymes restored the ability to form biofilms. The biofilm deficiency of *Pseudomonas aeruginosa* PAO1 and *Staphylococcus aureus* HG001 (p)ppGpp mutants (Δ*relAspoT* and *rsh*$_{Syn}$ respectively) was rescued by genetic complementation [Δ*relAspoT* + *relAspoT*$^{+}$ (+SR) as described (Nguyen et al., 2011) and *rsh*$^{+}$ (Geiger et al., 2010), respectively] leading to biofilm formation equivalent to WT shown in the left-most panels. After 3 days, bacteria were stained green with the all bacteria stain Syto-9 and red with the dead-bacteria stain propidium iodide (merge shows as yellow to red) prior to confocal imaging. Each panel shows reconstructions from the top in the large panel and sides in the right and bottom panels (xy, yz and xz dimensions). Reprinted from: de la Fuente-Núñez C, Reffuveille F, Haney EF, Strauss SK, Hancock REW. (2014).

Broad-spectrum anti-biofilm peptide that targets a cellular stress response. PLoS Pathog. 10: e1004152.

4.4.3 *relA* expression modulated biofilm formation and disassembly

To further demonstrate the role of (p)ppGpp in biofilm development and maintenance, the *relA* gene was placed under the control of an *araC* promoter and cloned into *P. aeruginosa* PAO1Δ*relAspoT* such that it expressed *relA* upon arabinose induction. Biofilms of this strain that were expressing *relA* due to the introduction of arabinose into the flow medium during the 3-day experiment, were able to form well-structured biofilms (Figure 4.3A). However, when induction of *relA* was stopped at day 2 (i.e. for the last 24 h of the experiment by removal of arabinose from the flow medium), analogous to delayed treatment by peptide 1018, pre-formed biofilms were dispersed (Figure 4.3A). Indeed, we performed viable cell counts of dispersed cells from these biofilms and found that repressing *relA* expression after 2 days of continuous induction led to biofilm dispersion (Figure 4.3B), while continued induction of *relA* for the 3 days of the experiment resulted in significantly reduced dispersal levels (Figure 4.3B) that were similar to that of the wild-type strain (data not shown). These results clearly highlighted the roles that *relA*-dependent (p)ppGpp production play both in biofilm formation and in biofilm maintenance, as well as the consequences of blocking (p)ppGpp synthesis.

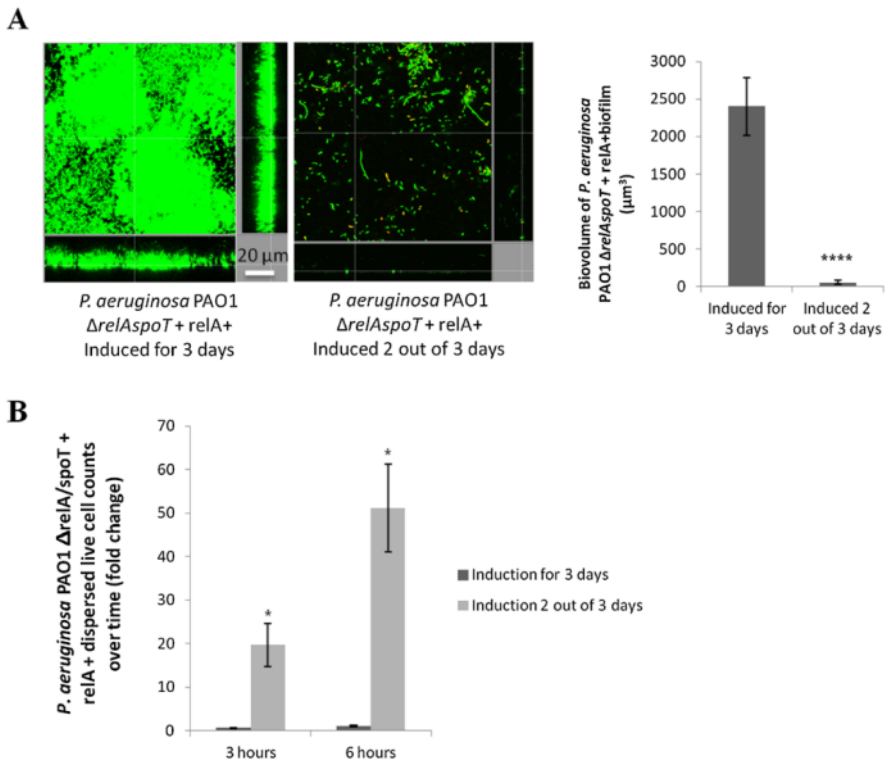

Figure 4.3. Modulation of *relA* expression impacts on biofilm development. (A) *relA* expression modulated biofilm formation and disassembly. The *relA* gene under the control of an arabinose-inducible promoter was introduced into a *P. aeruginosa* PAO1 Δ*relAspoT* background. Induction of *relA* led to biofilm formation in flow cells after 3 days. On the other hand, induction of *relA* for 2 days followed by 24 h of non-induction led to biofilm dispersal. Biofilm biovolume was calculated using Imaris software from Bitplane AG. Experiments were performed at least in triplicate. Student's *t* test was used (****, $P < 0.0001$). **(B)** Repression of *relA* expression (after 2 days of induction) led to biofilm dispersal in a *P. aeruginosa* PAO1 Δ*relAspoT* strain, while continuous induction of *relA* expression during the 3 days of the experiment resulted in significantly fewer cells dispersed from biofilms. Dispersed cells from 2-day old biofilms were collected and viable cell counts performed 3 and 6 h after induction of *relA* expression was either stopped or continued. Statistical significance was determined using Student's *t* test (*, $P < 0.05$). Reprinted from: de la Fuente-Núñez C, Reffuveille F, Haney EF, Strauss SK, Hancock REW. (2014). Broad-spectrum anti-biofilm peptide that targets a cellular stress response. PLoS Pathog. 10: e1004152.

4.4.4 Peptide 1018 prevented (p)ppGpp accumulation

The role of (p)ppGpp in the anti-biofilm mechanism of peptide 1018 was further assessed in multiple species. Direct measurement of the cellular levels of (p)ppGpp by thin layer chromatography (TLC) revealed that cells from multiple bacterial species treated with 5 µg/ml of peptide 1018 did not accumulate (p)ppGpp (Figure 4.4A). In contrast, the

conventional cationic antibiotics colistin, polymyxin B and tobramycin were unable to prevent (p)ppGpp accumulation (Figure 4.5, left panel; indeed the latter two actually increased ppGpp) or cause degradation of accumulated (p)ppGpp (Figure 4.5, right panel), thus demonstrating that these cationic antibiotics did not utilize a similar mechanism to that of peptide 1018.

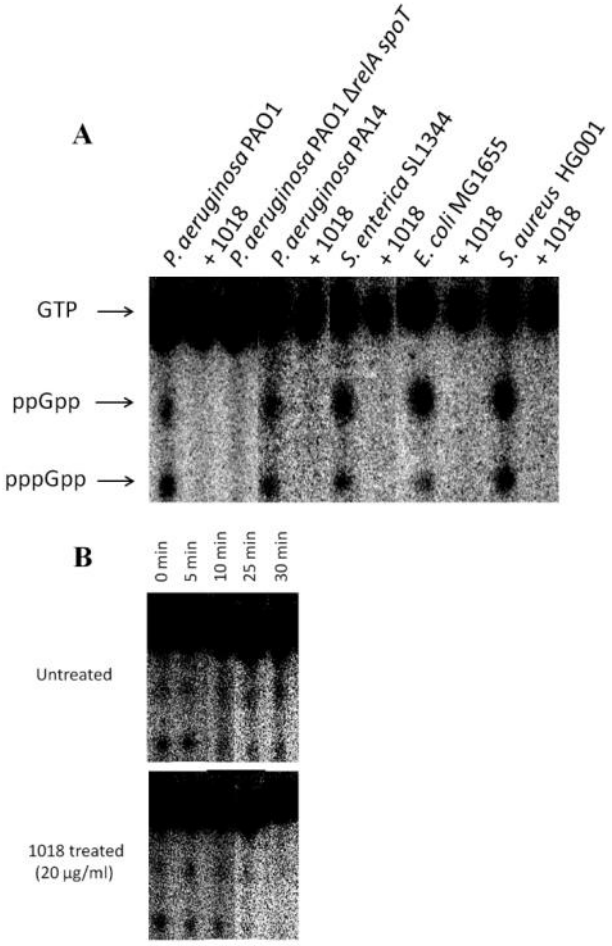

Figure 4.4. Peptide 1018 prevented (p)ppGpp accumulation *in vivo* as revealed by thin layer chromatography separation of guanine nucleotides extracted from intact cells**. (A)** Anti-biofilm peptide 1018 at 5 µg/ml directly prevented (p)ppGpp accumulation. **(B)** Treatment with peptide 1018 led to (p)ppGpp elimination within 30 min in *P. aeruginosa* PAO1 cells containing pre-accumulated (p)ppGpp due to SHX treatment. In panel **A**, bacteria were grown overnight in modified MOPS minimal medium containing 0.4% glucose, 2 mM phosphate (KH_2PO_4), and 0.2% CAA. For experiments evaluating the ability of the peptide to directly degrade (p)ppGpp in panel **B**, the cells were grown as described previously, induced with SHX and allowed to synthesize (p)ppGpp for 3 h prior to peptide treatment. After growth for both A and B, the cells were then diluted 1:20 in the same MOPS minimal medium except containing 0.4 mM phosphate (KH_2PO_4) and 500 µM serine hydroxamate (SHX) to induce (p)ppGpp synthesis, in the presence or absence of peptide 1018 and cells were labelled with

10 μCi/ml ^{32}P for 3 h. Samples were then extracted with frozen 13 M formic acid by three cycles of freeze-thaw. Aliquots of the supernatants were applied to 20×20 cm PEI cellulose TLC plates, resolved with 1.5 M KH_2PO_4, pH 3.4 for 4 h. After chromatography, nucleotides were visualized by autoradiography and quantified with a MolecularImager FX PhosphorImager and Quantity One software (Bio-Rad). Controls were performed to demonstrate that the Δ*relAspoT* mutation also prevented (p)ppGpp formation. Some of the experiments shown here were done at separate times and assembled together for the figure. Reprinted from: de la Fuente-Núñez C, Reffuveille F, Haney EF, Strauss SK, Hancock REW. (2014). Broad-spectrum anti-biofilm peptide that targets a cellular stress response. PLoS Pathog. 10: e1004152.

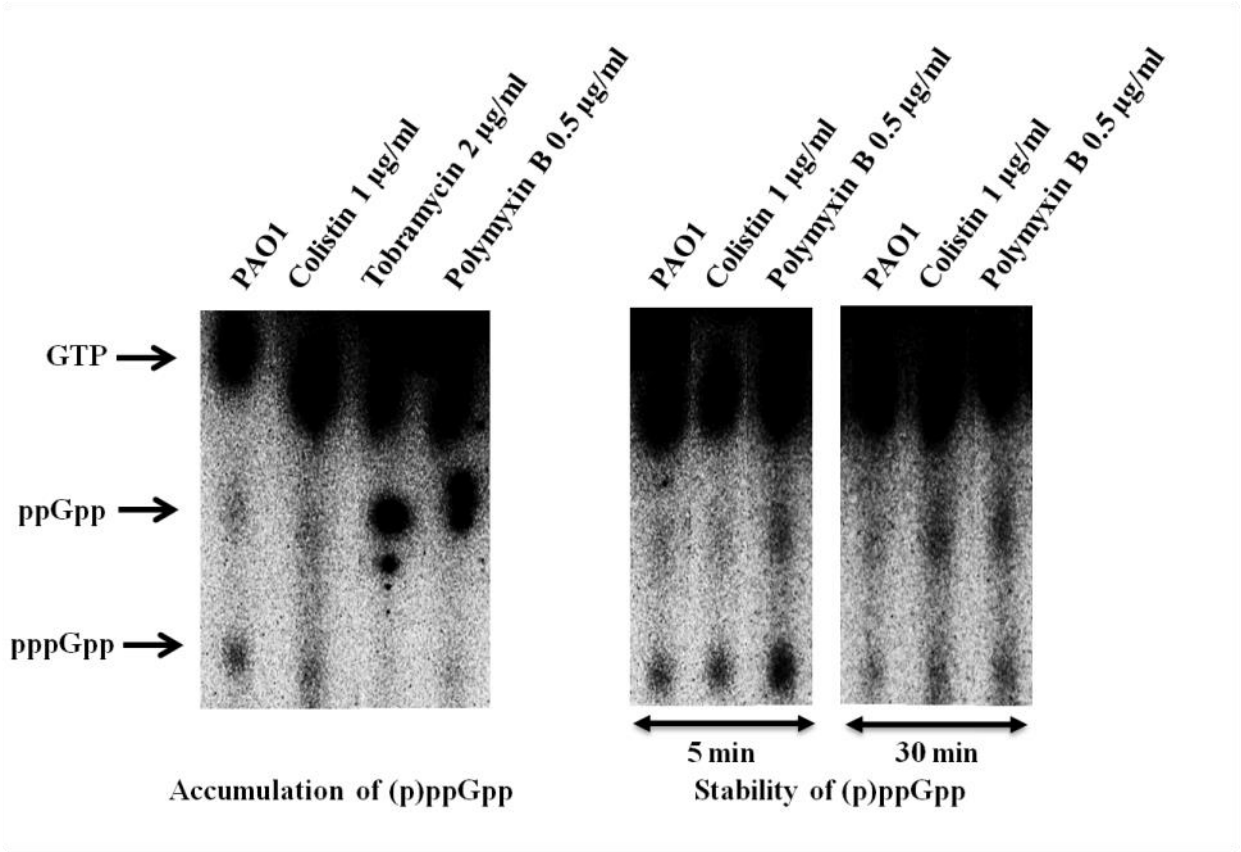

Figure 4.5. Conventional antibiotics did not prevent (p)ppGpp accumulation and did not degrade (p)ppGpp. To evaluate whether antibiotics inhibited (p)ppGpp formation they were added at the same time as SHX and (p)ppGpp pools were observed after 3 h using TLC (left panel). All antibiotics were unable to prevent ppGpp accumulation in fact both tobramycin and polymyxin B increased ppGpp levels (left panel). For degradation experiments, (p)ppGpp levels were allowed to increase by growth of cells for 3 h in the presence of SHX as described in the Methods and materials section and cells were then treated with the different antibiotics. After 5 and 30 min, levels of (p)ppGpp were determined using TLC. Treatment with colistin and polymyxin B for 30 minutes did not lead to direct degradation of (p)ppGpp (right panel). Accumulation of ppGpp upon polymyxin B treatment was more substantial in the inhibition experiments (left panel) than in the degradation experiments (right panel). Some of the experiments shown here were done at separate times and assembled together for the figure.

Reprinted from: de la Fuente-Núñez C, Reffuveille F, Haney EF, Strauss SK, Hancock REW. (2014). Broad-spectrum anti-biofilm peptide that targets a cellular stress response. PLoS Pathog. 10: e1004152.

4.4.5 Peptide 1018 bound to ppGpp and led to degradation of (p)ppGpp *in vivo*

The peptide was able to interact directly with ppGpp as demonstrated by co-precipitation (Figure 4.6A) and TLC of residual ppGpp (Figure 4.4A,B) and by nuclear magnetic resonance spectrometry (NMR) of the complexed molecules (Figure 4.6B-D), which were performed by Dr. Evan Haney and Dr. Suzana Straus. These studies further showed that peptide 1018 preferentially bound to ppGpp compared to other nucleotides such as GTP (Figure 4.6A and figure 4.7B).

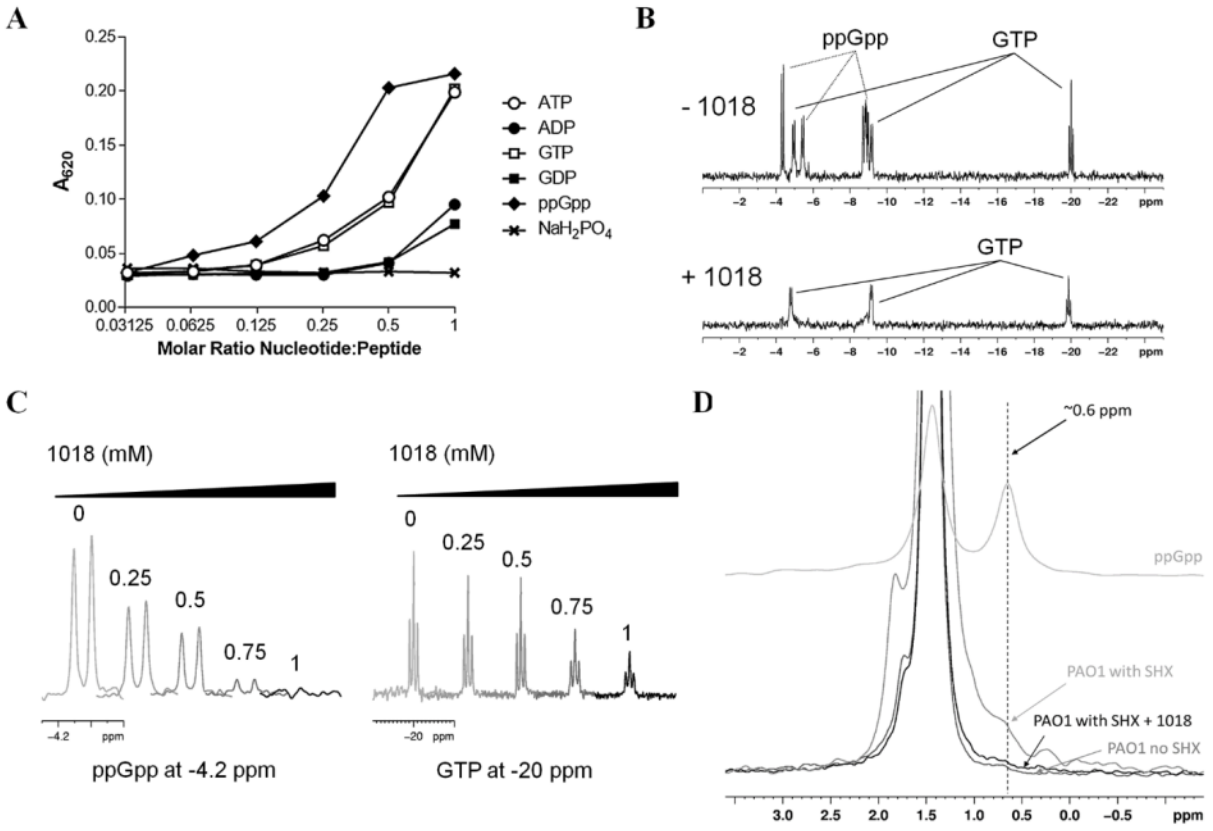

Figure 4.6. Peptide 1018 bound to ppGpp *in vitro* and led to degradation of ppGpp *in vivo*. (A) Binding of peptide 1018 to various nucleotides based on co-precipitation. Peptide 1018 (0.25 mM) was separately mixed with increasing amounts of ppGpp, GTP, ATP, GDP and ADP in buffer (50 mM Tris, pH 7.4) and the extent of co-precipitation was assessed by measuring the increase in absorbance at 620 nm. The amount of co-precipitation induced by peptide 1018 appeared to correlate with an increased negative charge on the nucleotides. A

separate sample containing NaH_2PO_4 revealed that phosphate ions did not induce precipitation of peptide 1018 in the concentration range tested. **(B)** Anti-biofilm peptide 1018 preferentially bound to ppGpp compared to GTP as revealed by ^{31}P-NMR spectroscopy. In the absence of peptide 1018 (top panel), a mixture of 0.5 mM ppGpp and 0.5 mM GTP revealed unique signals corresponding to the phosphorous atoms in ppGpp and GTP (indicated by arrows). Upon the addition of 1 mM of peptide 1018 (bottom panel), the peak intensity from the ppGpp signals was almost completely abolished, while the signals from GTP were reduced but to a lesser degree. **(C)** Samples containing an equimolar mixture of ppGpp and GTP at intermediate concentrations of 1018 were used to further evaluate the preferential binding of 1018 to ppGpp. Examination of specific spectral regions unique to ^{31}P signals from either ppGpp (~ -4.2 ppm) or GTP (~ -20 ppm) showed that the ppGpp peak intensity decreased more readily than those from GTP (peptide concentrations, in mM, are indicated above each trace). The preferential precipitation of ppGpp by peptide 1018 suggests that the peptide had a higher affinity for ppGpp over GTP under these conditions (See also figure 4.7B). **(D)** The ppGpp levels in nucleotide extracts from *P. aeruginosa* PAO1 cultures induced with SHX and treated with peptide 1018 were also measured using ^{31}P-NMR spectroscopy. In these spectra, the ppGpp phosphorous signals were shifted because of the presence of 6.5 M formic acid used to extract the nucleotides from the PAO1 cells. The chemical shifts of GTP and ppGpp in 6.5 M formic acid were determined separately using samples of pure nucleotide. Only the region from 3 ppm to -0.5 ppm is shown as this contained a unique ppGpp phosphorous peak at 0.6 ppm (for comparison, the spectra of 0.5 mM ppGpp in 6.5M formic acid is shown as the top trace). In the ^{31}P spectrum of nucleotide extracts from PAO1 induced with SHX, the ppGpp peak at 0.6 ppm appeared as a shoulder on the large phosphate peak at 1.5 ppm (middle grey trace). This shoulder was absent in samples taken from PAO1 cells grown without SHX (lowest grey trace). When PAO1 induced with SHX was treated with 20 μg/ml 1018, the ppGpp peak was essentially lost (black trace) demonstrating that the addition of 1018 to bacteria leads to the degradation of ppGpp *in vivo*. Reprinted from: de la Fuente-Núñez C, Reffuveille F, Haney EF, Strauss SK, Hancock REW. (2014). Broad-spectrum anti-biofilm peptide that targets a cellular stress response. PLoS Pathog. 10: e1004152.

The mechanism by which the peptide 1018-ppGpp interaction led to the loss of the ppGpp signal in cells was then investigated. One possibility was that the peptide sequestered the nucleotide, forming a peptide-ppGpp complex, which prevented ppGpp detection in our TLC and NMR assays. However, formic acid (used to extract nucleotides in both TLC and NMR experiments) was shown to lead to a disruption of the peptide-ppGpp complex while maintaining ppGpp in its intact form (Figure 4.7A, right panel), so this explanation seems unlikely since no free ppGpp was visible on TLC and NMR after formic acid treatment (Figures 4.4, 4.6D and 4.7A). Alternatively, peptide treatment could lead to ppGpp degradation. In agreement with this second possibility, TLC and NMR analysis of *in vivo* experiments showed that the addition of peptide led to the rapid degradation of (p)ppGpp within cells that had pre-accumulated these nucleotides (Figures 4.4B and 4.6D). In the TLC

experiments, (p)ppGpp synthesis was induced in *P. aeruginosa* PAO1 cultures by SHX for 3 h, after which 20 μg/ml of the peptide was added and the fate of (p)ppGpp was monitored over time, revealing elimination within only 30 min (Figure 4.4B). Likewise, after treatment with SHX to induce (p)ppGpp synthesis in *P. aeruginosa* PAO1 cells and then treatment with peptide for 1 h followed by extraction of nucleotides and NMR, the ppGpp peak observed in untreated cells was dramatically reduced (Figure 4.6D). Taken together, these results indicate that peptide 1018 directly and specifically interacts with (p)ppGpp and triggers its degradation, thus preventing its signaling effects within the cell (e.g. its role in biofilm development and maintenance).

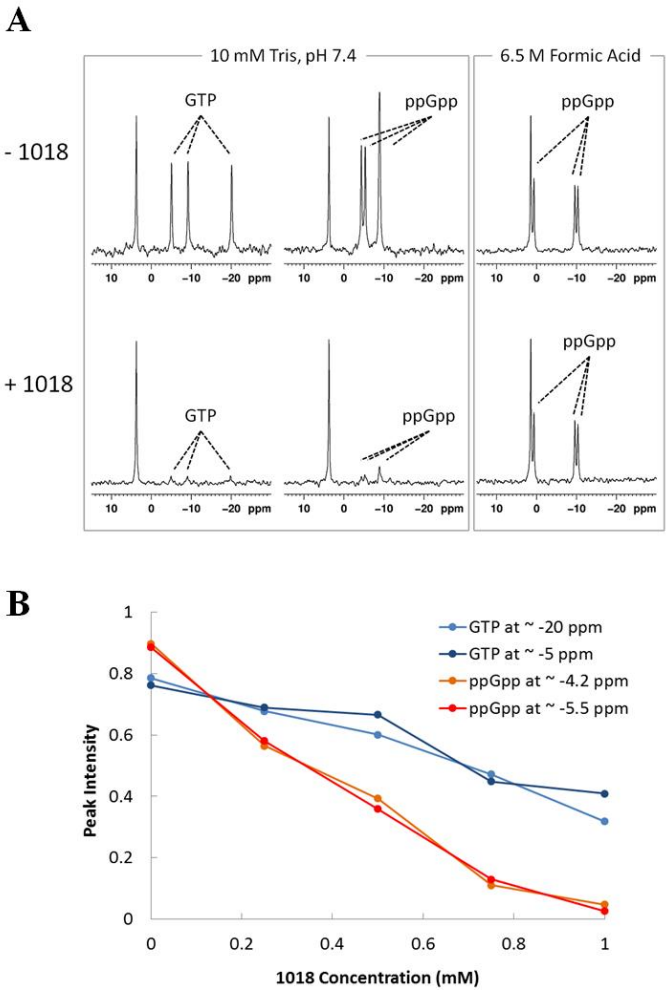

Figure 4.7. ^{31}P-NMR studies showed that peptide 1018 preferentially bound to ppGpp compared to GTP. (A) Binding of ppGpp and GTP by the anti-biofilm peptide 1018 monitored with ^{31}P-NMR. ^{31}P-NMR spectra were acquired for 0.5 mM samples of GTP or ppGpp in 10 mM Tris pH 7.4 or in 6.5 M Formic Acid (Top panel). Separate samples were prepared containing 0.5 mM nucleotide and 0.5 mM 1018 (Bottom panel). The samples were

centrifuged and the supernatant was collected and used as the NMR sample. For the samples prepared in Tris buffer, peptide 1018 precipitated GTP and ppGpp from solution resulting in a significant decrease in the amount of free nucleotide remaining in solution and a large reduction in the phosphorous signals in the ^{31}P NMR spectra (bottom panel). In contrast, no precipitate was observed between ppGpp and 1018 under acidic conditions (6.5 M formic acid). The peaks arising from the nucleotide of interest are indicated while the unlabelled peak corresponds to the 1 mM NaH_2PO_4 added to the sample as an internal standard. **(B) Effect of increasing amounts of 1018 on the ^{31}P-NMR signal intensities arising from ppGpp and GTP in NMR samples containing an equimolar mixture of both nucleotides (0.5 mM each).** Peak intensities were measured as a relative value compared to the internal reference peak of 1 mM phosphate at ~ 4 ppm. The preferential precipitation of ppGpp over GTP by 1018 is evident from the larger decrease in ppGpp phosphorous signals (at -4.2 and -5.5 ppm) compared to the GTP signals (at -5 and -20 ppm). It should be noted that the ppGpp and GTP phosphorous signals at approximately 9 ppm overlapped with one another and could therefore not be examined in this manner. Reprinted from: de la Fuente-Núñez C, Reffuveille F, Haney EF, Strauss SK, Hancock REW. (2014). Broad-spectrum anti-biofilm peptide that targets a cellular stress response. PLoS Pathog. 10: e1004152.

4.5 Discussion

The results described here indicate that the broad-spectrum anti-biofilm activity of peptide 1018 was due to its ability to depress (p)ppGpp levels in live bacterial cells. Previous studies have suggested that the stringent response might be involved in biofilm formation (Aberg et al., 2006; Balzer and McLean, 2002; Chávez de Paz et al., 2012; He et al., 2012; Lemos et al., 2004; Sugisaki et al., 2013; Taylor et al., 2002), although some controversy exists as to whether this may be due to the particular experimental conditions used, particularly flow rate and age of the biofilms examined. The stringent response is induced in reaction to bacterial stresses such as amino-acid starvation, fatty acid, iron or nutritional limitation, heat shock, and other stress conditions. It is signaled by the alarmone (p)ppGpp, and modulates transcription of up to one third of all genes in the cell. Conceptually it is designed to divert resources away from growth and division and toward metabolism in order to promote survival. Its specific role in biofilm formation is not known but it may be involved in initiating and/or perpetuating biofilm development. In addition, the results presented here indicate that it may actually suppress the tendency of biofilms to disperse (Figure 4.3), and even promote viability in adhered cells. Consistent with its effects on biofilms, *in vivo* studies have shown that (p)ppGpp-deficient mutants are easily cleared by the host, unable to establish chronic infections, incapable of long-term survival and overall more susceptible to exogenous stresses than their parent strains (Dahl et al., 2003; Vogt et al., 2011). Interestingly, various classes of

antibiotics are known to induce (p)ppGpp synthesis (Cortay and Cozzone, 1983; Erlich et al., 1971; Ikehara et al., 1985; Khan and Yamazaki, 1972; Figure 4.5), which in turn leads to antibiotic adaptive resistance (Nguyen et al., 2011; Gilbert et al., 1990). Importantly, recent efforts have identified molecules that target the stringent response (Wexselblatt et al., 2012).

In this Chapter it was demonstrated that peptide 1018, which triggers the degradation of the (p)ppGpp signal within the cell, acts as a broad-spectrum biofilm inhibitor. Given the importance of biofilms in human medicine, constituting at least 65% of all infections, and increasing antibiotic resistance which in biofilms is adaptive and broad spectrum, such a peptide offers considerable potential in the fight against the burgeoning resistance to antibiotics. Peptides with biofilm inhibitory activities have been previously identified (de la Fuente-Núñez et al., 2012; Overhage et al., 2008; Pompilio et al., 2011). However, the mechanism of action by which these peptides selectively target and kill biofilm cells of both Gram-negative and Gram-positive bacteria was previously postulated to involve changes in motility, adherence and quorum sensing (Chapter 2; Overhage et al., 2008), which are all species-specific and thus did not satisfactorily explain the action of peptide 1018 against a broad range of pathogens. In this Chapter evidence is provided that an anti-biofilm peptide, 1018, potently inhibited biofilm formation and eradicated existing mature biofilms in a broad-spectrum manner, through a direct interaction with ppGpp, which led to its degradation in live bacterial cells. The proposed mechanism of action involves direct contact between peptide 1018 and (p)ppGpp so the peptide must be able to cross the cell membranes to reach the cytoplasm. Previous studies have demonstrated that amphipathic cationic peptides, like 1018, have the characteristics of so-called cell penetrating peptides that are able to freely translocate across membranes (Fjell et al., 2011).

The peptide had at least three effects on biofilms, which might reflect the role of (p)ppGpp in cells. First when added prior to initiation of biofilms it prevented biofilm formation, second it specifically led to cell death in biofilms at concentrations that were not lethal for planktonic (free-swimming) cells (Table 3.1; Figs. 3.1 and 3.2), and third it promoted biofilm dispersal even in maturing (2-day old) biofilms (Figure 3.2), effects that were in fact reciprocated in mutants unable to accumulate (p)ppGpp (Figure 4.3). We suggest that the ability to cause cell death in biofilms might have been due to inhibition of cell wall biosynthesis and triggering of murine hydrolases, a known tendency for antimicrobial peptides (Friedrich

et al., 2000). Critically we propose that this is due in part to the impact of the stringent response in bacteria growing in the biofilm state, since stringent response is known to influence susceptibility to cell wall specific antibiotics, presumably through effects on cell wall synthesis (Gilbert et al., 1990), while the lack of ppGpp leads to cell death through the Slt soluble lytic transglycosylase (Betzner et al., 1990). Consistent with this, both peptide-treated biofilms and (p)ppGpp deficient mutants grown in flow cells demonstrated increased bacterial cell filamentation and cell lysis/death (Figures 3.1, 3.2 and 4.3).

Previous studies have demonstrated that the structure-activity relationships of anti-biofilm peptides vary substantially from antimicrobial peptides (de la Fuente-Núñez et al., 2012) despite certain common features (being amphipathic molecules with excess cationic and hydrophobic amino acids). Consistent with this, peptide 1018 was able to potently inhibit *Burkholderia cenocepacia* biofilms, despite the fact that this species is completely resistant to all antimicrobial peptides. Thus we have an opportunity to now develop more active peptides that have even more potent anti-biofilm activity. Indeed we have recently started to isolate such peptides and obtained preliminary evidence that they also act by inhibiting the stringent response.

4.6 Summary

Bacteria colonize most environments, including the host by forming biofilms, which are extremely (adaptively) resistant to conventional antibiotics. Biofilms cause at least 65% of all human infections, being particularly prevalent in device-related infections, infections on body surfaces and in chronic infections. Currently there is a severe problem with antibiotic-resistant organisms, given the explosion of antibiotic resistance whereby our entire arsenal of antibiotics is gradually losing effectiveness, combined with the paucity of truly novel compounds under development or entering the clinic. Thus the even greater resistance of biofilms adds to the major concerns being expressed by physicians and medical authorities. Consequently, there is an urgent need for new strategies to treat biofilm infections and we demonstrate in the present study an approach, based on the inhibition of (p)ppGpp by a small peptide, that eradicates biofilms formed by 4 of the so-called ESKAPE pathogens, identified by the Infectious Diseases Society of America as the most recalcitrant and resistant organisms in our society. The strategy presented here represents a significant advance in the search for new agents that specifically target bacterial biofilms.

Chapter 5: D-enantiomeric peptides that target bacterial biofilms formed by multidrug-resistant Gram-negative pathogens

5.1. Overview

Bacteria primarily exist in multicellular communities known as biofilms that are more resistant to antibiotics than their planktonic counterparts. Currently, there are no antimicrobial drugs available that specifically target biofilms. Despite the identification in earlier Chapters of peptides with excellent activities one of the potential deficits of such peptides is their susceptibility to proteases that abound at infection sites. Here, I identified several short D-enantiomeric, proteolytically stable peptides that even more potently inhibited biofilm development and eradicated pre-formed biofilms of multiple species of antibiotic resistant Gram-negative pathogens. The most potent peptides DJK-5 and DJK-6 effectively synergized with conventional antibiotics to treat bacterial biofilms. Indeed, these peptides reduced the concentrations of antibiotics required to inhibit biofilms by up to 64-fold. Furthermore, these lead peptides prevented the accumulation of (p)ppGpp, which was shown in Chapter 4 to be involved in biofilm development, and overproduction of (p)ppGpp by serine hydroxamate treatment led to reduced susceptibility of *Pseudomonas aeruginosa* biofilms to the peptide. In addition, both DJK-5 and DJK-6 protected the invertebrate organisms *Caenorhabditis elegans* and *Galleria mellonella* from *P. aeruginosa* biofilm infections.

5.2. Introduction

Bacteria predominantly form biofilms when growing on surfaces or at air-liquid interfaces (Costerton et al., 1999; de la Fuente-Núñez et al., 2013; López et al., 2010; O'Toole et al., 2000). Biofilms are encased in a protective extracellular matrix that contains water, polysaccharides, proteins, extracellular DNA and lipids (de la Fuente-Núñez et al., 2013; López et al., 2010). The transition from a planktonic to a biofilm lifestyle results in increased resistance to exogenous stresses including conventional antimicrobial therapy and host defense mechanisms (Davies, 2003; de la Fuente-Núñez et al., 2013; O'Toole et al., 2000). Therefore, biofilms are extremely difficult to treat with currently available antimicrobial agents. Indeed biofilms play an important role in the pathogenesis of numerous bacterial species because of their ability to persist on medical devices and in the host (Costerton et al., 1999; de la Fuente-Núñez et al., 2013).

In Chapters 2-4, cationic synthetic peptides with anti-biofilm activity were identified and characterized. Intriguingly, although these peptides seem superficially similar to the cationic antimicrobial peptides (that are active against planktonic bacteria), being short in size (12-50 amino acids long), and containing cationic amino acids (2 to 9 Arg or Lys residues) and a high proportion of hydrophobic residues (~50%), these activities can be clearly distinguished. Indeed, peptides with good anti-biofilm but little anti-planktonic activity have been demonstrated and vice versa (Chapters 2 and 3). Furthermore these peptides were active against *B. cenocepacia* biofilms even though planktonic *B. cenocepacia* are completely resistant to antimicrobial peptides. In Chapter 4, a broad-spectrum anti-biofilm peptide (peptide 1018) was shown to act by binding to and triggering the degradation of the stress-related second messenger nucleotides guanosine penta- and tetra- phosphate [(p)ppGpp], which play an important role in biofilm development in many bacterial species.

One limiting feature of the peptides made to date is that they are extremely labile to proteases that abound in the body, especially at sites of wounding, infection and inflammation. Therefore, novel short protease-resistant D-enantiomeric, peptides were tested and shown to have potent, broad-spectrum anti-biofilm activity, being up to 10-fold more potent than previously identified peptides. The lead anti-biofilm peptides DJK-5 and DJK-6 synergized with different classes of conventional antibiotics to prevent biofilm formation and led to the disassembly of pre-existing biofilms. These peptides also acted by inhibiting the accumulation of (p)ppGpp. Additionally, these peptides exhibited anti-biofilm activity *in vivo* as they protected the nematode *Caenorhabditis elegans* and the insect *Galleria mellonella* from *Pseudomonas aeruginosa* biofilm infections.

5.3. Methods and materials

5.3.1 Bacterial strains

Strains utilized included wild-type strains of *Pseudomonas aeruginosa* PA01 and PA14, *Burkholderia cenocepacia* genomovar IIIa isolate from a CF patient (Vancouver Children's Hospital clinical isolate 4813), *Escherichia coli* 0157, *Klebsiella pneumoniae*, multidrug-resistant *Acinetobacter baumannii* SENTRY C8 (a polymyxin B resistant blood clinical isolate from the U.S.A. obtained through the SENTRY surveillance system), and

Salmonella enterica serovar Typhimurium isolate 14028S were used.

5.3.2 Peptide Synthesis

All D-enantiomeric peptides were synthesized by CPC Scientific using solid-phase 9-fluorenylmethoxy carbonyl (Fmoc) chemistry and purified to a purity of ~95% using reverse-phase high-performance liquid chromatography. Peptide mass was confirmed by mass spectrometry.

5.3.3 BioFlux microfluidic studies

BioFlux studies were performed in collaboration by Dr. Shauna Reckseidler-Zenteno on peptides developed in the Hancock laboratory, as previously described (Benoit et al., 2010). Strains *Klebsiella pneumoniae* strain LM21 *gfp* (Balestrino et al., 2005) and *Pseudomonas aeruginosa gfp* were used. For biofilm experiments, LB cultures were grown to an OD_{620} of ~ 0.5. A BioFlux™ and associated 48-well flow-channel plates (Fluxion P/N 950-0010) were then used to support the growth of bacterial biofilms. To promote slow and even biofilm development while curtailing growth disruptive bubble formation within growth channels, degassed tryptic soy broth (TSB) diluted to 0.1 x working concentration was utilized as the assay medium. Channels were then primed using 100 µl of assay media, seeded for ~5 seconds using the prepared bacterial culture, and incubated with no flow for ~45 minutes to allow bacterial attachment. Following incubation, the remaining culture in the outlet wells was emptied and these wells were rinsed multiple times with sterile assay media. One ml of diluted synthetic peptide suspension was added to the inlet wells at the beginning of biofilm growth. Shear flow was applied at 5 dynes/cm^2 overnight. Negative and positive controls were established by adding 1 ml of 70% isopropanol and assay media to the flow channels. Inlet wells were topped off with media and outlet wells emptied every 6 to 8 hours as required. Biofilm development was periodically checked via brightfield microscopy. At the end of the experiment, channels were emptied of media and the outlet wells washed as described above. Detection of non-viable cells required the application of the fluorescent dead-cell stain propidium iodide (PI), a membrane impermeant, nucleic acid intercalating agent, as described (de la Fuente-Núñez et al., 2014). One hundred µl of 30 µM PI (Molecular Probes® 1304MP) and 0.85% saline were added to the inlet and outlet wells, respectively. Subsequently a shear flow was applied at 0.75 dynes/cm^2 for ~15 minutes. Excess dye was cleared from the system by emptying all wells and adding fresh saline, from inlet to outlet, at above shear flow for 20

minutes. Expression of GFP and staining by PI, allowed for differentiation and quantification of viable and non-viable cells. A Nikon Eclipse Ti inverted epifluorescence scope and associated digital camera were utilized for biofilm visualization and micrograph collection. Micrographs of each biofilm were obtained through bright-field (general observations), green fluorescent channel (GFP; viable cells), and red fluorescent channel (propidium iodide; non-viable cells) modes at identical positions and planes. Quantitative green and red fluorescent intensity data was extracted from the micrographs using Montage Offline (Fluxion 940-0004). GFP intensity values were compared against total micrograph fluorescence to determine percent viable cells. ImageJ (version 1.46) software (National Institutes of Health) was used to pseudo-colour representative micrographs from original black and white; no quantitative image parameters were modified.

5.3.4 Minimal Inhibitory Concentration (MIC, $MBIC_{50}$) assays

The broth microdilution method with minor modifications for cationic peptides (de la Fuente-Núñez et al., 2014; Wiegand et al., 2008) was used for measuring the MIC of all D-enantiomeric peptides used. The MIC was defined as the lowest concentration of peptide at which no planktonic growth was observed. Minimal biofilm inhibitory concentrations leading to 50% decrease in biofilm growth ($MBIC_{50}$) were obtained using 96-well plate assays and crystal violet staining of adherent biofilms as previously described (de la Fuente-Núñez et al., 2012).

5.3.5 Biofilm growth conditions in checkerboard assays

The medium used was generally LB, except for *Salmonella enterica* serovar Typhimurium isolate 14028S that was grown in BM2 minimal glucose medium (62 mM potassium phosphate buffer, pH 7.0, 7 mM [$(NH_4)_2SO_4$, 2 mM $MgSO_4$, 10 μM $FeSO_4$] containing 0.4% (wt/vol) glucose as a carbon source and 0.5% casamino acids. *Klebsiella pneumoniae* was grown in Todd Hewitt broth medium containing 0.4% yeast extract. Bacteria were grown for 24 h in all cases, except for *K. pneumoniae* that was allowed to grow for 48 h. In checkerboard assays, the MBIC values represented the concentration (or combinations of concentrations when using peptides in combination with antibiotic) at which 100 % biofilm inhibition was observed. The result was expressed as the fractional inhibitory concentration (FIC) index, calculated as follows: $FIC = [A]/MBIC_A + [B]/MBIC_B$, where $MBIC_A$ and $MBIC_B$ are the MBICs of peptides A and B alone and [A] and [B] are the MBICs of A and B

when in combination. An FIC index of 0.5 is considered to indicate good synergy (representing the equivalent of a four-fold decrease in the MBIC of each compound when used in combination). An FIC index of 1.0 represents additive activity (a two-fold decrease in the MBIC of each compound in combination), and an index of >4 would be indicative of antagonism.

5.3.6 Biofilm cultivation in flow cell chambers and microscopy

As described in detail in Chapters 2-3, biofilms were grown for 72 h, in the absence or presence of the desired concentration of peptides DJK-5, DJK-6 and/or the different antibiotics tested, at 37°C in flow chambers prior to live-dead staining and confocal microscopy. For treatment of pre-formed biofilms, bacteria were allowed to develop structured 2-day-old biofilms prior to peptide treatment for the following 24 h prior to live-dead staining and confocal microscopy.

5.3.7 (p)ppGpp measurement by thin layer chromatography

Bacteria were grown overnight in modified MOPS minimal medium containing 0.4% glucose, 2 mM phosphate (KH_2PO_4), and 0.2% CAA. The cells were then diluted 1:20 in the same MOPS minimal medium except containing 0.4 mM phosphate (KH_2PO_4) and 500 μM serine hydroxamate (SHX) to induce (p)ppGpp synthesis, in the presence or absence of peptides DJK-5 and DJK-6 and cells were labelled with 10 μCi/ml ^{32}P for 3 h. Subsequent processing of samples was as described in Chapter 4.

5.3.8 Strains and culture conditions for *in vivo* experiments

P. aeruginosa PAO1 was cultured in Mueller-Hinton broth (MH; Oxoid, Basingstoke, England) at 37°C. *Escherichia coli* OP50 was grown in TSB (Oxoid) at 37°C. *Caenorhabditis elegans* N2 (*glp-4*; *sek-1*) was propagated under standard conditions, synchronized by hypochlorite bleaching, and cultured on nematode growth medium using *E. coli* OP50 as a food source (Cooper et al, 2009; Stiernagle, 2006). Adult *Galleria mellonella* larvae (De Poorter, Gent, Belgium) were stored in wood chips at 15°C in darkness prior to use. Larvae weighing between 200 and 300 mg were used for all experiments.

5.3.9 *Caenorhabditis elegans* survival assay

The *C. elegans* survival assay was carried out in collaboration by Gilles Brackman and Tom Coeyne, U. Gent, as previously described (Brackman et al., 2011). In brief, synchronized

worms (L4 stage) were suspended in a medium containing 95% M9 buffer (3 g of KH_2PO_4, 6 g of Na_2HPO_4, 5 g of NaCl, and 1 ml of 1 M $MgSO_4 \cdot 7H_2O$ in 1 liter of water), 5% brain heart infusion broth (Oxoid), and 10 μg of cholesterol (Sigma-Aldrich) per ml. 0.5 ml of this suspension of nematodes was transferred to the wells of a 24-well microtitre plate. An overnight bacterial culture was centrifuged, resuspended in the assay medium, and standardized to 10^8 CFU/ml. Next, 250 μl of this standardized suspension were added to each well, while 250 μl of sterile medium was added to the positive control. Peptides were added to the test wells at a final concentration of 20 μg/ml. The assay plates were incubated at 25°C for up to 2 days. The fraction of dead worms was determined by counting the number of dead worms and the total number of worms in each well, using a dissecting microscope. Peptides were tested at least four times in each assay, and each assay was repeated at least three times ($n \geq 12$).

5.3.10 *G. mellonella* survival assay

The *G. mellonella* survival assay was carried out in collaboration by Gilles Brackman and Tom Coeyne, U. Gent, as previously described (Brackman et al., 2011). In brief, prior to injection in *G. mellonella*, bacterial cells were washed with PBS and then diluted to either 10^4 or 10^5 CFU per 10 μl. A Hamilton syringe was used to inject 10 μl in the *G. mellonella* last left proleg. The peptides (20 μg/10 μl) were administered by injecting 10 μl into a different proleg within 1 h after injecting the bacteria. Two control groups were used: the first group included uninfected larvae injected with PBS to monitor killing due to physical trauma; the second group included uninfected larvae receiving no treatment at all. Results from experiments in which one or more larvae in either control group died were discarded and the experiments were repeated. To evaluate the toxicity of the peptides, uninfected larvae were injected with peptides. Larvae were placed in the dark at 37°C and were scored as dead or alive 24 h and 48 h post-infection. Larvae were considered dead when they displayed no movement in response to shaking or touch. At least 20 larvae were injected for each treatment. For each treatment, data from at least six independent experiments were combined.

5.4 Results

5.4.1 D-enantiomeric peptide screen

With regards to the activity of antimicrobial peptides against planktonic organisms, in

many, but not all, cases one observes similar activity for the L- and D- amino acid enantiomers (Epand and Vogel, 1999). This has been taken to indicate that there is no receptor-mediated event involved in activity. Conversely similar activities for L- and retro-inverso (D- amino acids in reversed sequence) peptides of the same sequence can be consistent with receptor-mediated events since e.g. in an α-helix, despite the different rotation of the backbone, all side chains would end up in the same position in 3-dimensional space. Earlier peptide screening studies showed anti-biofilm activity to be completely independent of activity against planktonic cells and to involve both translocation into cells and interaction with the stress signal (p)ppGpp (Chapters 2-4). Here the impact of making both retro (D-amino acid) and retro inverso versions of a series of peptides conceptually related to anti-biofilm peptide 1018 was tested in collaboration with Dr. Shauna Reckseidler-Zenteno, Athabasca University, using the high throughput BioFlux apparatus (Benoit et al., 2010).

Intriguingly there was no obvious relationship between peptide enantiomeric composition and activity (Table 5.1). For example while the retro-inverso version of peptide 1018 retained pseudomonal anti-biofilm activity, it lost activity against *Klebsiella* biofilms. Conversely, RI-1002 was quite active but the L-version of this peptide was inactive. Overall the D-amino acid versions of the peptides tended to be more active, but there was substantial variability in activity between the D- and RI versions of several peptides. These data thus indicate that there is no simple relationship between enantiomeric composition or primary sequence and activity. Nevertheless because the D-versions of peptides tended to be more active and had the advantage of being protease resistant, it was decided to further evaluate these.

Table 5.1. Screen to assess the anti-biofilm activity of D-enantiomeric peptides against *Pseudomonas aeruginosa* and *Klebsiella pneumonia* using the BioFlux microfluidics system. Percentages represent proportion of dead cells cf. total number of cells in the biofilm population after treatment with 10 μg/ml of the different peptides at the beginning of biofilm growth, as detailed in the Experimental Procedures section. Hyphens (-) denote conditions that were not tested. BioFlux studies were done in collaboration with Dr. Shauna Reckseidler-Zenteno.

Peptide name	Type of peptide	Sequences (all peptides amidated)	% Biofilm Inhibition @ 10 μg/ml	
			Pa	Kp
L1018	Normal	VRLIVAVRIWRR	99	99
RI-1018	Retro-inverso	RRWIRVAVILRV	95	5
L1012	Normal	IFWRRIVIVKKF	41	1
RI1012	Retro-inverso	FKKVIVIRRWFI	95	0

Peptide name	Type of peptide	Sequences (all peptides amidated)	% Biofilm Inhibition @ 10 μg/ml	
			Pa	Kp
L1002	Normal	VQRWLIVWRIRK	7	0
RI1002	Retro-inverso	KRIRWVILWRQV	72	73
LJK1	Normal	VFLRRIRVIVIR	6	1
DJK1	D-Enantiomer	VFLRRIRVIVIR	85	87
RI-JK1	Retro-inverso	RIVIVRIRRLFV	0	-
LJK2	Normal	VFWRRIRVWVIR	43	-
DJK2	D-Enantiomer	VFWRRIRVWVIR	87	-
RIJK2	Retro-inverso	RIVWVRIRRWFV	91	91
LJK3	Normal	VQLRAIRVRVIR	0	-
RIJK3	Retro-inverso	RIVRVRIARLQV	100	99
DJK3	D-Enantiomer	VQLRAIRVRVIR	45	-
LJK4	Normal	VQLRRIRVWVIR	96	0
RIJK4	Retro-inverso	RIVWVRIRRLQV	99.8	71
DJK4	D-Enantiomer	VQLRRIRVWVIR	99	99
LJK5	Normal	VQWRAIRVRVIR	0	-
RI-JK5	Retro-inverso	RIVRVRAIRWQV	0	-
DJK5	D-Enantiomer	VQWRAIRVRVIR	99.7	99.8
LJK6	Normal	VQWRRIRVWVIR	69	0
RIJK6	Retro-inverso	RIVWVRIRRWQV	74	92
DJK6	D-Enantiomer	VQWRRIRVWVIR	98.4	98

Six of the more active D-enantiomeric peptides (Table 5.2) were screened for their relative ability to inhibit biofilm formation by the bacterial pathogen *P. aeruginosa* strain PA14. Analogous to previously reported anti-biofilm peptides (Chapters 2 and 3), these peptides exhibited modest direct antimicrobial activity (MIC) but relatively high anti-biofilm activity ($MBIC_{50}$). Peptides DJK-5 and DJK-6 were identified as the most active anti-biofilm peptides obtained to date as they had $MBIC_{50}$ values vs. *P. aeruginosa* of 1 μg/ml and 0.5 μg/ml, respectively (Table 5.2).

Table 5.2. Characterization of the most potent D-enantiomeric peptides against *Pseudomonas aeruginosa* PA14 biofilms. $MBIC_{50}$ values were determined using the 96-well plate biofilm assay and correspond to the ability of the peptides to prevent biofilm formation by 50%. The lowest $MBIC_{50}$ values obtained are shown in bold.

Peptide name	Amino acid sequence	MIC (μg/ml)	$MBIC_{50}$ (μg/ml)
DJK1	VFLRRIRVIVIR	20	10
DJK2	VFWRRIRVWVIR	10	5
DJK5	VQWRAIRVRVIR	16	**1**
DJK6	VQWRRIRVWVIR	16	**0.5**
RI-1002	KRIRWVILWRQV	10	5

Peptide name	Amino acid sequence	MIC (µg/ml)	$MBIC_{50}$ (µg/ml)
RI-1018	RRWIRVAVILRV	20	10

To confirm these results, the more sensitive flow cell method was used to assess the activity of these peptides on *P. aeruginosa* PA14 biofilms. Peptides were added to the flow medium in one of two ways: (1) Inhibition studies included 2.5 µg/ml of either DJK-5 or DJK-6 (well below their planktonic MICs of 16 µg/ml) from the beginning of biofilm growth and for the duration of the entire 3 days of the experiment; (2) Eradication studies were performed in which the same peptide concentration (2.5 µg/ml) was added after 2 days of biofilm formation when the biofilm structure was already evident. These studies showed that the peptides DJK-5 and DJK-6 were able to fully prevent biofilm formation in inhibition studies (Figure 5.1, center panels) and completely or partially disperse and kill *P. aeruginosa* PA14 mature biofilms (Figure 5.1, right panels).

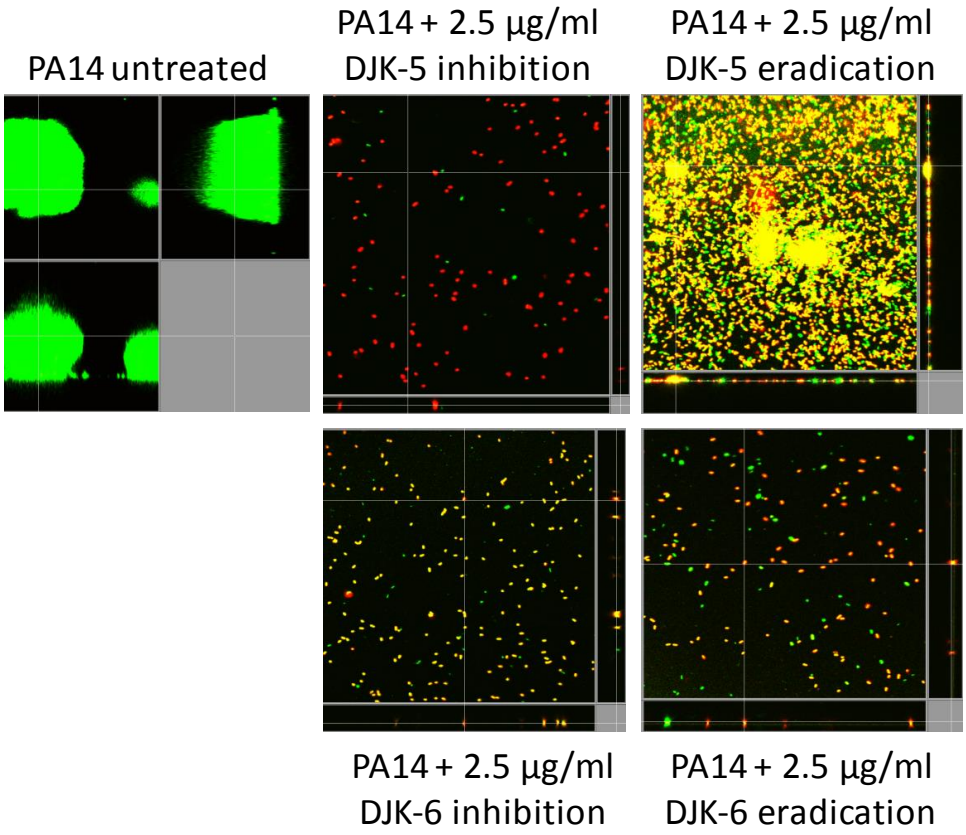

Figure 5.1. D-enantiomeric peptides completely prevented biofilm formation and eradicated *P. aeruginosa* biofilms. Sub-MIC concentrations (2.5 µg/ml) of peptides DJK-5

and DJK-6 were used. Inhibition of biofilm development was tested by immediately adding peptide into the flow-through medium of the flow cell apparatus and then monitoring biofilm formation for 3 days. Eradication conditions involved waiting two days before addition of either peptide into the flow-through medium. After 3 days, bacteria were stained green with the all bacteria stain Syto-9 and red with the dead-bacteria stain propidium iodide (merge shows as yellow to red) prior to confocal imaging. Each panel shows reconstructions from the top in the large panel and sides in the right and bottom panels (xy, yz and xz dimensions).

5.4.2 D-enantiomeric peptides exhibited broad-spectrum anti-biofilm activity

The spectrum of activity of the most active anti-biofilm peptides DJK-5 and DJK-6 was determined. In all cases both peptides prevented biofilm growth at levels below the MIC (Table 5.3). DJK-5 inhibited biofilms at concentrations ranging from 0.4 μg/ml to 2 μg/ml, while DJK-6 was most effective against *P. aeruginosa* PA14 (0.5 μg/ml) and showed less activity against enterohemorrhagic *Escherichia coli* isolate 0157 (8 μg/ml) (Table 5.3). Interestingly, the peptides did not affect planktonic growth of a clinical isolate of *Burkholderia cenocepacia*, known to be completely resistant to antimicrobial peptides, (MIC>256 μg/ml for DJK-5 and MIC>64 μg/ml for DJK-6), but inhibited biofilms of this multidrug-resistant strain at only 0.4 μg/ml and 2 μg/ml, respectively.

Table 5.3. Antimicrobial (MIC) and anti-biofilm ($MBIC_{50}$) activities of D-enantiomeric peptides DJK5 and DJK6. MIC refers to the concentration of peptide that results in 100% inhibition of planktonic growth. $MBIC_{50}$ corresponds to the peptide concentration that results in 50% biofilm inhibition.

Bacterial strains	DJK5		DJK6	
	MIC (μg/ml)	$MBIC_{50}$ (μg/ml)	MIC (μg/ml)	$MBIC_{50}$ (μg/ml)
Pseudomonas aeruginosa PA01	16	2	16	1
Burkholderia cenocepacia IIIa 4813	>256	0.4	>64	2
Escherichia coli 0157	1.6	0.8	16	8
Acinetobacter baumannii SENTRY C8	8	4	8	2
Klebsiella pneumoniae ATTC13883	3.2	1.6	4	2
Salmonella enterica sv Typhimurium 14028S	3.2	0.8	4	1

5.4.3 Broad-spectrum synergistic interactions between D-enantiomeric peptides and conventional antibiotics to treat biofilms

Synergy between peptides DJK-5 and DJK-6 and conventional antibiotics, was tested in collaboration with Dr. Fany Reffuveille, by using a variation of the checkerboard methodology that is widely used to determine interactions between compounds (Reffuveille et al., 2014; Yan and Hancock, 2001). Checkerboard titrations were performed within the context

of a simple biofilm assay, whereby one compound (peptide) was diluted along the rows of a microtitre plate and the other compound (antibiotic) was diluted along the columns. I Table 5.4 describes the results obtained when treating biofilms formed by different bacterial species when peptides DJK-5 and DJK-6 were combined with 4 of the most popular antibiotics used in human medicine, namely cephalosporin β-lactam ceftazidime, carbapenem β-lactam imipenem, fluoroquinolone ciprofloxacin and aminoglycoside tobramycin. In all cases, we observed either synergy (FIC < 0.5), near synergy (FIC < 0.56), or additive interactions (FIC=0.5-1) (Table 5.4). Overall 42.5% of the combinations showed synergy or near synergy. Interestingly, in most cases these peptides led to a substantial decrease in the concentration of antibiotic required for anti-biofilm activity, compared to the antibiotic alone when used alone, as depicted by a 2- to 64-fold drop in antibiotic concentration in combination (Table 5.4). For example, treatment of *S. enterica* with tobramycin in combination with DJK-5 led to a 32-fold decrease in the amount of tobramycin required to exhibit the same activity against biofilms formed by this bacterial species. The same 32-fold decrease in antibiotic concentration was observed for the combination of ciprofloxacin with DJK-6. An even more pronounced drop (64-fold) in the concentration of antibiotic was observed when treating multidrug-resistant *Acinetobacter baumannii* with tobramycin in combination with DJK-6.

Table 5.4. Antimicrobial (MIC), broad-spectrum anti-biofilm ($MBIC_{50}$) activities and synergistic interactions between D-enantiomeric peptides and conventional antibiotics. MIC refers to the concentration of peptide that resulted in 100% inhibition of planktonic growth. $MBIC_{50}$ corresponds to the peptide concentration that results in 50% biofilm inhibition. To test for synergy, checkerboard titrations were performed to assess synergistic interactions between D-enantiomeric peptides DJK-5 (A) and DJK-6 (B) and conventional antibiotics to prevent biofilm formation. The result was expressed as the fractional inhibitory concentration (FIC) with the FIC values indicating synergy (FIC<0.5) or near synergy (FIC<0.56) shown in bold. An FIC index of 0.5 is considered to indicate good synergy (representing the equivalent of a four-fold decrease in the MBIC of each compound when used in combination) and an FIC index of 1.0 represents additive activity (a two-fold decrease in the MBIC of each compound in combination). In most cases, peptides when combined with antibiotics reduced the antibiotic MBIC, here depicted as fold decrease in antibiotic concentration at the FIC. CTZ: ceftazidime; CIP: ciprofloxacin; IMI: imipenem; TOB: tobramycin. These experiments were done in collaboration with Dr. Fany Reffuveille.

DJK-5										
Strains	**MIC (µg/ml)**	**$MBIC_{50}$ (µg/ml)**	**FIC**				**Fold Decrease in Antibiotic Concentration**			
			CTZ	**CIP**	**IMI**	**TOB**	**CTZ**	**CIP**	**IMI**	**TOB**
P.aeruginosa	16	1	**0.5**	**0.14**	**0.5**	**0.5**	8X	16X	4X	2X
E. coli 0157	1.6	0.8	**0.54**	1	1	**0.56**	2X	16X	64X	16X
A. baumannii	8	4	0.75	1	0.75	**0.56**	2X	1X	2X	16X
K. pneumoniae	3.2	1.6	0.89	0.75	1	0.75	16X	2X	64X	4X
S. enterica	3.2	0.8	0.75	**0.56**	1	1.03	4X	2X	2X	32X
DJK-6										
P.aeruginosa	16	0.5	**0.48**	**0.46**	0.92	1.13	16X	4X	2X	1X
E. coli 0157	16	8	**0.35**	**0.5**	0.67	**0.5**	16X	32X	2X	4X
A. baumannii	8	2	**0.5**	**0.53**	**0.46**	0.75	16X	16X	4X	64X
K. pneumoniae	4	2	1	0.75	0.75	0.63	2X	4X	4X	4X
S. enterica	4	1	1	**0.56**	0.63	0.75	2X	16X	4X	4X

The more sensitive and physiologically-relevant flow cell chamber method was used to confirm these results. As this method has much lower throughput, assessments were performed only at the concentrations of peptide and antibiotic giving the lowest FIC against each bacterial species based on checkerboard assays. For example, the lowest FIC value obtained for *P. aeruginosa* PA14 was 0.14, corresponding to the combination 0.1 µg/ml of DJK-5 with 0.04 µg/ml ciprofloxacin (Table 5.4A). Flow cell experiments confirmed these results as the combination of 0.04 µg/ml of ciprofloxacin with 0.1 µg/ml of DJK-5 led to complete biofilm inhibition (Figure 5.2A). For all other species tested the best FIC peptide-antibiotic combination led to complete or nearly complete biofilm prevention, with only a few individual cells (some red-stained and thus dead) remaining attached to the surface of the flow cell chambers (Figure 5.2).

A) DJK-5

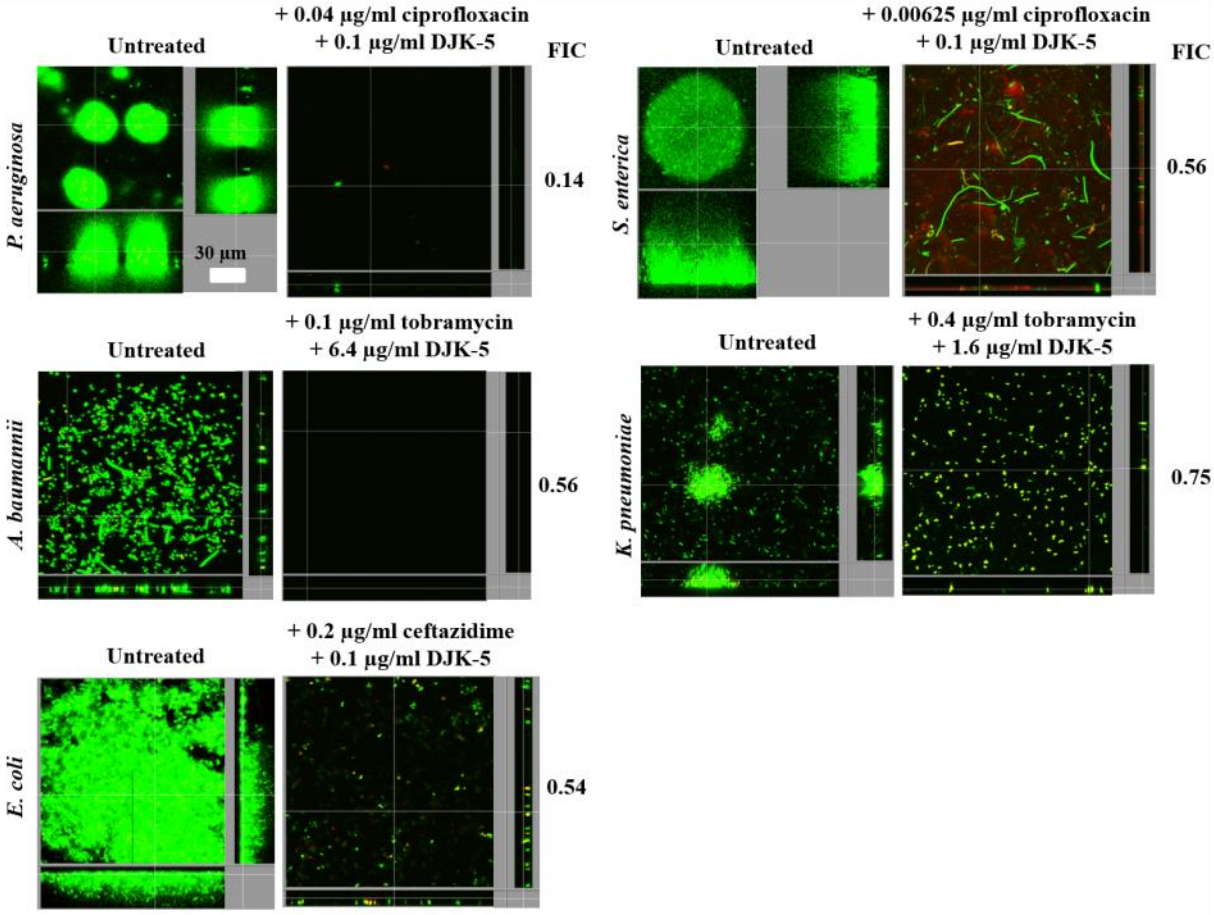
Untreated
+ 0.04 µg/ml ciprofloxacin
+ 0.1 µg/ml DJK-5
FIC
P. aeruginosa
30 µm
0.14
Untreated
+ 0.00625 µg/ml ciprofloxacin
+ 0.1 µg/ml DJK-5
FIC
S. enterica
0.56
Untreated
+ 0.1 µg/ml tobramycin
+ 6.4 µg/ml DJK-5
A. baumannii
0.56
Untreated
+ 0.4 µg/ml tobramycin
+ 1.6 µg/ml DJK-5
K. pneumoniae
0.75
Untreated
+ 0.2 µg/ml ceftazidime
+ 0.1 µg/ml DJK-5
E. coli
0.54

B) DJK-6

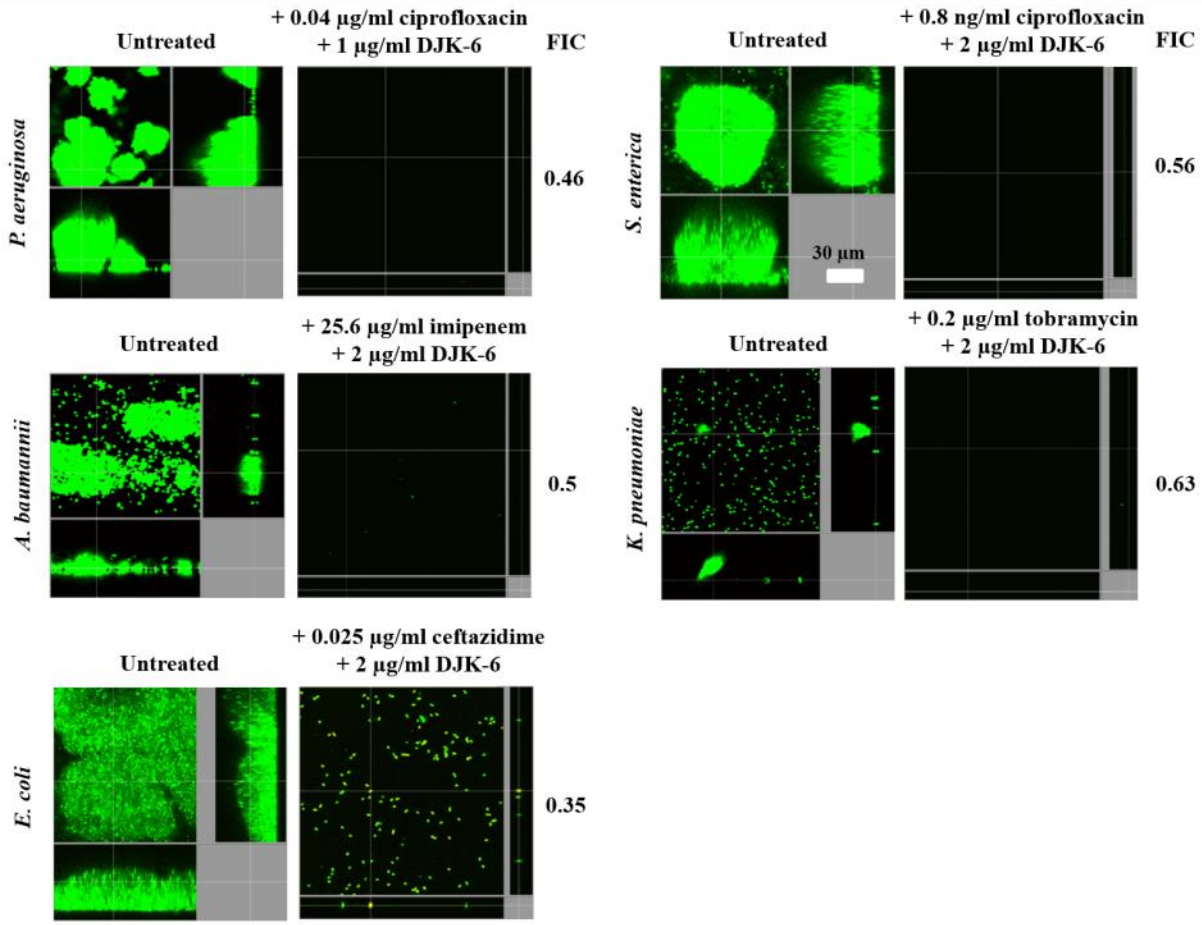

Figure 5.2. D-enantiomeric peptides DJK-5 (A) and DJK-6 (B) exhibited anti-biofilm activity in flow cells and synergized with conventional antibiotics in preventing biofilm formation by different bacterial species. Sub-inhibitory concentrations of peptides DJK-5 and DJK-6 in combination with antibiotics prevented biofilm development of Gram-negative bacteria. Inhibition of biofilm development was tested by immediately (at the beginning of biofilm growth at day 0) adding peptide plus antibiotic into the flow-through medium of the flow cell apparatus and then monitoring biofilm formation for 3 days. After 3 days, bacteria were stained green with the all bacteria stain Syto-9 and red with the dead-bacteria stain propidium iodide (merge shows as yellow to red) prior to confocal imaging. Each panel shows reconstructions from the top in the large panel and sides in the right and bottom panels (xy, yz and xz dimensions). The top FIC combinations of peptide + antibiotic (determined in checkerboard assays) were used. See Methods and materials section for more details.

Next, the same combinations of peptide and antibiotic were tested against pre-existing 2-day-old biofilms. For this purpose, biofilms of the different bacterial species were allowed to grow for 2 days untreated, and were subsequently treated with the peptide alone, the antibiotic alone or the combination peptide-antibiotic. Peptide DJK-5, when combined with

the antibiotics tobramycin, ceftazidime and ciprofloxacin led to eradication of *A. baumannii*, *Salmonella enterica* and *Klebsiella pneumoniae* mature biofilms, respectively (Figure 5.3A). On the other hand, the combination of DJK-5 with ciprofloxacin vs. *P. aeruginosa* PA14 caused much more limited dispersal but triggered cell death in remaining cells (Figure 5.3A). In contrast, the combination of DJK5 and ceftazidime vs. *E. coli* was not synergistic in eradication studies (Figure 5.3A). Combinations of DJK-6 with any of the antibiotics tested led to disruption of pre-formed biofilms in all cases (Figure 5.3B), with at most only a few cells remaining attached to the surface of the flow cell chambers.

A) DJK-5

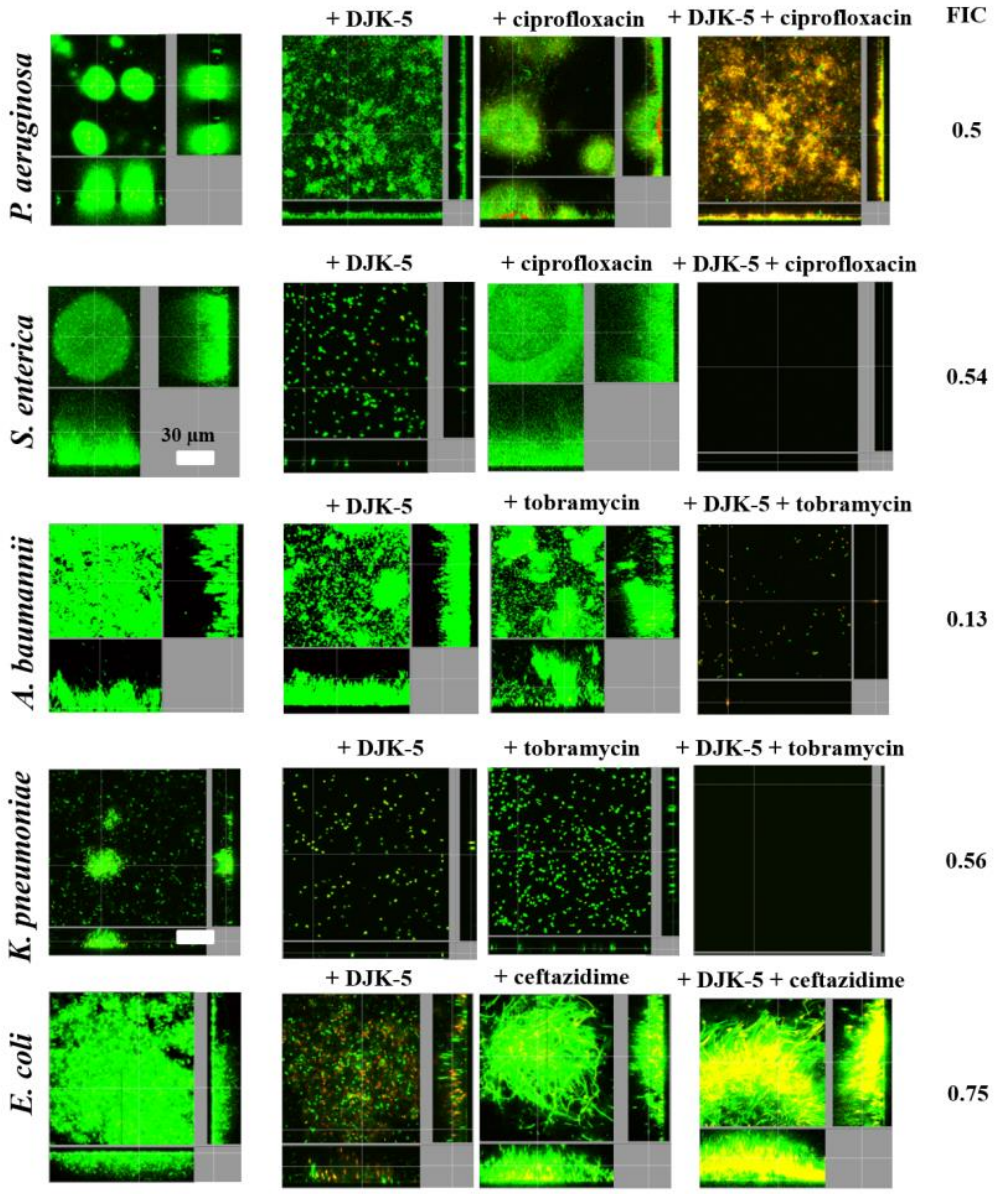

B) DJK-6

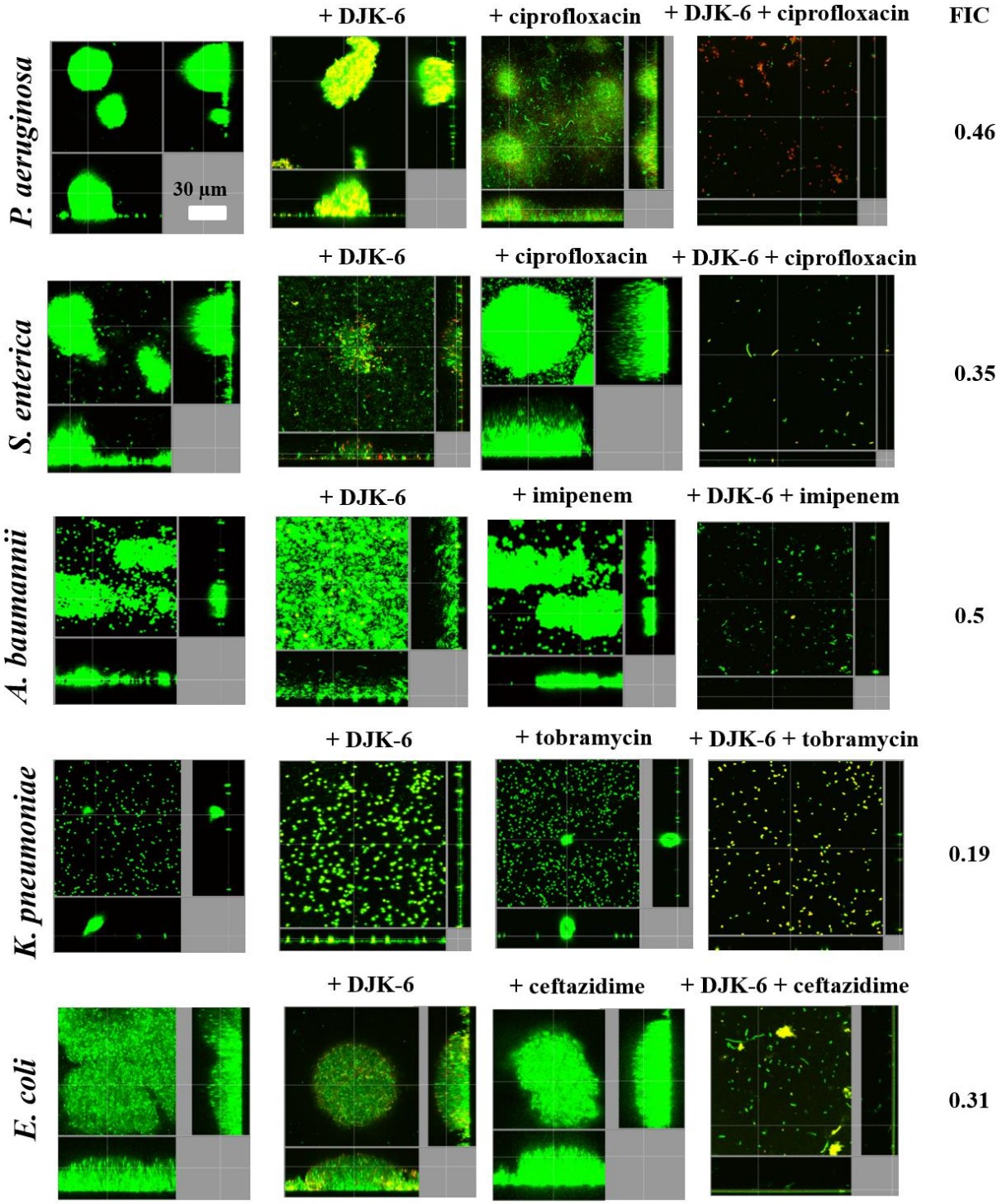

Figure 5.3. Synergistic interactions of D-enantiomeric peptides DJK-5 (A) and DJK-6 (B) with different classes of antibiotics in treating mature biofilms. Bacteria were grown in flow cells and treated at day 2 of biofilm formation with peptide, antibiotic, or the combination of both. The top FIC combinations of peptide + antibiotic (determined in checkerboard assays) were used (as in Figure 2). In some cases, at the concentrations selected, the activity of the

peptides led to complete eradication of the flow cell biofilms. Thus, we decreased the levels of peptide used, which lowered the FIC values (see on the right hand side of panels) compared to the checkerboard assay results shown in Table 2. Specifically, in (A) 0.8 μg/ml of DJK-5 (instead of 6.4 μg/ml) was used in combination with tobramycin vs *A. baumannii*. In (B), 0.5 μg/ml of DJK-6 were used instead of 2 μg/ml combined with imipenem vs. *A. baumannii*, 1 μg/ml of DJK-6 (as opposed to 2 μg/ml) was used in conjunction with ciprofloxacin vs *S. enterica*, and 0.5 μg/ml of DJK-6, instead of 2 μg/ml, was used in combination with tobramycin vs *K. pneumoniae*. After 3 days, bacteria were stained green with the all bacteria stain Syto-9 and red with the dead-bacteria stain propidium iodide (merge shows as yellow to red) prior to confocal imaging. Each panel shows reconstructions from the top in the large panel and sides in the right and bottom panels (xy, yz and xz dimensions). See Methods and materials section for more details.

5.4.4 Overproduction of (p)ppGpp led to altered susceptibility of biofilms to D-enantiomeric peptides and peptides inhibited (p)ppGpp accumulation

In Chapter 4, the less potent anti-biofilm peptide 1018 was shown to bind to and degrade the nucleotide(s) (p)ppGpp, which play a role in biofilm formation and maintenance. In this Chapter, I addressed whether D-enantiomeric peptides DJK-5 and DJK-6 operated through the same mechanism. First, we overproduced the potential target (p)ppGpp as previously described (de la Fuente-Núñez et al., 2014), as this is a well-established strategy for identifying drug targets. Overproduction of (p)ppGpp was achieved chemically by treating *P. aeruginosa* with 80 μM of serine hydroxamate (SHX), a structural analogue of L-serine that induces the stringent response by inhibiting charging of seryl-tRNA synthetase (Tosa and Pizer, 1971). This led to reduced susceptibility of *P. aeruginosa* biofilms to peptide action (Figure 5.4A). The concentration used here is known to inhibit seryl tRNA synthetase and thus induce the production of (p)ppGpp, based on previous reports (Tosa and Pizer, 1971; Raskin et al., 2007).

When planktonic cells were treated with 500 μM serine hydroxamate they accumulated (p)ppGpp (Nguyen et al., 2011). Starved bacterial cells produce ~5,000-50,000 pmol/g of ppGpp (Ochi et al., 1981; Ochi, 1990). Direct measurement of the cellular levels of (p)ppGpp by thin layer chromatography (TLC) revealed that treatment with 1 μg/ml of peptides DJK-5 and DJK-6 inhibited the accumulation of (p)ppGpp in these otherwise (p)ppGpp-expressing *P. aeruginosa* cells (Figure 5.4B). This would presumably prevent its signaling effects within the cell (e.g. its role in biofilm development and maintenance).

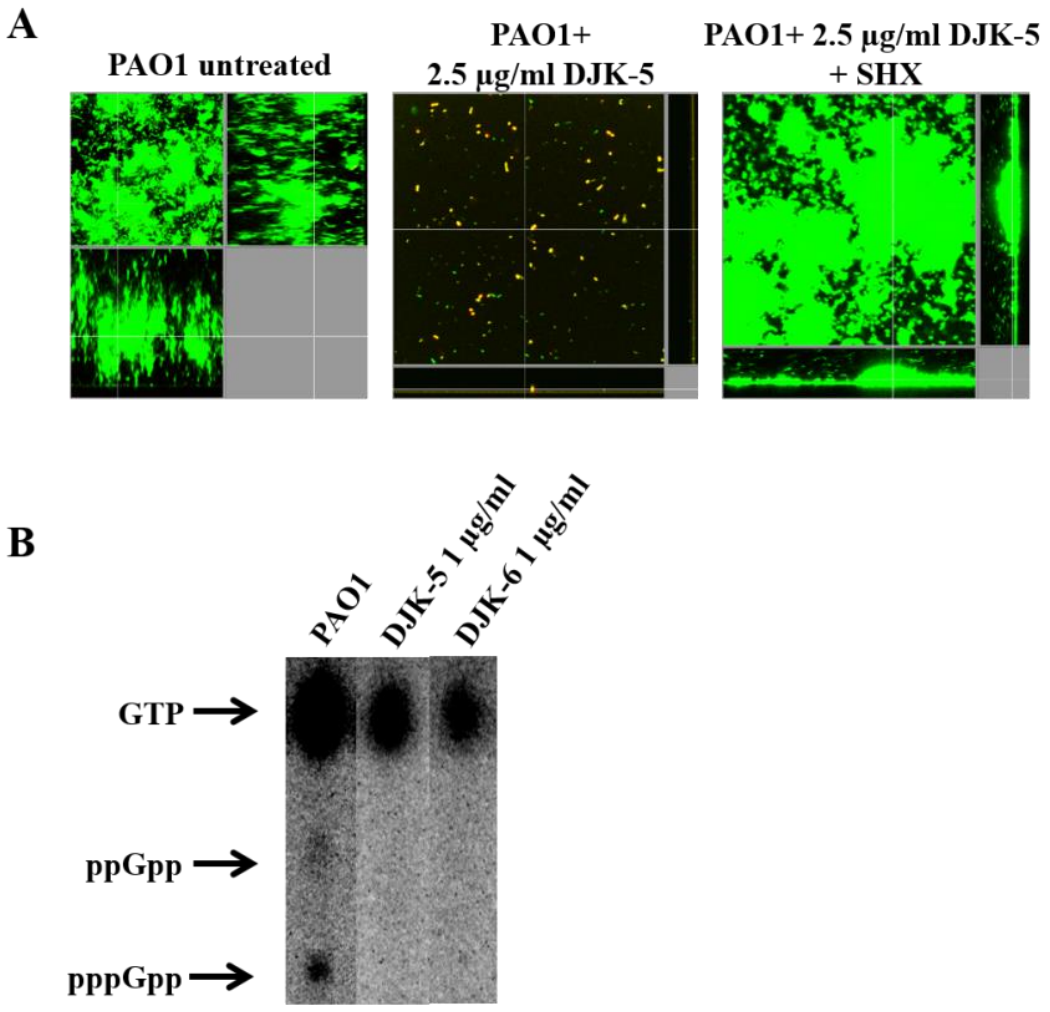

Figure 5.4. Overproduction of (p)ppGpp led to decreased biofilm susceptibility to D-enantiomeric peptides and peptides inhibited the accumulation of (p)ppGpp *in vivo*. (A) Addition of SHX, which leads to overproduction of (p)ppGpp, resulted in the resistance of flow cell biofilm formation to 2.5 µg/ml of peptide DJK-5. After 3 days, bacteria were stained green with the all bacteria stain Syto-9 prior to confocal imaging. Each panel shows reconstructions from the top in the large panel and sides in the right and bottom panels (xy, yz and xz dimensions). **(B)** Anti-biofilm peptides DJK-5 and DJK-6 at 1 µg/ml prevented (p)ppGpp accumulation as revealed by thin layer chromatography separation of guanine nucleotides extracted from intact cells as described in the Methods and materials section.

5.4.5 D-enantiomeric peptides protected *Caenorhabditis elegans* and *Galleria mellonella* from a lethal *P. aeruginosa* infection

D-enantiomeric peptides DJK-5, DJK-6 were tested *in vivo* for their ability to protect the nematode *C. elegans* and the moth *G. mellonella* from biofilm infections induced by *P. aeruginosa* PAO1, using previously-described models (Brackman et al., 2011; Cooper et al.,

2009; Stiernagle, 2006). The peptides did not display any toxic activity against *C. elegans*, since no significant differences in survival were observed after 24 h and 48 h in uninfected *C. elegans* nematodes treated with peptides compared to untreated animals (Table 5.5).

Untreated controls infected with *P. aeruginosa* PAO1 demonstrated 100% death after 48 h in both biofilm infection models (Table 5.5). As a control peptide, we used the previously characterized anti-biofilm peptide 1018 (de la Fuente-Núñez et al., 2014), and its D-enantiomeric retro-inverso version RI-1018. In the *C. elegans* experiments, all peptides significantly ($p<0.001$) protected the nematodes against *P. aeruginosa* PAO1-induced mortality after 24 h, with DJK-5 and DJK-6 giving nearly complete protection (Table 5.5). After 48 h of infection, significant protection ($p<0.001$) was still observed for groups treated with peptides DJK-5 and DJK-6, while mortality was close to 100% (and not significantly different from the peptide untreated control) for RI-1018 and 1018 (Table 5.5).

Table 5.5. *In vivo* anti-biofilm activity of D-enantiomeric peptides. *C. elegans* and *G. mellonella* biofilm survival assays. Percent survival of infected *C. elegans* and *G. mellonella* (average ± the SD) after treatment with peptides D-enantiomeric peptides RI-1018 (and its L-version 1018), DJK-5 and DJK-6 and *P. aeruginosa* strain PAO1. The results are expressed as the percent survival after both 24 h and 48 h of infection and peptide treatment. Statistical significance comparing peptide-treated groups to untreated was determined (*, P< 0.001). These assays were performed by Dr. Gilles Brackman and Dr. Tom Coenye.

	***C. elegans* survival (%)**			
	24h		**48h post infection**	
Peptide	**No infection**	***P. aeruginosa* PAO1**	**No infection**	***P. aeruginosa* PAO1**
None	100 ± 0	61 ± 21	95 ± 4	1 ± 2
RI1018	99 ± 1	83 ± 13*	81 ± 23	4 ± 6
1018	97 ± 4	91 ± 12*	88 ± 9	1 ± 3
DJK5	99 ± 2	99 ± 2*	99 ± 2	96 ± 4*
DJK6	99 ± 2	99 ± 2*	97 ± 4	90 ± 5*
***G. mellonella* survival (%)**				
None	100 ± 0	13 ± 11	100 ± 0	0 ± 0
RI1018	90 ± 14	50 ± 8*	80 ± 10	18 ± 7*
1018	90 ± 14	27 ± 11	90 ± 14	3 ± 5
DJK5	100 ± 0	90 ± 6*	100 ± 0	42 ± 7*
DJK6	100 ± 0	50 ± 8*	100 ± 0	30 ± 6*

*: survival significantly different from untreated control ($p<0.001$)

In experiments performed using the *Galleria* biofilm model, in which moths were infected with 10^4 CFU, no protective effect was observed after 24 h with peptide 1018, a

moderate but significant protective effect was observed for RI-1018 and DJK-6, and a strong and significant protective effect was conferred by DJK-5 (Table 5.5). After 48 h, RI-1018 and particularly peptides DJK-5 and DJK-6 resulted in increased survival (18-42% survival cf. complete killing in the control group) (Table 5.5).

5.5 Discussion

Today, multidrug-resistant Gram-negative pathogens are becoming increasingly prevalent, including members of the ESKAPE pathogens, *Pseudomonas, Klebsiella* and *Acinetobacter*, for which no fundamentally new drugs are under development in the antibiotic pipeline (Boucher et al., 2009; Payne et al., 2007). Of increasing concern is the rise of adaptive resistance whereby the growth state of the organism leads to non-mutational high-level resistance to most antibiotics currently available (de la Fuente-Núñez et al., 2013). For example, biofilm growth leads to multidrug adaptive resistance (up to 10- to 1000-fold increased resistance compared to planktonic bacteria) and is associated with at least 65% of all human clinical infections (Costerton et al., 1999; Davies, 2003; de la Fuente-Núñez et al., 2013; López et al., 2010). However, there are currently no specific treatments for such biofilm-related infections.

In the present study, D-enantiomeric peptides were identified and extensively characterized for their anti-biofilm activities against a range of Gram-negative species, showing that there was no relationship between killing of planktonic bacteria and anti-biofilm activity, in accordance with other reports (Dean et al., 2011; Overhage et al., 2008; Chapters 2 and 3).

In addition, these peptides acted either additively or synergistically with antibiotics commonly used in the clinic to both prevent biofilm formation and treat pre-established mature biofilms. Thus, the peptides have two very potent and novel activities for countering drug resistance. First, they counteract biofilms that are known to cause more than two thirds of all infections in humans, and are notoriously (adaptively) resistant to multiple classes of antibiotics. Second, the peptides showed excellent synergy (or additive effects) with conventional antibiotics providing a potent strategy to make biofilms more susceptible to these agents. Thus the combination of D-enantiomeric peptides with antibiotics enhanced the activity of antibiotics to treat bacterial biofilms, both at the initial stages of growth and in their mature state.

Bacterial resistance strategies to antimicrobial peptides have been previously described that include enzymatic degradation of peptides. Here this limitation, and the lability of peptides to host proteases, was overcome by designing D-enantiomeric peptides, which cannot be recognized by bacterial and host proteases that abound during infections and that cleave peptides composed entirely of L-amino acids (Sieprawska-Lupa et al., 2004). Twelve amino acid peptides were identified with the most potent activity observed to date against biofilms formed by Gram-negative bacteria that are notorious for multi-drug resistance. The data favored a mechanism similar to that observed for peptide 1018 (Chapter 4), whereby peptides DJK-5 and DJK-6 inhibited biofilm formation and suppressed mature biofilms by entering cells and subsequently targeting and causing the degradation of the intracellular nucleotides (p)ppGpp, which are important for the formation and maintenance of biofilms.

For the first time, it was possible to demonstrate anti-biofilm activity in animal models, as shown here for 3 different D-enantiomeric peptides. The most effective peptides were peptides DJK-5 and DJK-6 that protected *C. elegans* and *Galleria mellonella* (wax moth) against *Pseudomonas* biofilm infections. Indeed, DJK-5 and DJK-6 demonstrated much higher levels of protection in both hosts compared to the previously identified anti-biofilm peptide 1018 and its retro-inverso version RI-1018, indicating higher potency after both 24 h and 48 h of infection.

These data indicate many desirable features against multi-species biofilms. In particular, the combination of conventional antibiotics and D-enantiomeric anti-biofilm peptides offers an exciting potential as a therapeutic strategy for treating biofilms formed by multidrug-resistant Gram-negative pathogens for which few alternatives exist.

5.6 Summary

In an era in which there are relatively few novel compounds or strategies under development or entering the clinic to treat multidrug-resistant Gram-negative bacterial pathogens, we have identified and characterized protease-resistant D-enantiomeric peptides that exhibit potent abilities to counteract the adaptive antibiotic resistance associated with biofilms, a common growth state responsible for >65% of all human clinical infections. Second, when combined with different classes of commonly used antibiotics, these peptides showed excellent synergy or additive effects against biofilms, thus providing a strategy to make biofilms more susceptible to conventional therapies. Finally, these peptides conferred

protection to the nematode *C. elegans* and the larvae *Galleria mellonella* against *P. aeruginosa* biofilm infections thus proving their potential *in vivo*. D-enantiomeric anti-biofilm peptides such as DJK-5 and DJK-6 may form the basis for novel adjuvant therapies that might be effective in combination with antibiotics against biofilms formed by antibiotic-resistant bacteria.

Chapter 6: Conclusions

6.1 Conclusion

Throughout their evolution, bacteria have gradually adapted to endure situations of environmental stress. One such adaptation entails the formation of biofilms, multicellular specialized structures that have become very efficient at tolerating external insults. On the basis of our current knowledge about the biology of biofilms, we can speculate that the evolutionary adaptation to the biofilm mode of growth may have been driven by stress signals present in the natural environment that would in turn trigger the production of (p)ppGpp from ATP and either GDP or GTP. Since GTP is used extensively in protein synthesis, inhibition of this process by (p)ppGpp-inducing stimuli (such as amino acid starvation) may have been selected through evolution due to the critical regulatory function of (p)ppGpp in bacterial survival. Indeed, it is now known that (p)ppGpp plays a key role in triggering drug resistance mechanisms in bacteria (Figure 1.4). One consequence of this adaptation is the adaptive resistance to antimicrobial compounds that is displayed by biofilm-forming cells. This characteristic has made biofilms a particular challenge for the treatment of infectious diseases linked to biofilm formation. However, during the last decade we have made considerable progress in the understanding of the signalling pathways and molecular mechanisms that govern the cycle of biofilm formation and dispersal. This knowledge has opened the door to the development of new therapeutic strategies directed at inhibiting biofilm formation and inducing biofilm dispersal. One of these approaches, and the focus of this thesis, is the use of synthetic cationic peptides (originally designed based on the amino acid sequence of host defence peptides) that exhibit anti-biofilm activity. With this in mind, we anticipate that in the near future some of these therapeutics will be introduced into clinical trials and will eventually help in the treatment of biofilm-related infections. At the same time, further research on the molecular biology of biofilms and the exogenous stress signals responsible for their formation will be decisive in discerning the role that these structured colonies play in the bacterial world. Furthermore, it is tempting to speculate that this knowledge might perhaps hint at the processes that led to the origin of multicellular organisms.

Overall, in any given environment, bacteria predominantly exist as multicellular communities called biofilms. These surface-associated structures are highly (adaptively) resistant to exogenous stresses, allowing bacterial populations to survive in conditions that

would kill their planktonic counterparts. Biofilms thus constitute a significant problem in the clinic, as they are estimated to cause at least 65% of all human infections and cells within a biofilm are 10 to 1000 times more resistant to antibiotics than planktonic bacteria. Unfortunately, there are currently no approved drugs that target biofilms.

In Chapter 2 of this thesis, I identified a very small peptide composed of only 9 amino acids in length that was capable of preventing biofilm formation in a broad-spectrum manner despite its inability to affect planktonic growth in the tested organisms. Further studies done using *P. aeruginosa* concluded that the peptide was affecting different types of motility, quorum-sensing and other biofilm-associated genes, and that these effects were proposed to responsible for the anti-biofilm activity observed, although subsequent work made this seem less likely.

In Chapter 3, I described in detail the improved broad-spectrum anti-biofilm activity of peptide 1018 compared to peptide 1037 and further showed that at low concentrations the peptide triggered cell dispersal from biofilms, while higher levels of the peptide caused cell death. In addition, the peptide was shown to act synergistically with a variety of different classes of conventional antibiotics in acting against bacterial biofilms.

Previous conclusions made in Chapter 2 were consistent with the biofilm inhibitory activity of peptide 1037 in the context of *P. aeruginosa* but did not clarify the broad-spectrum activity of the peptide. Thus, concentrating on our lead peptide 1018, I hypothesized that this peptide targeted a cellular process that was common in both Gram-negative and Gram-positive bacteria and that this process might be the stringent response. A series of experiments described in Chapter 4 showed that indeed peptide 1018 bound to and led to the degradation of (p)ppGpp, the signaling molecule produced during the stringent response in bacteria.

As outlined in Chapter 5, additional peptide screens helped to identify several D-enantiomeric peptides that exhibited increased anti-biofilm activity, and the two lead compounds were very potent, were highly synergistic with conventional antibiotics, prevented (p)ppGpp accumulation and showed activity *in vivo* since they protected *C. elegans* and *G. mellonella* from *P. aeruginosa* biofilm infections.

In summary, this thesis has made important breakthoughs in defining a unique set of peptides conceptually based on natural templates. In so doing it has provided molecules that can be considered as anti-resistance strategies that can be developed clinically as novel

therapeutic strategies addressing the massively concerning issue of burgeoning resistance. Thus the peptides described in the thesis, or derivatives therof, in combination with conventional antibiotics may provide the basis for novel therapeutic strategies designed to target difficult-to-treat bacterial biofilm infections.

6.2. Future directions

Future studies will be directed towards the identification of D-enantiomeric peptides with even more potent activity than those presented in this thesis. Structure-activity relationship studies using our most active anti-biofilm peptides will be performed to pinpoint what amino acids and in what positions within the peptide sequence contribute to the overall anti-biofilm activity. This will allow the design and synthesis of novel, improved, D-enantiomeric anti-biofilm peptides. Another objective will be to try to reduce peptide size, as this will bring down the production cost. The lead peptide derivatives will then be tested in murine biofilm infection models to assess whether their broad-spectrum anti-biofilm activity is conserved under *in vivo* conditions. These studies will test the stand-alone anti-biofilm activity of the peptides and their efficacy at eradicating biofilm infections when combined with conventional antibiotics.

The work presented in this thesis has served to identify small peptides that target drug-resistant biofilms at low concentrations and potentiate the activity of conventional antibiotics that are otherwise inactive against biofilms at the concentrations tested. Further, the mechanism of action of one of these peptides (i.e., 1018) has been shown to involve targeting of the second messenger signaling nucleotides (p)ppGpp. Peptides 1018 and the D-enantiomers DJK-5 and DJK-6, or derivatives thereof, possess biological and physical properties that make them ideal therapeutic leads for further development.

6.2.1 Clinical development

Several strategies are needed to take the lead peptides presented in this thesis to the clinic. These include testing the peptides in animal models that better mimic biofilm-related infections in humans. Initial pharmacokinetic studies in mice also need to be performed to understand the fate of the peptides in a living organism. Toxicity can also be a problem when administering peptides systemically, so thorough toxicity studies will need to be performed. However the potency of these peptides may help overcome this limitation, as lower concentrations may be needed for these peptides to exert anti-biofilm activity *in vivo*.

Importantly, as these peptides are highly synergistic with conventional antibiotics, all these studies may be performed using the peptides as adjuvants for antibiotic therapy.

Once all these studies have been done, it will be essential to define the type of infection(s) that are most susceptible and suitable to the characteristics of the peptide. Next, the Food and Drug Administrations's (FDA) Investigational New Drug (IND) program will allow the pharmaceutical company responsible for the development of the peptide to obtain permission to ship the peptide across state lines, before a marketing application for the peptide is approved. The FDA then reviews the IND application to ensure the research subjects will not be exposed to unreasonable risk when taking the drug. Subsequently, the peptide would enter clinical trials that are commonly classified into four phases (phases 0-4). In phase 0, sub-therapeutic doses of the drug are given to a small number of subjects (10-15) to collect preliminary data on the drugs's pharmacodynamics and pharmacokinetics. In phase 1 trials, the peptide would be administered to a small subset of patients (20-80) to evaluate its safety, and determine its potential side effects. Phase 2 trials involve a larger group of subjects (100-300) and would evaluate the effectiveness and safety of the drug. In phase 3 trials, the peptide would be administered to 1000-3000 people to confirm its activity, monitor its side effects, and compare these to already approved agents. This would then lead to an application for New Drug Approval (NDA). Finally, in phase 4 trials, an FDA review and postmarketing studies would outline information such as the risks, benefits and optimal use of the peptide.

Bibliography

Aberg A, Shingler V, Balsalobre C. (2006). (p)ppGpp regulates type 1 fimbriation of *Escherichia coli* by modulating the expression of the site-specific recombinase FimB. Mol. Microbiol. 60:1520-33.

Achtman AH, Pilat S, Law CW, Lynn DJ, Janot L, Mayer ML, Ma S, Kindrachuk J, Finlay BB, Brinkman FS, Smyth GK, Hancock REW, Schofield L. (2012). Effective adjunctive therapy by an innate defense regulatory peptide in a preclinical model of severe malaria. Sci. Transl. Med. 4:135ra64.

Allison KR, Brynildsen MP, Collins JJ. (2011). Metabolite-enabled eradication of bacterial persisters by aminoglycosides. Nature. 473:216-20.

Amato SM, Orman MA, Brynildsen MP. (2013). Metabolic control of persister formation in Escherichia coli. Mol. Cell. 50:475-87.

Amer, L.S., B.M. Bishop, and M.L. van Hoek. (2010). Antimicrobial and antibiofilm activity of cathelicidins and short, synthetic peptides against Francisella. Biochem. Biophys. Res. Commun. 396:246-51.

Anderl JN, Franklin MJ, Stewart PS. (2000). Role of antibiotic penetration limitation in *Klebsiella pneumoniae* biofilm resistance to ampicillin and ciprofloxacin. Antimicrob. Agents Chemother. 44:1818-1824.

Balaban N, Cirioni O, Giacometti A, Ghiselli R, Braunstein JB, Silvestri C, Mocchegiani F, Saba V, Scalise G. (2007). Treatment of *Staphylococcus aureus* biofilm infection by the quorum-sensing inhibitor RIP. Antimicrob. Agents Chemother. 51:2226-9.

Balaban NQ, Merrin J, Chait R, Kowalik L, Leibler S. (2004). Bacterial persistence as a phenotypic switch. Science. 305:1622-5.

Balázsi G, van Oudenaarden A, Collins JJ. (2011). Cellular decision making and biological noise: from microbes to mammals. Cell. 144:910-25.

Balzer GJ, McLean RJ. (2002). The stringent response genes *relA* and *spoT* are important for *Escherichia coli* biofilms under slow-growth conditions. Can. J. Microbiol. 48:675-80.

Banin E, Brady KM, Greenberg EP. (2006). Chelator-induced dispersal and killing of *Pseudomonas aeruginosa* cells in a biofilm. Appl. Environ. Microbiol. 72:2064-9.

Barraud N, Schleheck D, Klebensberger J, Webb JS, Hassett DJ, Rice SA, Kjelleberg S. (2009). Nitric oxide signaling in *Pseudomonas aeruginosa* biofilms mediates phosphodiesterase activity, decreased cyclic di-GMP levels, and enhanced dispersal. J. Bacteriol. 191:7333-42.

Baugh S, Ekanayaka AS, Piddock LJ, Webber MA. (2012). Loss of or inhibition of all multidrug resistance efflux pumps of *Salmonella enterica* serovar Typhimurium results in impaired ability to form a biofilm. J. Antimicrob. Chemother. 67:2409-2417.

Beaudoin T, Zhang L, Hinz AJ, Parr CJ, Mah TF. (2012). The biofilm-specific antibiotic resistance gene *ndvB* is important for expression of ethanol oxidation genes in *Pseudomonas aeruginosa* biofilms. J. Bacteriol. 194:3128-3136.

Beyth N, Yudovin-Farber I, Perez-Davidi M, Domb AJ, Weiss EI. (2010). Polyethyleneimine nanoparticles incorporated into resin composite cause cell death and trigger biofilm stress *in vivo*. Proc. Natl. Acad. Sci. U. S. A. 107:22038-43.

Bernier SP, Lebeaux D, DeFrancesco AS, Valomon A, Soubigou G, Coppée JY, Ghigo JM, Beloin C. (2013). Starvation, together with the SOS response, mediates high biofilm-specific tolerance to the fluoroquinolone ofloxacin. PLoS Genet. 9:e1003144.

Betzner AS, Ferreira LC, Höltje JV, Keck W. (1990). Control of the activity of the soluble

lytic transglycosylase by the stringent response in *Escherichia coli*. FEMS Microbiol. Lett. 55:161-4.
Bjarnsholt T, Ciofu O, Molin S, Givskov M, Høiby N. (2013). Applying insights from biofilm biology to drug development - can a new approach be developed? Nat. Rev. Drug. Discov. 12:791-808.
Borriello G, Werner E, Roe F, Kim AM, Ehrlich GD, Stewart PS. (2004). Oxygen limitation contributes to antibiotic tolerance of *Pseudomonas aeruginosa* in biofilms. Antimicrob. Agents Chemother. 48:2659-2664.
Boucher HW, Talbot GH, Bradley JS, Edwards JE, Gilbert D, Rice LB, Scheld M, Spellberg B, Bartlett J. (2009). Bad bugs, no drugs: no ESKAPE! An update from the Infectious Diseases Society of America. Clin. Infect. Dis. 48:1-12.
Boyd CD, O'Toole GA. (2012). Second messenger regulation of biofilm formation: breakthroughs in understanding c-di-GMP effector systems. Annu. Rev. Cell Dev. Biol. 28:439-62.
Brackman G, Cos P, Maes L, Nelis HJ, Coenye T. (2011). Quorum sensing inhibitors increase the susceptibility of bacterial biofilms to antibiotics *in vitro* and *in vivo*. Antimicrob. Agents Chemother. *55*, 2655-61.
Breidenstein EBM, Bains M, Hancock REW (2012) Involvement of the lon protease in the SOS response triggered by ciprofloxacin in *Pseudomonas aeruginosa* PAO1. Antimicrob. Agents Chemother. 56:2879-87.
Breidenstein EBM, de la Fuente-Núñez C, Hancock REW. (2011). *Pseudomonas aeruginosa*: all roads lead to resistance. Trends Microbiol. 19:419-26.
Brogden KA. (2005). Antimicrobial peptides: pore formers or metabolic inhibitors in bacteria? Nat. Rev. Microbiol. 3:238-50.
Brötz-Oesterhelt H, Beyer D, Kroll HP, Endermann R, Ladel C, Schroeder W, Hinzen B, Raddatz S, Paulsen H, Henninger K, Bandow JE, Sahl HG, Labischinski H. (2005). Dysregulation of bacterial proteolytic machinery by a new class of antibiotics. Nat. Med. 11:1082-7.
Butler MT, Wang Q, Harshey RM. (2010). Cell density and mobility protect swarming bacteria against antibiotics. Proc. Natl. Acad. Sci. U. S. A. 107:3776-81.
Camilli A, Bassler BL. (2006). Bacterial small-molecule signaling pathways. Science. 311:1113-6.
Cashel M. (1975). Regulation of bacterial ppGpp and pppGpp. Annu. Rev. Microbiol. 29:301-18.
Cashel M, Gallant J. (1969). Two compounds implicated in the function of the RC gene of *Escherichia coli*. Nature. 221:838-41.
Cegelski L, Pinkner JS, Hammer ND, Cusumano CK, Hung CS, Chorell E, Aberg V, Walker JN, Seed PC, Almqvist F, Chapman MR, Hultgren SJ. (2009). Small-molecule inhibitors target *Escherichia coli* amyloid biogenesis and biofilm formation. Nat. Chem. Biol. 5:913-9.
Chávez de Paz LE, Lemos JA, Wickström C, Sedgley CM. (2012). Role of (p)ppGpp in biofilm formation by *Enterococcus faecalis*. Appl. Environ. Microbiol. 78:1627-30.
Cherkasov A, Hilpert K, Jenssen H, Fjell CD, Waldbrook M, Mullaly SC, Volkmer R, Hancock REW. (2009). Use of artificial intelligence in the design of small peptide antibiotics effective against a broad spectrum of highly antibiotic-resistant superbugs. ACS Chem. Biol. 4:65-74

Chung J, Goo E, Yu S, Choi O, Lee J, Kim J, Kim H, Igarashi J, Suga H, Moon JS, Hwang I, Rhee S. (2011). Small-molecule inhibitor binding to an N-acyl-homoserine lactone synthase. Proc. Natl. Acad. Sci. U. S. A. 108:12089-94.

Cohen NR, Lobritz MA, Collins JJ. (2013). Microbial persistence and the road to drug resistance. Cell Host Microbe. 13:632-42.

Conlon BP, Nakayasu ES, Fleck LE, LaFleur MD, Isabella VM, Coleman K, Leonard SN, Smith RD, Adkins JN, Lewis K. (2013). Activated ClpP kills persisters and eradicates a chronic biofilm infection. Nature. 503:365-70.

Cook L, Chatterjee A, Barnes A, Yarwood J, Hu WS, Dunny G. (2011). Biofilm growth alters regulation of conjugation by a bacterial pheromone. Mol. Microbiol. 81:1499-1510.

Cooper VS, Carlson WA, LiPuma JJ. (2009). Susceptibility of *Caenorhabditis elegans* to *Burkholderia* infection depends on prior diet and secreted bacterial attractants. PLoS One. 4:e7961.

Cortay JC, Cozzone AJ. (1983). Accumulation of guanosine tetraphosphate induced by polymixin and gramicidin in *Escherichia coli*. Biochim. Biophys. Acta. 755:467-73.

Costerton JW, Stewart PS, Greenberg EP. (1999). Bacterial biofilms: a common cause of persistent infections. Science. 284:1318-22.

Dahl JL, Kraus CN, Boshoff HI, Doan B, Foley K, Avarbock D, Kaplan G, Mizrahi V, Rubin H, Barry CE 3rd. (2003). The role of RelMtb-mediated adaptation to stationary phase in long-term persistence of *Mycobacterium tuberculosis* in mice. Proc. Natl. Acad. Sci. U. S. A. 100:10026-31.

Dalebroux ZD, Svensson SL, Gaynor EC, Swanson MS. (2010). ppGpp conjures bacterial virulence. Microbiol. Mol. Biol. Rev. 74:171-99.

Dangel A, Ackermann N, Abdel-Hadi O, Maier R, Önder K, Francois P, Müller CW, Pané-Farré J, Engelmann S, Schrenzel J, Heesemann J, Lindermayr C. (2013). A *de novo*-designed antimicrobial peptide with activity against multiresistant *Staphylococcus aureus* acting on RsbW kinase. FASEB J. 27:4476-88.

Davies D. (2003). Understanding biofilm resistance to antibacterial agents. Nat. Rev. Drug Discov. 2:114-22.

Davies DG, Parsek MR, Pearson JP, Iglewski BH, Costerton JW, Greenberg EP. (1998). The involvement of cell-to-cell signals in the development of a bacterial biofilm. Science. 280:295-8.

Dean SN, Bishop BM, van Hoek ML (2011). Susceptibility of *Pseudomonas aeruginosa* biofilm to alpha-helical peptides: D-enantiomer of LL-37. Front. Microbiol. 2:128.

de la Fuente-Núñez C, Reffuveille F, Haney EF, Strauss SK, Hancock REW. (2014). Broad-spectrum anti-biofilm peptide that targets a cellular stress response. PLoS Pathog. 10: e1004152.

de la Fuente-Núñez C, Reffuveille F, Fernández L, Hancock REW. (2013). Bacterial biofilm development as a multicellular adaptation: antibiotic resistance and new therapeutic strategies. Curr. Opin. Microbiol. 16:580-9.

de la Fuente-Núñez C, Korolik V, Bains M, Nguyen U, Breidenstein EB, Horsman S, Lewenza S, Burrows L, Hancock REW. (2012). Inhibition of bacterial biofilm formation and swarming motility by a small synthetic cationic peptide. Antimicrob. Agents Chemother. 56:2696-704.

Drenkard E, Ausubel FM. (2002). *Pseudomonas* biofilm formation and antibiotic resistance are linked to phenotypic variation. Nature. 416:740-3.

Driffield K, Miller K, Bostock JM, O'Neill AJ, Chopra I. (2008). Increased mutability of *Pseudomonas aeruginosa* in biofilms. J. Antimicrob. Chemother. 61:1053-1056.
Easton DM, Nijnik A, Mayer ML, Hancock REW. (2009). Potential of immunomodulatory host defense peptides as novel anti-infectives. Trends Biotechnol. 27:582-90.
Edwards S, Kjellerup BV. (2012). Exploring the applications of invertebrate host-pathogen models for *in vivo* biofilm infections. FEMS Immunol. Med. Microbiol. 65:205-14.
Erlich H, Laffler T, Gallant J. (1971). ppGpp formation in *Escherichia coli* treated with rifampicin. J. Biol. Chem. 246:6121-3.
Fjell CD, Hiss JA, Hancock REW, Schneider G. (2011). Designing antimicrobial peptides: form follows function. Nat. Rev. Drug Discov. 11:37-51.
Fernández L, Breidenstein EBM, Hancock REW. (2011). Creeping baselines and adaptive resistance to antibiotics. Drug Resist. Updat. 14:1-21.
Flemming HC, Wingender J. (2010). The biofilm matrix. Nat. Rev. Microbiol. 8:623-33.
Freitag NE, Port GC, Miner MD. (2009). *Listeria monocytogenes* - from saprophyte to intracellular pathogen. Nat. Rev. Microbiol. 7:623-8.
Friedrich CL, Moyles D, Beveridge TJ, Hancock REW. (2000). Antibacterial action of structurally diverse cationic peptides on Gram-positive bacteria. Antimicrob. Agents Chemother. 44:2086-92.
Fux CA, Costerton JW, Stewart PS, Stoodley P. (2005). Survival strategies of infectious biofilms. Trends Microbiol. 13:34-40.
Gao W, Chua K, Davies JK, Newton HJ, Seemann T, Harrison PF, Holmes NE, Rhee HW, Hong JI, Hartland EL, Stinear TP, Howden BP. (2010). Two novel point mutations in clinical *Staphylococcus aureus* reduce linezolid susceptibility and switch on the stringent response to promote persistent infection. PLoS Pathog. 6:e1000944.
Geiger T, Francois P, Liebeke M, Fraunholz M, Goerke C, Krismer B, Schrenzel J, Lalk M, Wolz C. (2012). The stringent response of *Staphylococcus aureus* and its impact on survival after phagocytosis through the induction of intracellular PSMs expression. PLoS Pathog. 8:e1003016.
Geiger T, Goerke C, Fritz M, Schäfer T, Ohlsen K, Liebeke M, Lalk M, Wolz C. (2010). Role of the (p)ppGpp synthase RSH, a RelA/SpoT homolog, in stringent response and virulence of *Staphylococcus aureus*. Infect. Immun. 78:1873-83.
Germain E, Castro-Roa D, Zenkin N, Gerdes K. (2013). Molecular mechanism of bacterial persistence by HipA. Mol. Cell. 52:248-54.
Gilbert P, Collier PJ, Brown MR. (1990). Influence of growth rate on susceptibility to antimicrobial agents: biofilms, cell cycle, dormancy, and stringent response. Antimicrob. Agents Chemother. 34:1865-8.
Gillis RJ, White KG, Choi KH, Wagner VE, Schweizer HP, Iglewski BH. (2005). Molecular basis of azithromycin-resistant *Pseudomonas aeruginosa* biofilms. Antimicrob. Agents Chemother. 49:3858-67.
Gooderham WJ, Gellatly SL, Sanschagrin F, McPhee JB, Bains M, Cosseau C, Levesque RC, Hancock REW. (2009). The sensor kinase PhoQ mediates virulence in *Pseudomonas aeruginosa*. Microbiology. 155:699-711.
Hall MJ, Middleton RF, Westmacot D. (1983). The fractional inhibitory concentration (FIC) index as a measure of synergy. J. Antimicrob. Chemother. 11:427-433.
Hall-Stoodley L, Stoodley P. (2005). Biofilm formation and dispersal and the transmission of human pathogens. Trends Microbiol. 13:7-10.

Hall-Stoodley L, Costerton JW, Stoodley P. (2004). Bacterial biofilms: from the natural environment to infectious diseases. Nat. Rev. Microbiol. 2:95-108.
Hancock REW, Sahl HG. (2006). Antimicrobial and host-defense peptides as new anti-infective therapeutic strategies. Nat. Biotechnol. 24:1551-7.
Hancock REW, Speert DP. (2000). Antibiotic resistance in *Pseudomonas aeruginosa*:mechanisms and impact on treatment. Drug Resist. Updat. 3:247-255.
Hara A, Sy J. (1983). Guanosine 5'-triphosphate, 3'-diphosphate 5'-phosphohydrolase. Purification and substrate specificity. J. Biol. Chem. 258:1678-83.
He H, Cooper JN, Mishra A, Raskin DM. (2012). Stringent response regulation of biofilm formation in *Vibrio cholerae*. J. Bacteriol. 194:2962-72.
He J, Furmanski P. (1995). Sequence specificity and transcriptional activation in the binding of lactoferrin to DNA. Nature. 373:721-4.
Hengge R. (2009). Principles of c-di-GMP signalling in bacteria. Nat Rev Microbiol. 7:263-73.
Hilpert K, McLeod B, Yu J, Elliott MR, Rautenbach M, Ruden S, Bürck J, Muhle-Goll C, Ulrich AS, Keller S, Hancock REW. (2010) Short cationic antimicrobial peptides interact with ATP. Antimicrob. Agents Chemother. 54:4480-3.
Hilpert K, Volkmer-Engert R, Walter T, Hancock REW. (2005). High-throughput generation of small antibacterial peptides with improved activity. Nat. Biotechnol. 23:1008-12.
Hobley L, Kim SH, Maezato Y, Wyllie S, Fairlamb AH, Stanley-Wall NR, Michael AJ. (2014). Norspermidine is not a self-produced trigger for biofilm disassembly. Cell. 156:844-54.
Hochbaum AI, Kolodkin-Gal I, Foulston L, Kolter R, Aizenberg J, Losick R. (2011). Inhibitory effects of D-amino acids on *Staphylococcus aureus* biofilm development. J. Bacteriol. 193:5616-22.
Hoffman LR, D'Argenio DA, MacCoss MJ, Zhang Z, Jones RA, Miller SI. (2005). Aminoglycoside antibiotics induce bacterial biofilm formation. Nature. 436:1171-5.
Høiby N, Ciofu O, Johansen HK, Song ZJ, Moser C, Jensen PØ, Molin S, Givskov M, Tolker-Nielsen T, Bjarnsholt T. (2011). The clinical impact of bacterial biofilms. Int. J. Oral Sci. 3:55-65.
Huisman GW, Kolter R. (1994). Sensing starvation: a homoserine lactone—dependent signaling pathway in *Escherichia coli*. Science. 265:537-9.
Ikehara K, Kamitani E, Koarata C, Ogura A (1985) Induction of stringent response by streptomycin in *Bacillus subtilis* cells. J Biochem 97:697-700.
Ito A, Taniuchi A, May T, Kawata K, Okabe S. (2009). Increased antibiotic resistance of *Escherichia coli* in mature biofilms. Appl. Environ. Microbiol. 75:4093-100.
Jacobs MA, Alwood A, Thaipisuttikul I, Spencer D, Haugen E, Ernst S, Will O, Kaul R, Raymond C, Levy R, Chun-Rong L, Guenthner D, Bovee D, Olson MV, Manoil C. (2003). Comprehensive transposon mutant library of *Pseudomonas aeruginosa*. Proc. Natl. Acad. Sci. U.S.A. 100:14339-44.
Johansson EM, Crusz SA, Kolomiets E, Buts L, Kadam RU, Cacciarini M, Bartels KM, Diggle SP, Cámara M, Williams P, Loris R, Nativi C, Rosenau F, Jaeger KE, Darbre T, Reymond JL. (2008). Inhibition and dispersion of *Pseudomonas aeruginosa* biofilms by glycopeptide dendrimers targeting the fucose-specific lectin LecB. Chem. Biol. 15:1249-57.
Johnson L, Mulcahy H, Kanevets U, Shi Y, Lewenza S. (2012). Surface-localized spermidine

protects the *Pseudomonas aeruginosa* outer membrane from antibiotic treatment and oxidative stress. J. Bacteriol. 194:813-826.

Junker LM, Clardy J. (2007). High-throughput screens for small-molecule inhibitors of *Pseudomonas aeruginosa* biofilm development. Antimicrob. Agents Chemother. 51:3582-90.

Kaplan JB, Velliyagounder K, Ragunath C, Rohde H, Mack D, Knobloch JK, Ramasubbu N. (2004). Genes involved in the synthesis and degradation of matrix polysaccharide in *Actinobacillus actinomycetemcomitans* and *Actinobacillus pleuropneumoniae* biofilms. J. Bacteriol. 186:8213-20.

Kazmierczak BI, Lebron MB, Murray TS. (2006). Analysis of FimX, a phosphodiesterase that governs twitching motility in *Pseudomonas aeruginosa*. Mol. Microbiol. 60:1026-43.

Kaspy I, Rotem E, Weiss N, Ronin I, Balaban NQ, Glaser G. (2013). HipA-mediated antibiotic persistence via phosphorylation of the glutamyl-tRNA-synthetase. Nat. Commun. 4:3001

Keasling JD, Bertsch L, Kornberg A. (1993). Guanosine pentaphosphate phosphohydrolase of *Escherichia coli* is a long-chain exopolyphosphatase. Proc Natl Acad Sci U S A. 90:7029-33.

Keren I, Kaldalu N, Spoering A, Wang Y, Lewis K. (2004). Persister cells and tolerance to antimicrobials. FEMS Microbiol. Lett. 230:13-8.

Khan SR, Yamazaki H. (1972). Trimethoprim-induced accumulation of guanosine tetraphosphate (ppGpp) in *Escherichia coli*. Biochem. Biophys. Res. Commun. 48:169-74.

Kindrachuk KN, Fernández L, Bains M, Hancock REW. (2011). Involvement of an ATP-dependent protease, PA0779/AsrA, in inducing heat shock in response to tobramycin in *Pseudomonas aeruginosa*. Antimicrob. Agents Chemother. 55:1874-82.

Klinkenberg LG, Lee JH, Bishai WR, Karakousis PC. (2010). The stringent response is required for full virulence of *Mycobacterium tuberculosis* in guinea pigs. J. Infect. Dis. 202:1397-404.

Köhler T, Curty LK, Barja F, van Delden C, Pechère JC. (2000). Swarming of *Pseudomonas aeruginosa* is dependent on cell-to-cell signaling and requires flagella and pili. J. Bacteriol. 182:5990-6.

Kolodkin-Gal I, Cao S, Chai L, Böttcher T, Kolter R, Clardy J, Losick R. (2012). A self-produced trigger for biofilm disassembly that targets exopolysaccharide. Cell. 149:684-92.

Kolodkin-Gal I, Romero D, Cao S, Clardy J, Kolter R, Losick R. (2010). D-amino acids trigger biofilm disassembly. Science. 328:627-9.

Korch SB, Henderson TA, Hill TM. (2003). Characterization of the *hipA7* allele of *Escherichia coli* and evidence that high persistence is governed by (p)ppGpp synthesis. Mol. Microbiol. 50:1199-213

Kriel A, Bittner AN, Kim SH, Liu K, Tehranchi AK, Zou WY, Rendon S, Chen R, Tu BP, Wang JD. (2012). Direct regulation of GTP homeostasis by (p)ppGpp: a critical component of viability and stress resistance. Mol. Cell. 48:231-41

Kuczyńska-Wiśnik D, Matuszewska E, Laskowska E. (2010). *Escherichia coli* heat-shock proteins IbpA and IbpB affect biofilm formation by influencing the level of extracellular indole. Microbiology. 156:148-57.

Kumon H, Tomochika K, Matunaga T, Ogawa M, Ohmori H. (1994). A sandwich cup method for the penetration assay of antimicrobial agents through *Pseudomonas*

exopolysaccharides. Microbiol. Immunol. 38:615-619.
Kuroda A, Murphy H, Cashel M, Kornberg A. (1997). Guanosine tetra- and pentaphosphate promote accumulation of inorganic polyphosphate in *Escherichia coli*. J. Biol. Chem. 272:21240-3.
Leiman SA, May JM, Lebar MD, Kahne D, Kolter R, Losick R. (2013). D-amino acids indirectly inhibit biofilm formation in *Bacillus subtilis* by interfering with protein synthesis. J. Bacteriol. 195:5391-5.
Lellouche J, Kahana E, Elias S, Gedanken A, Banin E. (2009). Antibiofilm activity of nanosized magnesium fluoride. Biomaterials. 30:5969-78.
Lemos JA, Brown TA Jr, Burne RA. (2004). Effects of RelA on key virulence properties of planktonic and biofilm populations of *Streptococcus mutans*. Infect. Immun. 72:1431-40.
Lewis K. (2010). Persister cells. Annu. Rev. Microbiol. 64:357-72.
Lewis K. (2008). Multidrug tolerance of biofilms and persister cells. Curr. Top. Microbiol. Immunol. 322:107-131.
Lewis K. (2007). Persister cells, dormancy and infectious disease. Nat. Rev. Microbiol. 5:48-56.
Linares JF, Gustafsson I, Baquero F, Martinez JL. (2006). Antibiotics as intermicrobial signaling agents instead of weapons. Proc. Natl. Acad. Sci. U.S.A. 103:19484-9.
Lynch SV, Dixon L, Benoit MR, Brodie EL, Keyhan M, Hu P, Ackerley DF, Andersen GL, Matin A. (2007). Role of the *rapA* gene in controlling antibiotic resistance of *Escherichia coli* biofilms. Antimicrob. Agents Chemother. 51:3650-3658.
López D, Vlamakis H, Kolter R. (2010). Biofilms. Cold Spring Harb. Perspect. Biol. 2:a000398.
Losick R, Desplan C. (2008). Stochasticity and cell fate. Science. 320:65–68.
Loutet SA, Valvano MA. (2010). A decade of *Burkholderia cenocepacia* virulence determinant research. Infect. Immun. 78:4088-100.
Loutet SA, Valvano MA. (2011). Extreme antimicrobial peptide and polymyxin B resistance in the genus *Burkholderia*. Front Microbiol. 2:159.
Lu TK, Collins JJ. (2009). Engineered bacteriophage targeting gene networks as adjuvants for antibiotic therapy. Proc. Natl. Acad. Sci. U. S. A. 106:4629-34.
Lu TK, Collins JJ. (2007). Dispersing biofilms with engineered enzymatic bacteriophage. Proc. Natl. Acad. Sci. U. S. A. 104:11197-202.
Magnusson LU, Farewell A, Nyström T. (2005). ppGpp: a global regulator in *Escherichia coli*. Trends Microbiol. 13:236-42.
Mah TF, Pitts B, Pellock B, Walker GC, Stewart PS, O'Toole GA. (2003). A genetic basis for *Pseudomonas aeruginosa* biofilm antibiotic resistance. Nature. 426:306-10.
Maisonneuve E, Castro-Camargo M, Gerdes K. (2013). (p)ppGpp controls bacterial persistence by stochastic induction of toxin-antitoxin activity. Cell. 154:1140-50
Matsumura K, Furukawa S, Ogihara H, Morinaga Y. (2011). Roles of multidrug efflux pumps on the biofilm formation of *Escherichia coli* K-12. Biocontrol. Sci. 16:69-72.
Moore RA, Hancock REW. (1986). Involvement of outer membrane of *Pseudomonas cepacia* in aminoglycoside and polymyxin resistance. Antimicrob. Agents Chemother. 30:923-6.
Moreau-Marquis S, Stanton BA, O'Toole GA. (2008). *Pseudomonas aeruginosa* biofilm formation in the cystic fibrosis airway. Pulm. Pharmacol. Ther. 21:595-9.
Müh U, Schuster M, Heim R, Singh A, Olson ER, Greenberg EP. (2006). Novel *Pseudomonas aeruginosa* quorum-sensing inhibitors identified in an ultra-high-throughput screen.

Antimicrob. Agents Chemother. 50:3674-9.
Mulcahy H, Charron-Mazenod L, Lewenza S. (2008). Extracellular DNA chelates cations and induces antibiotic resistance in *Pseudomonas aeruginosa* biofilms. PLoS Pathog. 4:e1000213.
Mwangi MM, Kim C, Chung M, Tsai J, Vijayadamodar G, Benitez M, Jarvie TP, Du L, Tomasz A. (2013). Whole-genome sequencing reveals a link between β-lactam resistance and synthetases of the alarmone (p)ppGpp in *Staphylococcus aureus*. Microb. Drug Resist. 19:153-9.
Nguyen D, Joshi-Datar A, Lepine F, Bauerle E, Olakanmi O, Beer K, McKay G, Siehnel R, Schafhauser J, Wang Y, Britigan BE, Singh PK. (2011). Active starvation responses mediate antibiotic tolerance in biofilms and nutrient-limited bacteria. Science. 334:982-6.
Nickel JC, Wright JB, Ruseska I, Marrie TJ, Whitfield C, Costerton JW. (1985). Antibiotic resistance of *Pseudomonas aeruginosa* colonizing a urinary catheter *in vitro*. Eur. J. Clin. Microbiol. 4:213-218.
Ochi K. (1990). *Streptomyces relC* mutants with an altered ribosomal protein ST-L11 and genetic analysis of a *Streptomyces griseus relC* mutant. J. Bacteriol. 172:4008-16.
Ochi K, Kandala JC, Freese E. (1981). Initiation of Bacillus subtilis sporulation by the stringent response to partial amino acid deprivation. J. Biol. Chem. 256:6866-75.
O'Loughlin CT, Miller LC, Siryaporn A, Drescher K, Semmelhack MF, Bassler BL. (2013). A quorum-sensing inhibitor blocks *Pseudomonas aeruginosa* virulence and biofilm formation. Proc. Natl. Acad. Sci. U. S. A. 110:17981-6.
Ooga T, Ohashi Y, Kuramitsu S, Koyama Y, Tomita M, Soga T, Masui R. (2009). Degradation of ppGpp by nudix pyrophosphatase modulates the transition of growth phase in the bacterium *Thermus thermophilus*. J. Biol. Chem. 284:15549-56.
O'Toole G, Kaplan HB, Kolter R. (2000). Biofilm formation as microbial development. Annu. Rev. Microbiol. 54:49-79.
O'Toole GA, Kolter R. (1998). Flagellar and twitching motility are necessary for *Pseudomonas aeruginosa* biofilm development. Mol. Microbiol. 30:295-304.
Otto M. (2006). Bacterial evasion of antimicrobial peptides by biofilm formation. Curr. Top. Microbiol. Immunol. 306:251-8.
Overhage J, Bains M, Brazas MD, Hancock REW. (2008). Swarming of *Pseudomonas aeruginosa* is a complex adaptation leading to increased production of virulence factors and antibiotic resistance. J. Bacteriol. 190:2671-9.
Overhage J, Campisano A, Bains M, Torfs EC, Rehm BH, Hancock REW. (2008). Human host defense peptide LL-37 prevents bacterial biofilm formation. Infect. Immun. 76:4176-82.
Pamp SJ, Gjermansen M, Johansen HK, Tolker-Nielsen T. (2008). Tolerance to the antimicrobial peptide colistin in *Pseudomonas aeruginosa* biofilms is linked to metabolically active cells, and depends on the *pmr* and *mexAB-oprM* genes. Mol. Microbiol. 68:223-240.
Payne DJ, Gwynn MN, Holmes DJ, Pompliano DL. (2007). Drugs for bad bugs: confronting the challenges of antibacterial discovery. Nat. Rev. Drug. Discov. 6:29-40.
Pesavento C, Hengge R. (2009). Bacterial nucleotide-based second messengers. Curr. Opin. Microbiol. 12:170-6.
Picioreanu C, Kreft JU, Klausen M, Haagensen JA, Tolker-Nielsen T, Molin S. (2007).

Microbial motility involvement in biofilm structure formation--a 3D modelling study. Water Sci. Technol. 55:337-43.
Pompilio A, Scocchi M, Pomponio S, Guida F, Di Primio A, Fiscarelli E, Gennaro R, Di Bonaventura G. (2011). Antibacterial and anti-biofilm effects of cathelicidin peptides against pathogens isolated from cystic fibrosis patients. Peptides. 32:1807-14.
Poole K. (2012). Bacterial stress responses as determinants of antimicrobial resistance. J. Antimicrob. Chemother. 67:2069-89.
Potrykus K, Cashel M. (2008). (p)ppGpp: still magical? Annu. Rev. Microbiol. 62:35-51.
Powers JP, Martin MM, Goosney DL, Hancock REW. (2006). The antimicrobial peptide polyphemusin localizes to the cytoplasm of *Escherichia coli* following treatment. Antimicrob. Agents Chemother. 50:1522-1524.
Qiu D, Damron FH, Mima T, Schweizer HP, Yu HD. (2008). PBAD-based shuttle vectors for functional analysis of toxic and highly regulated genes in *Pseudomonas* and *Burkholderia* spp. and other bacteria. Appl. Environ. Microbiol. 74:7422-6.
Qu Y, Daley AJ, Istivan TS, Rouch DA, Deighton MA. (2010). Densely adherent growth mode, rather than extracellular polymer substance matrix build-up ability, contributes to high resistance of *Staphylococcus epidermidis* biofilms to antibiotics. J. Antimicrob. Chemother. 65:1405-1411.
Ramasubbu N, Thomas LM, Ragunath C, Kaplan JB. (2005). Structural analysis of dispersin B, a biofilm-releasing glycoside hydrolase from the periodontopathogen *Actinobacillus actinomycetemcomitans*. J. Mol. Biol. 349:475-86.
Reffuveille F, de la Fuente-Núñez C, Mansour S, Hancock REW. (2014). A broad-spectrum anti-biofilm peptide enhances antibiotic action against bacterial biofilms. Antimicrob. Agents Chemother. 58:5363-71.
Riera E, Macià MD, Mena A, Mulet X, Pérez JL, Ge Y, Oliver A. (2010). Anti-biofilm and resistance suppression activities of CXA-101 against chronic respiratory infection phenotypes of *Pseudomonas aeruginosa* strain PAO1. J. Antimicrob. Chemother. 65:1399-404.
Rivas-Santiago B, Castañeda-Delgado JE, Rivas Santiago CE, Waldbrook M, González-Curiel I, León-Contreras JC, Enciso-Moreno JA, del Villar V, Mendez-Ramos J, Hancock RE, Hernandez-Pando R. (2013). Ability of innate defence regulator peptides IDR-1002, IDR-HH2 and IDR-1018 to protect against *Mycobacterium tuberculosis* infections in animal models. PLoS One. 8:e59119.
Rendueles O, Travier L, Latour-Lambert P, Fontaine T, Magnus J, Denamur E, Ghigo JM. (2011). Screening of *Escherichia coli* species biodiversity reveals new biofilm-associated antiadhesion polysaccharides. MBio. 2:e00043-11
Römling U, Kjelleberg S, Normark S, Nyman L, Uhlin BE, Akerlund B. (2014). Microbial biofilm formation: a need to act. J. Intern. Med. 276:98-110.
Römling U, Galperin MY, Gomelsky M. (2013). Cyclic di-GMP: the first 25 years of a universal bacterial second messenger. Microbiol Mol Biol Rev. 77:1-52.
Römling U, Balsalobre C. (2012). Biofilm infections, their resilience to therapy and innovative treatment strategies. J. Intern. Med. 272:541-561.
Sauer K, Camper AK, Ehrlich GD, Costerton JW, Davies DG. (2002). *Pseudomonas aeruginosa* displays multiple phenotypes during development as a biofilm. J. Bacteriol. 184:1140-54.
Savage VJ, Chopra I, O'Neill AJ. (2013). *Staphylococcus aureus* biofilms promote horizontal

transfer of antibiotic resistance. Antimicrob. Agents Chemother. 57:1968-1970.
Schaible B, Taylor CT, Schaffer K. (2012). Hypoxia increases antibiotic resistance in *Pseudomonas aeruginosa* through altering the composition of multidrug efflux pumps. Antimicrob. Agents Chemother. 56:2114-2118.
Scott MG, Dullaghan E, Mookherjee N, Glavas N, Waldbrook M, Thompson A, Wang A, Lee K, Doria S, Hamill P, Yu JJ, Li Y, Donini O, Guarna MM, Finlay BB, North JR, Hancock REW. (2007). An anti-infective peptide that selectively modulates the innate immune response. Nat. Biotechnol. 25:465-72.
Scott MG, Yan H, Hancock REW. (1999). Biological properties of structurally related alpha-helical cationic antimicrobial peptides. Infect. Immun. 67:2005-9.
Sharma SV, Lee DY, Li B, Quinlan MP, Takahashi F, Maheswaran S, McDermott U, Azizian N, Zou L, Fischbach MA, Wong KK, Brandstetter K, Wittner B, Ramaswamy S, Classon M, Settleman J. (2010). A chromatin-mediated reversible drug-tolerant state in cancer cell subpopulations. Cell. 141:69–80.
Shrout JD, Chopp DL, Just CL, Hentzer M, Givskov M, Parsek MR. (2006). The impact of quorum sensing and swarming motility on *Pseudomonas aeruginosa* biofilm formation is nutritionally conditional. Mol. Microbiol. 62:1264-77.
Shyp V, Tankov S, Ermakov A, Kudrin P, English BP, Ehrenberg M, Tenson T, Elf J, Hauryliuk V. (2012). Positive allosteric feedback regulation of the stringent response enzyme RelA by its product. EMBO Rep. 13:835-9.
Sieprawska-Lupa M, Mydel P, Krawczyk K, Wójcik K, Puklo M, Lupa B, Suder P, Silberring J, Reed M, Pohl J, Shafer W, McAleese F, Foster T, Travis J, Potempa J. (2004). Degradation of human antimicrobial peptide LL-37 by *Staphylococcus aureus*-derived proteinases. Antimicrob. Agents Chemother. 48:4673-9.
Singh PK, Parsek MR, Greenberg EP, Welsh MJ. (2002). A component of innate immunity prevents bacterial biofilm development. Nature. 417:552-5.
Singh PK, Schaefer AL, Parsek MR, Moninger TO, Welsh MJ, Greenberg EP. (2000). Quorum-sensing signals indicate that cystic fibrosis lungs are infected with bacterial biofilms. Nature. 407:762-4.
Singh R, Ray P, Das A, Sharma M. (2010). Penetration of antibiotics through *Staphylococcus aureus* and *Staphylococcus epidermidis* biofilms. J. Antimicrob. Chemother. 65:1955-1958.
Stiernagle T. (2006). Maintenance of *C. elegans*. Wormbook. 11:1-11.
Sugisaki K, Hanawa T, Yonezawa H, Osaki T, Fukutomi T, Kawakami H, Yamamoto T, Kamiya S. (2013). Role of (p)ppGpp in biofilm formation and expression of filamentous structures in *Bordetella pertussis*. Microbiology. 159:1379-89.
Sun S, Kjelleberg S, McDougald D. (2013). Relative contributions of *Vibrio* polysaccharide and quorum sensing to the resistance of *Vibrio cholerae* to predation by heterotrophic protists. PLoS One. 8:e56338.
Svitil AL, Cashel M, Zyskind JW. (1993). Guanosine tetraphosphate inhibits protein synthesis *in vivo*. A possible protective mechanism for starvation stress in *Escherichia coli*. J. Biol. Chem. 268:2307-11.
Taylor CM, Beresford M, Epton HA, Sigee DC, Shama G, Andrew PW, Roberts IS. (2002). *Listeria monocytogenes relA* and *hpt* mutants are impaired in surface-attached growth and virulence. J. Bacteriol. 184:621-8.
Tedin K, Norel F. (2001). Comparison of Delta*relA* strains of *Escherichia coli* and *Salmonella*

enterica serovar Typhimurium suggests a role for ppGpp in attenuation regulation of branched-chain amino acid biosynthesis. J. Bacteriol. 183:6184-96.
Tomkins GM. (1975). The metabolic code. Science. 189:760-3.
Tosa T, Pizer LI. (1971). Biochemical bases for the antimetabolite action of L-serine hydroxamate. J. Bacteriol. 106:972-82.
Valle J, Da Re S, Henry N, Fontaine T, Balestrino D, Latour-Lambert P, Ghigo JM. (2006). Broad-spectrum biofilm inhibition by a secreted bacterial polysaccharide. Proc. Natl. Acad. Sci. U.S.A. 103:12558-63.
van Delden C, Comte R, Bally AM. (2001). Stringent response activates quorum sensing and modulates cell density-dependent gene expression in *Pseudomonas aeruginosa*. J. Bacteriol. 183:5376-84.
van der Veen S, Abee T. (2010). HrcA and DnaK are important for static and continuous-flow biofilm formation and disinfectant resistance in *Listeria monocytogenes*. Microbiology. 156:3782-90.
Vogt SL, Green C, Stevens KM, Day B, Erickson DL, Woods DE, Storey DG. (2011). The stringent response is essential for *Pseudomonas aeruginosa* virulence in the rat lung agar bead and *Drosophila melanogaster* feeding models of infection. Infect. Immun. 79:4094-104.
Wexselblatt E, Oppenheimer-Shaanan Y, Kaspy I, London N, Schueler-Furman O, Yavin E, Glaser G, Katzhendler J, Ben-Yehuda S. (2012). Relacin, a novel antibacterial agent targeting the Stringent Response. PLoS Pathog. 8:e1002925.
Wieczorek M, Jenssen H, Kindrachuk J, Scott WR, Elliott M, Hilpert K, Cheng JT, Hancock REW, Straus SK. (2010). Structural studies of a peptide with immune modulating and direct antimicrobial activity. Chem. Biol. 17:970-80.
Wiegand I, Hilpert K, Hancock REW. (2008). Agar and broth dilution methods to determine the minimal inhibitory concentration (MIC) of antimicrobial substances. Nat. Protoc. 3:163-75.
Whitchurch CB, Tolker-Nielsen T, Ragas PC, Mattick JS. (2002). Extracellular DNA required for bacterial biofilm formation. Science. 295:1487.
Xiao H, Kalman M, Ikehara K, Zemel S, Glaser G, Cashel M. (1991). Residual guanosine 3',5'-bispyrophosphate synthetic activity of *relA* null mutants can be eliminated by *spoT* null mutations. J. Biol. Chem. 266:5980-90
Yang L, Nilsson M, Gjermansen M, Givskov M, Tolker-Nielsen T. (2009). Pyoverdine and PQS mediated subpopulation interactions involved in *Pseudomonas aeruginosa* biofilm formation. Mol. Microbiol. 74:1380-92.
Yan H, Hancock REW. (2001). Synergistic interactions between mammalian antimicrobial defense peptides. Antimicrob. Agents Chemother. 45:1558-60.
Yoon SS, Hennigan RF, Hilliard GM, Ochsner UA, Parvatiyar K, Kamani MC, Allen HL, DeKievit TR, Gardner PR, Schwab U, Rowe JJ, Iglewski BH, McDermott TR, Mason RP, Wozniak DJ, Hancock RE, Parsek MR, Noah TL, Boucher RC, Hassett DJ. (2002). *Pseudomonas aeruginosa* anaerobic respiration in biofilms: relationships to cystic fibrosis pathogenesis. Dev. Cell. 3:593-603.
Zhang L, Hinz AJ, Nadeau JP, Mah TF. (2011). *Pseudomonas aeruginosa tssC1* links type VI secretion and biofilm-specific antibiotic resistance. J. Bacteriol. 193:5510-5513.
Zhang L, Mah TF. (2008). Involvement of a novel efflux system in biofilm-specific resistance to antibiotics. J. Bacteriol. 190:4447-4452.